Polyhydroxyalkanoate granules: surface protein topology and rational design of functionalised biobeads

A thesis presented to Massey University in partial fulfilment of the requirements for the degree of

Doctor of Philosophy

in

Microbiology

at Massey University, Manuwatu, New Zealand.

David O. Hooks

2014

Acknowledgements

Prof. Bernd Rehm for the topics and ideas to work on as well as all the guidance in the various aspects of science.

Dr Zoe Jordens helped and supported me though the process.

Friends in the lab who have come and gone over the last four years, a close 'bunch' we were and great to bounce new theories off.

Financial support from Massey University and the Institute of Fundamental Sciences.

Preface

All chapters published as separate manuscripts are listed below. These contributions do not appear in chronological order.

Chapter 2

Draper, J.; Du, J.; Hooks, D. O.; Lee, J. W.; Parlane, N. A.; Rehm, B. H. A. **Polyhydroxyalkanoate inclusions: Polymer synthesis, self-assembly and display technology.** In *Bionanotechnology: Biological Self-assembly and Its Applications*; Rehm, B. H. A., Ed.; Caister Academic Press: Norfolk, **2013**; pp. 1–36.

Chapter 3

Hooks, D. O.; Venning-Slater, M.; Du, J.; Rehm, B. H. A. **Polyhydroxyalkanoate Synthase Fusions as a Strategy for Oriented Enzyme Immobilisation.** *Molecules* **2014**, *19*, 8629–8643.

Chapter 4

Hooks, D. O.; Blatchford, P. A.; Rehm, B. H. A. **Bioengineering of bacterial polymer inclusions catalyzing the synthesis of N-acetyl neuraminic acid.** *Appl. Environ. Microbiol.* **2013**, *79*, 3116–3121.

Chapter 5

Hooks, D. O.; Rehm, B. H. A. **Insights into the surface topology of polyhydroxyalkanoate synthase: self-assembly of functionalized supramolecular inclusions.** *Applied Microbiology and Biotechnology* 2015, 1-9.

Chapter 6

Hooks, D. O.; Rehm, B. H. A. **Surface display of highly-stable *Desulfovibrio vulgaris* carbonic anhydrase on polyester beads for CO_2 capture.** *Biotechnology Letters* 2015, 1-6.

Listed below are contributions to each published chapter performed by David Hooks:

Chapter 2: This book chapter was partly written by David Hooks focussing on the genetics of PhaC, its catalytic mechanism, and application in enzyme immobilisation as well as contributions to other sections.

Chapter 3: This review was partly written and extensively edited by David Hooks focussing on the *in vivo* and *in vitro* methods of PhaC-fusion immobilisation along with current and potential applications.

Chapter 4: All experiments were performed by David Hooks. Paul Blatchford is acknowledged for construction of several plasmids as well as sample collection for GCMS analysis. Manuscript prepared by David Hooks.

Chapter 5: All experiments performed and manuscript prepared by David Hooks.

Chapter 6: All experiments performed and manuscript prepared by David Hooks.

DNA sequencing, GCMS, and MALDI-TOF/MS were provided by external services.

This is to certify that the above research was performed by David Hooks:

(Signature, Date)

Prof. Bernd H. A. Rehm

(Signature, Date)

David O. Hooks

Abstract

This thesis examined aspects of the polyhydroxyalkanoate (PHA) biobead system for immobilisation of proteins. Three separate studies have expanded the scope of this platform technology into different applications. New flexible regions along the length of the PhaC protein were discovered and functionalised with IgG binding domains. The bioremediation and fine-chemical synthesis aspects of the PHA biobeads were developed with active enzymes of interest immobilised to the bead surface. Additionally, functional dual fusion of enzymes to both the N- and C-terminus of PhaC was demonstrated for the first time. The enhanced scope of the PHA biobeads will lead to further applications in fields such as protein purification, vaccines, and diagnostics.

The first study assessed the ability of the PHA synthase (PhaC) based immobilisation system to tolerate dual enzyme fusions allowing the recapitulation of a biosynthetic pathway. *N*-acetyl neuraminic acid aldolase and *N*-acetyl glucosamine 2-epimerase allow for the synthesis of the medically relevant fine-chemical *N*-acetyl neuraminic acid (Neu5Ac). Ultimately, biobeads establishing the entire Neu5Ac synthesis pathway were able to convert up to 22% of the initial *N*-acetyl glucosamine into Neu5Ac which compares favourably with the theoretical maximum from chemi-enzymatic synthesis of 33%.

Despite intense research interest, the structure of PhaC has not yet been solved. Structural information of the exposed regions of granule-associated PhaC was gathered by the application of biotinylation labels. Six amino acid sites were found to be surface

exposed and four were able to tolerate FLAG-tag insertion. Three of these sites were chosen to functionalise with the IgG binding domain. These beads were able to mediate the binding and elution of IgG, with a maximum capacity of 16 mg IgG/g wet PHA beads.

The enhanced carbonic anhydrase from *Desulfovibrio vulgaris* str. "Miyazaki F" (DvCA) was fused the N-terminus of PhaC and immobilised on the surface of PHA beads. The DvCA beads had a specific activity of 114 U/mg enzyme. PHA-immobilised DvCA retained 54% of its initial activity after incubation at 90 °C for 1 h and 77% of its initial activity after incubation at pH 12 for 30 min. This stability indicates its usefulness in the challenging industrial environments where it may be deployed.

Table of Contents

List of Figures

List of Tables

Chapter 1

1. Introduction

Polyhydroxyalkanoates (PHA) are a class of bacterial polymer synthesised in times of unbalanced nutrient availability when carbon is readily available but other nutrients, such as nitrogen or oxygen, are depleted (Anderson & Dawes, 1990; Hoffmann & Rehm, 2004; Jendrossek & Pfeiffer, 2014; Rehm, 2010). These polyoxoesters are stored as water-insoluble inclusion bodies, or carbonosomes, referred to as PHA granules (Jendrossek, 2009). These granules can be catabolised when a carbon or energy source is required (Jendrossek & Handrick, 2002; Jendrossek, Schirmer, & Schlegel, 1996). PHA accumulation is seen commonly in bacteria and occasionally in *Archaea* with bacteria accumulating up to 80% of their dry weight as PHA (Hezayen, Rehm, Eberhardt, & Steinbüchel, 2000; Poli, Di Donato, Abbamondi, & Nicolaus, 2011). PHA is composed of monomers classified as either short or medium chain length and the most common PHA is the short-chain length poly-(*R*)-3-hydroxybutyrate (PHB) (G.-Q. Chen, 2009; Draper & Rehm, 2012; Leong, Show, Ooi, Ling, & Lan, 2014; Rehm, 2003).

PHB has been in industrial-scale production since 1982 as an alternative to plastics derived from petrochemicals. It is fully biodegradable by environmental microbial populations in contrast to traditional plastics which generate environmental pollution (Braunegg, Lefebvre, & Genser, 1998; Jendrossek & Handrick, 2002; Jendrossek et al., 1996). PHB has a similar tight helical structure and degree of crystallinity to polypropylene making it suitable for use in the biomedical industry where biocompatibility and biodegradability are important (Lenz & Marchessault, 2005). These properties give PHA the potential to be used in applications as diverse as packaging, surgical medicine, fisheries, enantiomerically pure chemical synthesis, and pharmacology. However, due to

the comparatively high cost of production, PHAs are limited to specialised applications such as sutures or medical implants (Hazer & Steinbüchel, 2007).

PHB biosynthesis (Fig. 1.1) has been extensively studied in the Gram-negative bacterium *Ralstonia eutropha* (also called *Cupriavidus necator*). The three enzymes involved are expressed from a single operon (Steinbüchel & Schlegel, 1991). Starting from acetyl-coenzyme A, two molecules of which are condensed by the enzyme β-ketothiolase (PhaA) to form acetoacetyl-CoA. Acetoacetyl-CoA reductase (PhaB) then reduces acetoacetyl-CoA to (R)-3-hydroxybutyryl-CoA which is polymerised into PHB by PHB synthase. For other PHAs different hydroxyacyl-CoA precursors are derived from alternate metabolic pathways. However, the final step is always catalysed by a specific PHA synthase (PhaC) (Peoples & Sinskey, 1989a, 1989b; Steinbüchel & Schlegel, 1991).

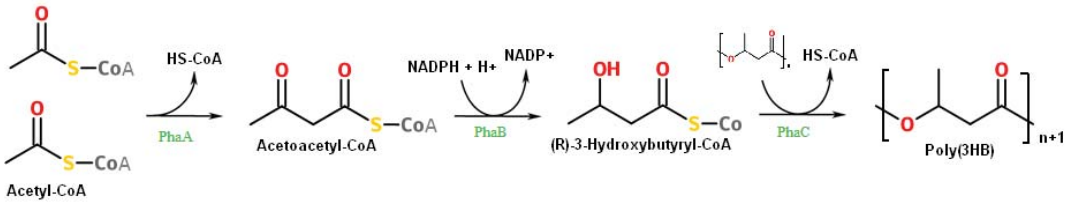

Figure 1.1: The biosynthetic pathway of PHB production.

Genetic modification has allowed the production of PHB granules in a number of heterologous expression systems. The first system was established in *Escherichia coli* (Slater, Voige, & Dennis, 1988). A short restriction enzyme fragment from a *R. eutropha* cosmid library containing *phaA*, *phaB*, and *phaC* was ligated into a multicopy vector. This expression system achieved PHB levels approaching 80% of bacterial cell dry weight. It appears possible that PHB biosynthetic pathway can be implemented in almost any species (Suriyamongkol, Weselake, Narine, Moloney, & Shah,

2007). Low levels of PHB production have been achieved in *Saccharomyces cerevisiae* (Leaf, Peterson, Stoup, Somers, & Sriencl, 1996). Expressing the *phaB* and *phaC* genes from *R. eutropha* in transgenic cotton fibre resulted in high levels of PHB production and an improvement in thermal insulation properties (John & Keller, 1996). Because plants produce their own carbon source, this method of PHB production is carbon-neutral.

The PHA synthase (PhaC) is the key enzyme and remains covalently attached to the nascent polymer chain (Rehm & Steinbüchel, 1999; Rehm, 2003, 2010; Stubbe & Tian, 2003; Stubbe et al., 2005). As the amphipathic protein/polyester chains extend, they form spherical inclusions within the cell of 50 - 500 nm diameter (Grage et al., 2009). The role of PHA in bacterial metabolism, the metabolic pathway of PHB, and genetics of *phaC* is discussed in Chapter 1. Recently, this process of *in vivo* PHB granule formation has been exploited as a protein immobilisation platform by fusing proteins of interest to the PhaC and expressing the resulting constructs in transgenic hosts such as *Escherichia coli* (Brockelbank, Peters, & Rehm, 2006). Examples include vaccines, diagnostic tests, affinity purification, and enzyme immobilisation as fully described in Chapter 1 (Blatchford, Scott, French, & Rehm, 2012; Brockelbank et al., 2006; S. Chen et al., 2014; Hooks, Blatchford, & Rehm, 2013; Hooks, Venning-Slater, Du, & Rehm, 2014; Parlane et al., 2011).

PHB has many attractive properties which make PHB biobeads useful in various applications. It is biodegradable, non-toxic, and well tolerated by mammalian systems (Braunegg et al., 1998). The small size of the granules (50 – 500 nm) gives the biobeads a large surface to volume ratio and makes them small enough for drug delivery or antigen display in vaccination. Immobilisation of enzymes and peptides to a solid support has many advantages over the use of free protein. Immobilisation facilitates purification, enhances stability of the immobilised product under harsh

conditions, and allows for efficient re-use of the expensive input (Fernandez-Lafuente, 2009; Mateo, Palomo, Fernandez-Lorente, Guisan, & Fernandez-Lafuente, 2007). Additionally, immobilisation of multiple enzymes co-localised to a solid-support surface allows for the generation of synthetic multienzyme complexes which more closely mimic the structures found in nature (Jia, Narasimhan, & Mallapragada, 2013). Enzyme immobilisation to PHA biobeads as well as the advantage of an oriented attachment process is the focus of Chapter 2.

Thesis Scope

Problem statement

PHAs are seen as alternatives to petroleum based plastics due to their renewable and biodegradable properties. Intense research interest has focussed on PhaC, the final enzyme in the PHA production pathway. As PhaC remains covalently attached to the PHA inclusion these biological "nanobeads" have also been used as a platform for protein immobilisation including applications in enzyme display, vaccine production, and bioseparation. Although there have been multiple demonstrations of functionalised biobeads, there is scope for enhancing this functionality through an improved understanding of granule surface proteins, especially PhaC. Examining the orientation, arrangement, and topology of the granule surface proteins will allow the production of biobeads with enhanced bioremediation, separation, and enzymatic abilities.

Aim

Apply empirically derived knowledge of PhaC and PhaC fusion proteins to the design of functionalised PHA granules demonstrating an enhanced commercial scope for this platform technology.

Objectives

First, the immobilisation of two enzymes involved in the synthesis of the medically relevant fine chemical N-acetyl neuraminic acid to PHA beads. Although single enzyme fusions to either the N- or C-terminus had been successfully demonstrated this was the first example of a dual enzyme

fusion recapitulating a biosynthetic pathway and resulted in a new field of application for PHA biobeads in fine chemical synthesis.

Structural information of PhaC would be useful in the rational design of functionalised biobeads. Despite many attempts, the structure of PhaC is yet to be solved. By exploring the granule-associated PhaC with amino acid specific biotinylation labels, the surface exposed regions of PhaC were located. These sites were further examined as potential modification sites for the functionalisation of PHA biobeads. The functionalities assessed were the synthetic epitope FLAG and the IgG binding domain of *Stapholoccoccus aureus* protein A for affinity purification.

The final objective of this PhD was to introduce carbon dioxide bioremediation functionality to the PHA biobeads by immobilisation of the engineered carbonic anhydrase from *Desulfovibrio vulgaris* str. "Mikazaki F". Immobilisation frequently improves enzyme stability which may provide advantages in high temperature or extreme pH operating environments. The aim of this aspect of the research was to develop biobeads with an application in carbon dioxide adsorption and conversion in power plant exhaust streams.

References

Anderson, A. J., & Dawes, E. A. (1990). Occurrence, metabolism, metabolic role, and industrial uses of bacterial polyhydroxyalkanoates. *Microbiological Reviews*, *54*(4), 450–472. doi:0146-0749/90/040450-23$02.00/0

Blatchford, P. A., Scott, C., French, N., & Rehm, B. H. A. (2012). Immobilization of organophosphohydrolase OpdA from Agrobacterium radiobacter by overproduction at the surface of polyester inclusions inside engineered Escherichia coli. *Biotechnology and Bioengineering*, *109*(5), 1101–8. doi:10.1002/bit.24402

Braunegg, G., Lefebvre, G., & Genser, K. F. (1998). Polyhydroxyalkanoates, biopolyesters from renewable resources: Physiological and engineering aspects. *Journal of Biotechnology*, *65*(2-3), 127–161. doi:10.1016/S0168-1656(98)00126-6

Brockelbank, J. A., Peters, V., & Rehm, B. H. A. (2006). Recombinant Escherichia coli strain produces a ZZ domain displaying biopolyester granules suitable for immunoglobulin G purification. *Applied and Environmental Microbiology*, *72*(11), 7394–7. doi:10.1128/AEM.01014-06

Chen, G.-Q. (2009). A microbial polyhydroxyalkanoates (PHA) based bio- and materials industry. *Chemical Society Reviews*, *38*(8), 2434–2446. doi:10.1039/b812677c

Chen, S., Parlane, N. A., Lee, J., Wedlock, D. N., Buddle, B. M., & Rehm, B. H. A. (2014). New skin test for detection of bovine tuberculosis on the basis of antigen-displaying polyester inclusions produced by recombinant Escherichia coli. *Applied and Environmental Microbiology*, *80*(8), 2526–35. doi:10.1128/AEM.04168-13

Draper, J. L., & Rehm, B. H. A. (2012). Engineering bacteria to manufacture functionalized polyester beads. *Bioengineered*. doi:10.4161/bbug.19567

Fernandez-Lafuente, R. (2009). Stabilization of multimeric enzymes: Strategies to prevent subunit dissociation. *Enzyme and Microbial Technology*, *45*(6-7), 405–418. doi:10.1016/j.enzmictec.2009.08.009

Grage, K., Jahns, A. C., Parlane, N., Palanisamy, R., Rasiah, I. A., Atwood, J. A., & Rehm, B. H. A. (2009). Bacterial polyhydroxyalkanoate granules: biogenesis, structure, and potential use as nano-/micro-beads in biotechnological and biomedical applications. *Biomacromolecules*, *10*(4), 660–9. doi:10.1021/bm801394s

Hazer, B., & Steinbüchel, A. (2007). Increased diversification of polyhydroxyalkanoates by modification reactions for industrial and medical applications. *Applied Microbiology and Biotechnology*, *74*(1), 1–12. doi:10.1007/s00253-006-0732-8

Hezayen, F. F., Rehm, B. H. A., Eberhardt, R., & Steinbüchel, A. (2000). Polymer production by two newly isolated extremely halophilic archaea: application of a novel corrosion-resistant

bioreactor. *Applied Microbiology and Biotechnology*, *54*(3), 319–325. Retrieved from http://www.ncbi.nlm.nih.gov/pubmed/11030566

Hoffmann, N., & Rehm, B. H. A. (2004). Regulation of polyhydroxyalkanoate biosynthesis in Pseudomonas putida and Pseudomonas aeruginosa. *FEMS Microbiology Letters*, *237*(1), 1–7. doi:10.1016/j.femsle.2004.06.029

Hooks, D. O., Blatchford, P. A., & Rehm, B. H. A. (2013). Bioengineering of bacterial polymer inclusions catalyzing the synthesis of N-acetylneuraminic acid. *Applied and Environmental Microbiology*, *79*(9), 3116–21. doi:10.1128/AEM.03947-12

Hooks, D. O., Venning-Slater, M., Du, J., & Rehm, B. H. A. (2014). Polyhydroyxalkanoate synthase fusions as a strategy for oriented enzyme immobilisation. *Molecules (Basel, Switzerland)*, *19*(6), 8629–43. doi:10.3390/molecules19068629

Jendrossek, D. (2009). Polyhydroxyalkanoate granules are complex subcellular organelles (carbonosomes). *Journal of Bacteriology*, *191*(10), 3195–202. doi:10.1128/JB.01723-08

Jendrossek, D., & Handrick, R. (2002). Microbial degradation of polyhydroxyalkanoates. *Annual Review of Microbiology*, *56*, 403–432. doi:10.1146/annurev.micro.56.012302.160838

Jendrossek, D., & Pfeiffer, D. (2014). New insights in the formation of polyhydroxyalkanoate granules (carbonosomes) and novel functions of poly(3-hydroxybutyrate). *Environmental Microbiology*. doi:10.1111/1462-2920.12356

Jendrossek, D., Schirmer, A., & Schlegel, H. G. (1996). Biodegradation of polyhydroxyalkanoic acids. *Applied Microbiology and Biotechnology*. doi:10.1007/s002530050844

Jia, F., Narasimhan, B., & Mallapragada, S. (2013). Materials-based strategies for multi-enzyme immobilization and co-localization: A review. *Biotechnology and Bioengineering*, *111*(2), 209–222. doi:10.1002/bit.25136

John, M. E., & Keller, G. (1996). Metabolic pathway engineering in cotton: biosynthesis of polyhydroxybutyrate in fiber cells. *Proceedings of the National Academy of Sciences of the United States of America*, *93*(23), 12768–73. Retrieved from http://www.pubmedcentral.nih.gov/articlerender.fcgi?artid=23995&tool=pmcentrez&rendertype=abstract

Leaf, T. A., Peterson, M. S., Stoup, S. K., Somers, D., & Sriencl, F. (1996). Saccharornyces cerevisiae. *Microbiology*, (1996), 1169–1180.

Lenz, R. W., & Marchessault, R. H. (2005). Bacterial polyesters: Biosynthesis, biodegradable plastics and biotechnology. *Biomacromolecules*. doi:10.1021/bm049700c

Leong, Y. K., Show, P. L., Ooi, C. W., Ling, T. C., & Lan, J. C. W. (2014). Current trends in polyhydroxyalkanoates (PHAs) biosynthesis: Insights from the recombinant Escherichia coli. *Journal of Biotechnology*, *180*, 52–65. doi:10.1016/j.jbiotec.2014.03.020

Mateo, C., Palomo, J. M., Fernandez-Lorente, G., Guisan, J. M., & Fernandez-Lafuente, R. (2007). Improvement of enzyme activity, stability and selectivity via immobilization techniques. *Enzyme and Microbial Technology*, *40*(6), 1451–1463. doi:10.1016/j.enzmictec.2007.01.018

Parlane, N. A., Grage, K., Lee, J. W., Buddle, B. M., Denis, M., & Rehm, B. H. A. (2011). Production of a particulate hepatitis C vaccine candidate by an engineered Lactococcus lactis strain. *Applied and Environmental Microbiology*, *77*(24), 8516–22. doi:10.1128/AEM.06420-11

Peoples, O. P., & Sinskey, A. J. (1989a). Poly-β-hydroxybutyrate (PHB) biosynthesis in Alcaligenes eutrophus H16. Identification and characterization of the PHB polymerase gene (phbC). *Journal of Biological Chemistry*, *264*(26), 15298–15303.

Peoples, O. P., & Sinskey, A. J. (1989b). Poly-β-hydroxybutyrate biosynthesis in Alcaligenes eutrophus H16. Characterization of the genes encoding β-ketothiolase and acetoacetyl-CoA reductase. *Journal of Biological Chemistry*, *264*(26), 15293–15297.

Poli, A., Di Donato, P., Abbamondi, G. R., & Nicolaus, B. (2011). Synthesis, production, and biotechnological applications of exopolysaccharides and polyhydroxyalkanoates by Archaea. *Archaea*. doi:10.1155/2011/693253

Rehm, B. H. A. (2003). Polyester synthases: natural catalysts for plastics. *The Biochemical Journal*, *376*(Pt 1), 15–33. doi:10.1042/BJ20031254

Rehm, B. H. A. (2010). Bacterial polymers: biosynthesis, modifications and applications. *Nature Reviews Microbiology*, *8*(8), 578–92. doi:10.1038/nrmicro2354

Rehm, B. H. A., & Steinbüchel, A. (1999). Biochemical and genetic analysis of PHA synthases and other proteins required for PHA synthesis. *International Journal of Biological Macromolecules*, *25*(1-3), 3–19. Retrieved from http://www.ncbi.nlm.nih.gov/pubmed/10416645

Slater, S. C., Voige, W. H., & Dennis, D. E. (1988). Cloning and expression in Escherichia coli of the Alcaligenes eutrophus H16 poly-beta-hydroxybutyrate biosynthetic pathway. *Journal of Bacteriology*, *170*(10), 4431–6. Retrieved from http://www.pubmedcentral.nih.gov/articlerender.fcgi?artid=211473&tool=pmcentrez&rendertype=abstract

Steinbüchel, A., & Schlegel, H. G. (1991). Physiology and molecular genetics of poly(β-hydroxyalkanoic acid) synthesis in Alcaligenes eutrophus. *Molecular Microbiology*, *5*(3), 535–542. doi:10.1111/j.1365-2958.1991.tb00725.x

Stubbe, J., & Tian, J. (2003). Polyhydroxyalkanoate (PHA) hemeostasis: the role of PHA synthase. *Natural Product Reports*, *20*(5), 445–457. doi:10.1039/b209687k

Stubbe, J., Tian, J., He, A., Sinskey, A. J., Lawrence, A. G., & Liu, P. (2005). Nontemplate-dependent polymerization processes: polyhydroxyalkanoate synthases as a paradigm. *Annual Review of Biochemistry*, *74*, 433–480. doi:10.1146/annurev.biochem.74.082803.133013

Suriyamongkol, P., Weselake, R., Narine, S., Moloney, M., & Shah, S. (2007). Biotechnological approaches for the production of polyhydroxyalkanoates in microorganisms and plants - A review. *Biotechnology Advances*. doi:10.1016/j.biotechadv.2006.11.007

Chapter 2

2. Polyhydroxyalkanoate inclusions: Polymer synthesis, self-assembly and display technology

*Jenny Draper, Jinping Du, David Hooks, Jason Lee, Natalie Parlane[1], Bernd Rehm**

Institute of Molecular Biosciences, Massey University, Palmerston North, New Zealand,

[1] AgResearch, Hopkirk Research Institute, Palmerston North, New Zealand

* corresponding author: b.rehm@massey.ac.nz

Abstract

Biopolyesters are a class of carbon storage polymers synthesized by a wide variety of bacteria in response to nutrient stress. Production of these polyhydroxyalkanoates (PHAs = polyesters) is catalyzed by PHA synthases, which polymerize *(R)*-3-hydroxyacyl-CoA thioesters into polyester. There are several different classes of PHA synthases which preferentially utilize different CoA thioester precursors, generating PHAs with varying material properties such as

elasticity and melting point. Genetic engineering and growth on varied carbon sources can be used to modify the type of polyester produced. The general biopolyester properties of biocompatibility, biodegradability, and production from renewable carbon sources have led to considerable interest in PHAs as biomaterials for medical applications as well as alternatives to petrochemical plastics.

Biopolyesters are generated in the cell as water-insoluble granules coated with structural, regulatory, and synthase proteins. Recently, the natural structure of the granules has been exploited to generate functionalized nanoparticles for use in a wide variety of applications, including bioseparation, drug delivery, protein purification, enzyme immobilization, diagnostics, and vaccine delivery.

1) Introduction

Polyhydroxyalkanoates (PHAs) are biopolyesters produced naturally as intracellular inclusions by a wide range of bacteria and archaea when a carbon source is available in excess and other nutrients are growth–limiting. These PHA granules serve as a carbon and energy reserve which can be accessed by depolymerizing enzymes during periods of carbon starvation.

The key enzyme for PHA production is the PHA synthase, which catalyzes the enantiomer-selective conversion of *(R)*-3-hydroxyacyl-CoA thioesters into polyester, while releasing CoA **[Figure 2.1.1]**. The thioester precursors are generated from intermediates of primary metabolism. This is exemplified by the production of *(R)*-3-polyhydroxybutyrate (PHB) from acetyl CoA in *R. eutropha*: first, the PhaA β-ketothiolase condenses two acetyl-CoA monomers into acetoacetyl-CoA; these are reduced into *(R)*-3-hydroxybutyryl-CoA by the acetoacetyl-CoA

reductase PhaB, and finally the PhaC synthase uses the *(R)*-3-hydroxybutyryl-CoA monomers to synthesize PHB. Together, the *phaABC* genes are sufficient for production of PHB in the presence of acetyl-CoA.

However, the intermediates can also be diverted from the β-oxidation cycle or fatty acid *de novo* biosynthesis pathways when other carbon sources are used. Incorporation of *(R)*-3-hydroxy fatty acids with different monomer chain lengths generates PHAs with varied properties such as melting point and crystallinity. The four major classes of PHA synthases preferentially utilize different precursors, thus favoring formation of different PHA types. However, most of the PHA synthases studied are able to utilize a broad range of precursors. Genetic engineering to modify the precursor-generating pathways, such as *fadAB* knockout mutants disrupting β-oxidation, can influence the type and amount of PHA produced. Mutagenesis of the PHA synthases or growth on varied carbon sources also affects PHA production.

Much research has been done on PHA production; PHAs are highly biocompatible, biodegradable, and produced naturally from renewable carbon resources, making them an attractive alternative to petrochemical-based plastics. However, due to the cost of

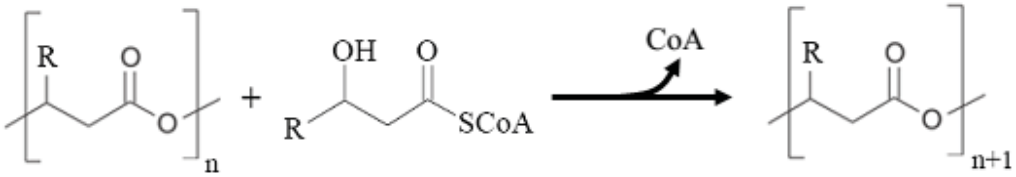

Figure 2.1.1 *The PHA production reaction catalyzed by PHA synthases. (Reproduced from Rehm 2007 [111].)*

fermentation and purification, PHAs currently remain more expensive to produce than conventional plastics. Thus, they are primarily manufactured for higher value niche applications, especially in the biomedical field where they are currently used as suture material, tissue scaffolds, or potentially for drug delivery.

PHAs are deposited in the cell cytoplasm as granules with a hydrophobic biopolyester core surrounded by attached or embedded surface proteins [**Figures 2.1.2, 2.1.3]**. The surface-attached proteins include the PHA synthase, which remains covalently attached to the polyester chain it synthesized, as well as structural proteins (phasins), depolymerases, and regulatory proteins bound to the polyester core by hydrophobic interactions. However, aside from the PHA synthase these surface proteins are not necessary for granule formation. Granules can form *in vitro*, merely by providing purified PHA synthase with precursor *(R)*-3-hydroxyacyl-CoA thioesters. Additionally, PHA granules are produced efficiently in recombinant bacteria lacking the structural and regulatory proteins. In naturally PHA-producing cells the surface proteins are involved in regulation of granule size, number, and

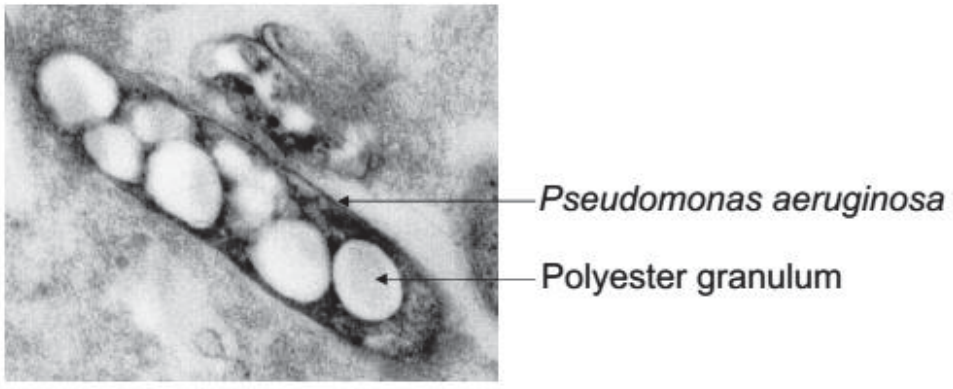

***Figure* 2.1.2** *Electron microscopy image of* Pseudomonas aeruginosa *containing PHA granules. (Reproduced from Rehm 2007 [111].)*

distribution during cell division.

The natural production of PHAs as protein-coated granules has recently been exploited to produce functionalized biopolyester “nanobeads”. This new technology uses genetic fusions of naturally granule-attached proteins to functional proteins of interest; expression of these proteins in PHA-producing bacteria results in one-step production of functionalized granules. PHA nanobeads suitable for bioseparation, diagnostics and imaging, enzyme immobilization, protein purification, and delivery of drugs and vaccines have already been developed. The potential applications of this technology are only limited by the ability to express functional protein in a host cell. Most bacteria are capable of producing PHA either naturally or

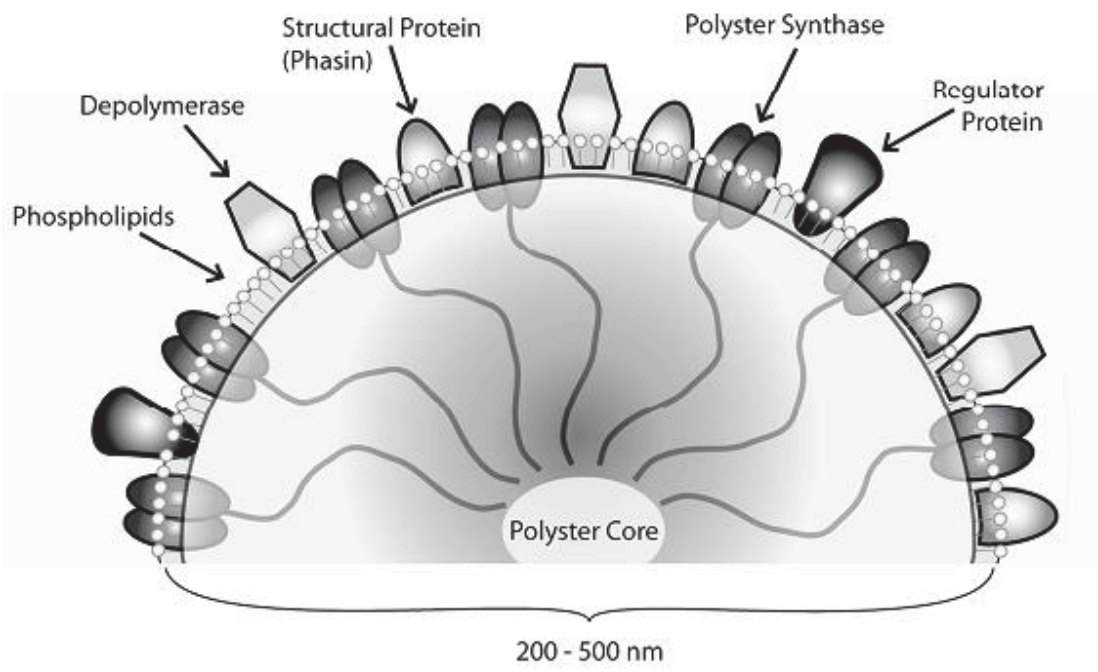

Figure 2.1.3 *Schematic representation of a PHA granule and its associated proteins.*

recombinantly; currently *Escherichia coli*, *Pseudomonas sp., Ralstonia eutropha*, and *Lactococcus lactis* are the primary producers of recombinant functionalized polyester granules.

2) Polyester diversity

PHAs are high molecular weight (5 x 10^5 to 5 x 10^6) linear polyesters composed of *(R)*-3-hydroxyfatty acids with different monomer chain lengths **[Figure 2.2]** [1, 2]. Short-chain-length PHAs (PHA_{SCL}) comprise 3-5 carbon atoms and are produced by a wide-range of bacteria and archaea. These PHAs have a high melting point, crystallinity, and brittleness. Medium-chain-length PHAs (PHA_{MCL}) with 6-14 carbon atoms are produced primarily by pseudomonads; these PHAs are more elastomeric and have a lower melting point and crystallinity. Long chain-length PHAs (PHA_{LCL}) have more than 14 carbon atoms. Intracellular PHB was first discovered in *Bacillus megaterium* in 1925 [3]. Examples of other PHAs include poly 4-hydroxybutyrate (P4HB), copolymers of 3-hydroxybutyrate and 3-hydroxyvalerate (PHBV), copolymers of 3-hydroxybutyrate and 3-hydroxyhexanoate (PHBHHx), and poly 3-hydroxyoctanoate (PHO). produced PHAs have since been described [4, 56].

In contrast to the high-molecular weight carbon-storage PHA produced by prokaryotes, many prokaryotic and eukaryotic organisms produce non-storage, low molecular weight PHA [7-10]. These 130-170 monomer unit molecules known as cPHB are complexed with other macromolecules such as polyphosphates and are found in lipoproteins, cell membranes, and cytoplasm. cPHBs can dissolve salts and facilitate their transfer across hydrophobic barriers. For example, cPHBs can form channels in the cytoplasmic membrane, allowing import of calcium ions [11]. This plays a part in acquisition of competence by *E. coli*, most likely by

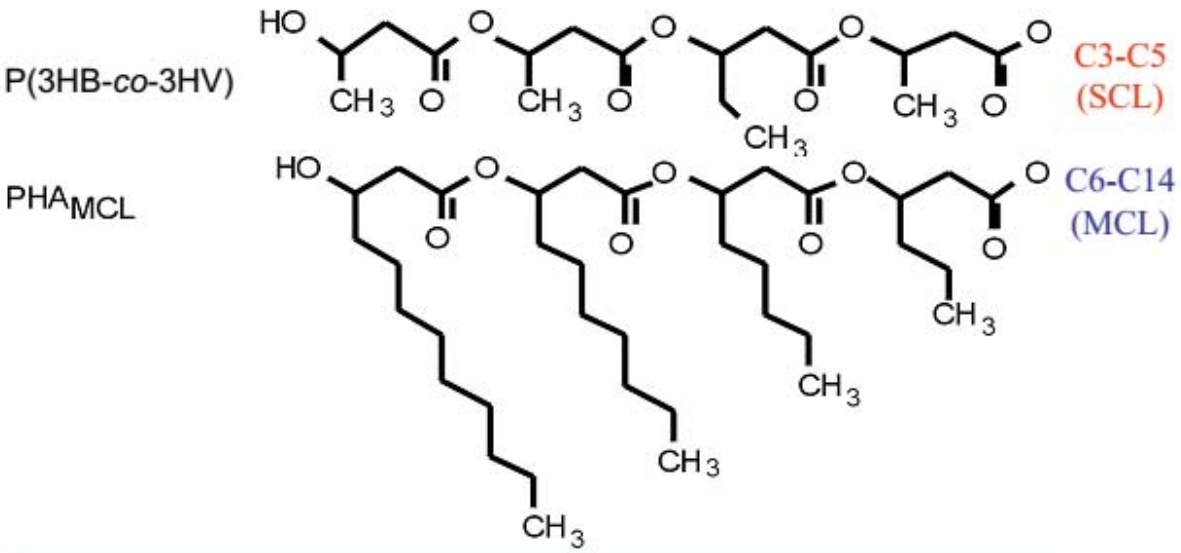

Material Properties	PHA_{SCL}	PHA_{MCL}	PP
T_m (°C)	177	61	176
T_g (°C)	2	-36	-10
Crystallinity (%)	70	30	60
Elongation at break (%)	5	300	400

PP, polypropylene

***Figure* 2.2** *Chemical structure and material properties of the two major classes of bacterial polyesters, compared to polypropylene. (Reproduced from Rehm 2007 [111].)*

replacing the inorganic polyphosphate in the PHB channel with organic DNA polyphosphate, resulting in DNA being drawn into the cell [12]. Reusch *et al* have also shown an involvement of cPHB in atherogenic plaques and diabetes and suggested plasma PHB levels may serve as a disease marker [13]. No synthesis genes or enzymes for cPHB production have yet been identified.

Some eukaryotic organisms such as slime-moulds and fungi are able to produce the polyester poly(*β*,L-malic acid) (PMLA) [14]. PMLAs probably function as carrier molecules for proteins involved in synchronization of cell nucleus division [15]. Although PMLA can be produced chemically, an enantiomerically pure product is obtained by biological fermentation, often using myxomycetes such as *Physarum polycephalum*. PMLA is highly water-soluble, biodegradable, biocompatible, and can be chemically modified. It is often produced as co-polymer microspheres [16] for use as slow release drug-delivery agents combined with active drugs for cancer treatment [17, 18], broncho-dilators [19], or to treat pulmonary hypertension [20].

In contrast to traditional petrochemical-based plastics, PHA is produced from renewable carbon sources such as glucose, cane or beet molasses [21, 22], waste oil [23], or xylose and by transgenic plants [24-26]. Furthermore, the biodegradability of PHAs is desirable in many environments and ecosystems. Numerous microorganisms secrete extracellular polymerases that hydrolyse PHA into water-soluble oligomers and monomers and subsequently utilise these as cell nutrients.

Some PHAs have properties similar to the main commodity plastics (e.g. polypropylene and polystyrene), and they can be heat-processed using current plastic industry techniques [27].

PHAs have already been used in the packaging, pharmaceutical, and medical industries for a wide range of products. Additionally, the chiral hydroxy acids that compose PHA can be used as building blocks for the synthesis of enantiomerically pure fine chemicals such as antibiotics or vitamins [28]. However, it is presently more expensive to produce plastic from renewable biological sources than non-renewable petrochemical sources. Therefore, the use of PHA is currently targeted at niche medical applications which benefit from its biocompatibility and biodegradability, such as drug delivery, suture material, and bone scaffolds.

3) Polyester synthases: genetics

Polyester synthases are the key enzymes for PHA biosynthesis. The four major classes of PHA synthase are distinguished primarily by subunit composition and sequence similarity and to a lesser extent by substrate specificity **[Figure 2.3]**.

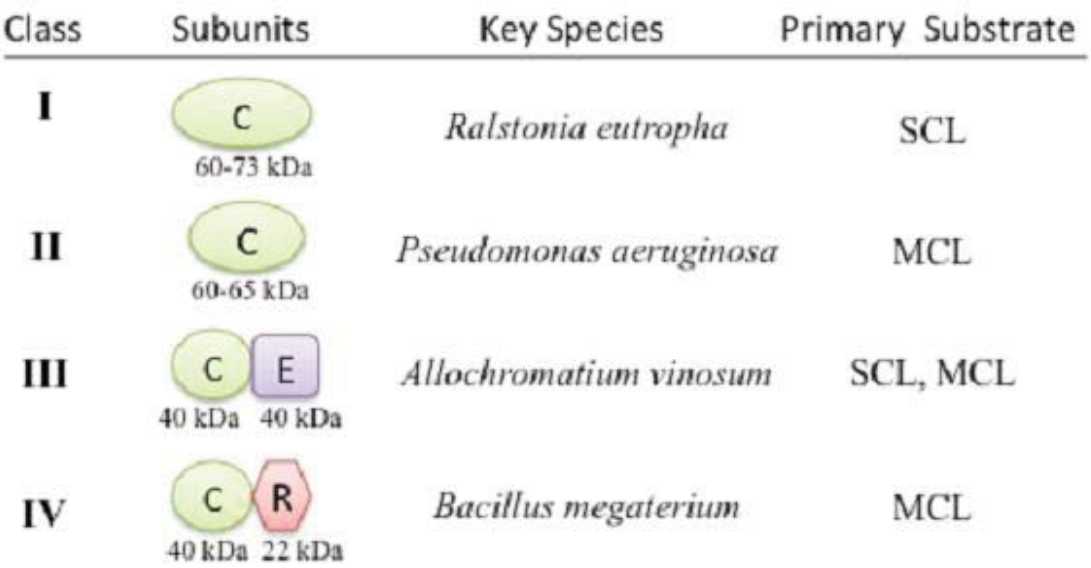

Figure 2.3 *The four classes of polyester synthases.*

3.1) Class I

Class I synthases are composed of a single PhaC subunit with a relatively large molecular weight of 60 – 73 kDa. The class I PHA synthases from *R. eutropha* H16 preferentially utilise SCL CoA thioesters of (*R*)-3-hydroxy fatty acids of 3-5 carbon atoms. However, medium chain length monomers can also be incorporated by the class I PhaC from *R. eutropha* B5786 which shows a 99% sequence similarity to the PhaC from H16 [29]. The class I synthases from *Aeromonas punctata* FA440 also produce polymers from SCL and MCL CoA thioesters of (*R*)-3-hydroxy fatty acids [30]. Recently, a highly active PHA synthase from *Chromobacterium* sp. USM2 has been isolated and characterised [31]. This enzyme can utilize a broad substrate range (3HB, 3HV, and 3HHx). Compared to the activity of PhaC from *R. eutropha* (307 ± 24 U/g), the new synthase has an eight-fold higher activity (2,462 ± 80 U/g) with respect to the polymerisation of 3-hydroxybutyryl-coenzyme A.

3.2) Class II

This class of synthases is found in *Pseudomonas* species; it is also composed of a single PhaC subunit with a slightly smaller molecular weight of 60 – 65 kDa. Class II synthases usually utilise MCL CoA thioesters of (*R*)-3-hydroxy fatty acids (e.g. *P. putida, P. aeruginosa, P. oleovorans*) [32]. However the PHA synthase from *Pseudomonas sp.* 61-3 produces polymers from both SCL and MCL CoA thioesters of (*R*)-3-hydroxy fatty acids [33]. It should be noted that pseudomonads can also produce class I synthases [34].

3.3) Class III

In contrast to the previous two classes, class III synthases are composed of two subunits, PhaC and PhaE. The ~40 kDa PhaC subunit from *Allochromatium vinosum* has only 24.7% similarity to PhaC from *R. eutropha* [35, 36]. The ~40 kDa PhaE subunit shows no homology to PhaC. Class III synthases from *Allochromatium vinosum* prefer SCL CoA thioesters of (*R*)-3-hydroxy fatty acids of 3-5 carbon atoms. Phylogenetic trees of PhaC or PhaE sequences suggest the synthases found in a number of haloarchaeons belong to a sub-group of class III and possibly result from horizontal gene transfer [37]. The *Haloferax mediterranei* synthase from this subgroup synthesizes poly(3-hydroxybutyrate-co-3-hydroxyvalerate) (PHBV) [37].

3.4) Class IV

Class IV synthases such as those from *Bacillus megaterium* are similar to class III synthases, except the PhaE subunit is replaced with a smaller 20 kDa PhaR subunit; they also prefer SCL CoA thioesters [38]. The class IV synthase from *Bacillus cereus* YB-4 can incorporate 3HHx when grown on longer-chain fatty acids (e.g. palm or soybean oil) whereas the synthase from *B. megaterium* could not [39].

3.5) The genetics of PHA production

PHA synthesis and regulatory genes are often clustered, although such clustering is not strictly conserved. Class I synthases such as *phaC1* from *R. eutropha* typically occur in a *phaCAB* operon with the *phaA* (β-ketothiolase) and *phaB* (acetoacetyl-CoA reductase) genes, which together generate the *(R)*-3-hydroxybutyryl-CoA monomers required for synthesis of PHB; additionally, a *phaR* regulator gene is often located just downstream of the *phaCAB* operon.

Class II synthases such as PhaC1 and PhaC2 from *P. aeruginosa* are typically organized in a *phaC1 - phaZ - phaC2 - phaD* operon*;* PhaZ is a depolymerase, while PhaD is a structural protein. This operon is followed by another transcribed in the opposite direction which encodes the structural and regulatory proteins PhaI and PhaF. Class III synthases are typically encoded as a *phaC-phaE* synthase operon, adjacent to an operon (usually transcribed in the opposite direction) encoding *phaA, phaB,* and a phasin *phaP.* Class IV synthases are less consistently organised, but the two subunits (PhaRC) are typically encoded by a *phaR-phaB-phaC* operon; in *Bacillus* species, this is adjacent to genes encoding the PhaP phasin and PhaQ regulator genes.

4) Polyester synthases: structure & function

4.1) Structural Features

Currently no structural data for polyester synthases is available, although they do contain a conserved functional α/β hydrolase domain that can be threaded onto solved structures **[Figure 2.4.1]** [40, 41]. The class I PHA synthase from *R. eutropha* has been studied in the most

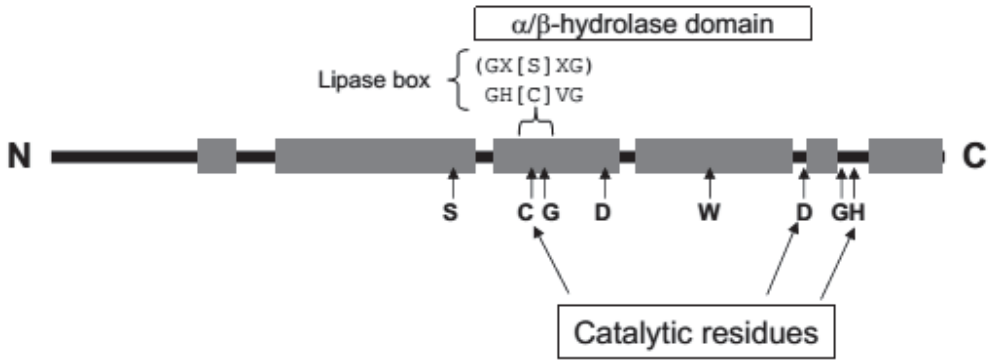

Figure 2.4.1 *Primary structure of the R. eutropha PHA synthase. (Reproduced from Rehm 2007 [111].)*

detail, and the majority of mutagenesis approaches have used the enzyme from this model PHA producer [4]. Mutational analysis of the non-conserved N-terminal region, including deleting the first 100 amino acid residues, indicated it was not essential for synthase activity. However, replacement of residues involved in a putative α-helix (D70-E88) with proline enhanced PHA accumulation [42], suggesting a role for the N-terminus in regulatory protein-protein interactions. The high hydrophobicity of the conserved C-terminal region suggests it may associate with the hydrophobic PHA granule core. Deletions of five and twelve amino acids from the C-terminal region caused inactivation of the synthase, showing this region is essential for activity [43]. Fusion proteins of class I and class II synthases with the fusion point inside the α/β hydrolase fold are not active, confirming the presence of an essential functional domain [43].

Polyester synthases exist in both monomeric and dimeric forms; however, dimerization is strongly induced in the presence of substrate or analogues such as (3-hydroxybutyryl)$_3$-CoA [44]. Dimerization of the PHA synthase from *R. eutropha* reduces enzyme lag phase and increases specific activity [44]. Polyester synthases have been localised to the surface of PHA granules from *R. eutropha* by immunoelectron microscopy and gold-labeled anti-PHA synthase antibodies [45]. The class III enzyme (PhaEC) from *A. vinosum* has also been localised to the granule surface, where it exists as a complex with a native molecular mass of 400 kDa (representing about ten subunits) [46].

4.2) Catalytic reaction mechanism

Griebel and colleagues first noted the inhibition of PHA synthase by the sulfhydral inhibitors *N*-ethylmaleimide and *p*-mercuribenzoate [47]. They proposed a mechanistic model for the

PhaC enzyme that shared features with fatty acid synthesis [48]. Their model for PHA chain elongation suggested two thiol groups from the PHA synthase would be involved in the polymerization reaction. The growing PHA chain would cycle between the two thiol groups as the other was loaded with the next HB monomer.

Initially, the conserved residues cysteine-319 and cysteine-459 from the class I PhaC of *Ralstonia eutropha* were thought to provide the two sulfhydral groups necessary for PHB chain extension. However, site-directed mutagenesis revealed only cysteine-319 was involved in covalent catalysis, whereas cysteine-459 was clearly not required for enzyme activity [49].

In fatty acid synthesis the second thiol is provided by post-translational modification. Therefore, a second thiol group was postulated to become available from the covalent modification of the conserved serine-260 from *R. eutropha* by 4-phosphopantetheine. However, expression of the PHA synthase gene in a β-alanine mutant of *R. eutropha* followed by detection of 4-phosphopantetheinylated protein did not reveal this post-translational modification of PhaC. Nonetheless, site-directed mutagenesis of serine-260 abolishes enzyme activity indicating an important role for this residue [50].

Currently, the active form of PHA synthase is considered to be a homodimer (class I and II) or a multimeric heterodimer (class III and IV). The dimerisation of PhaC suggests that each monomer could provide one of the two necessary thiol groups, allowing the catalytic mechanism to proceed once the dimer is formed **[Figure 2.4.2].** Tryptophan-398 in *P. aeruginosa* is hypothesised to generate a hydrophobic surface which allows for PhaC dimerisation, due to its surface-exposure in threading models [40]. Replacing the highly conserved tryptophan-425 in *R. eutropha* and tryptophan-398 in *P. aeruginosa* with alanine

caused inactivation of the respective synthases, suggesting that dimerisation is indeed necessary for enzyme function [40].

All PHA synthases possess a lipase box-like sequence (G-X-[S/C]-X-G), and structural modelling comparing PhaC to lipases identified conserved residues with a potential role in covalent catalysis. The first enzyme compared to the lipase model was a class III PHA synthase from *Allochromatium vinosum*. Site-directed mutations in each of the conserved residues cysteine-

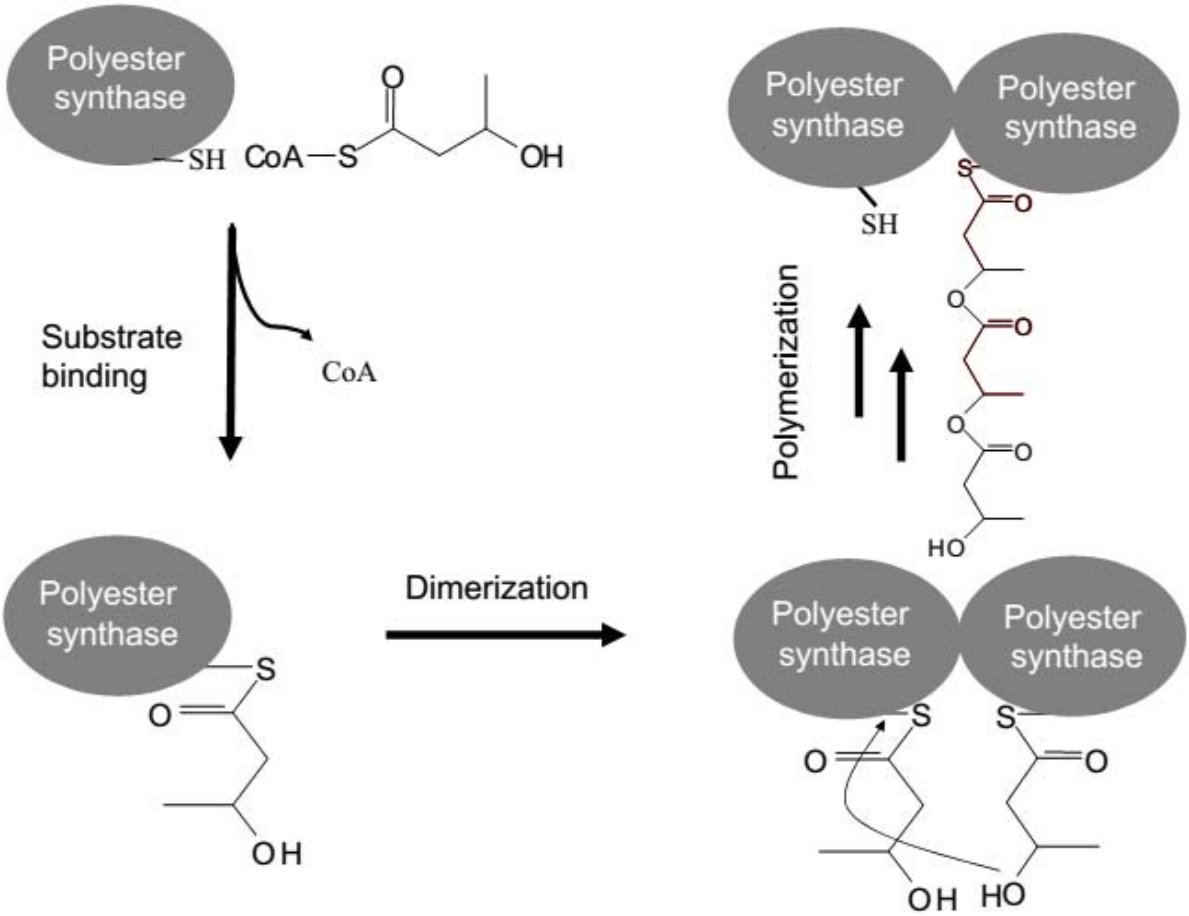

Figure 2.4.2 *Model of the polyester synthase catalytic mechanism. (Reproduced from Rehm 2007 [111].)*

149, histidine-331, and aspartate-302 almost abolished enzyme activity [41]. Thus, these three residues were hypothesised to form the catalytic mechanism, with cysteine-149 as the nucleophile for covalent catalysis and histidine-331 as its general base catalyst. Aspartate-302 appeared to function as a general base catalyst for the substrate, activating the 3-hydroxyl of 3-hydroxybutyryl CoA thioester for nucleophilic attack and allowing formation of the acylated thiolester intermediate. Further support for the role of aspartate-302 in elongation rather than activating cysteine-139 for acylation was provided by the detection of polymeric HB covalently bound only to peptides containing cysteine-139 after a tryptic digest of the mutant synthase (D302A-PhaCPhaE) from *A. vinosum*. Additional *in vivo* experiments using the same mutant synthase resulted in production of very small (<0.05 μm) diameter PHA granules in a *R. eutropha* host compared to the ~0.4 μm granules in the wildtype strain, possibly due to shorter HB polymer lengths [51].

The equivalent amino acid residues cysteine-319, histidine-508, and aspartate-480 from the class I *R. eutropha* PhaC were also subjected to site-directed mutagenesis resulting in greatly diminished enzyme activity, suggesting a similar catalytic mechanism to the class III enzyme [52]. However, the use of a saturated trimer of 3-HB-CoA as an artificial primer of synthesis demonstrated the conserved aspartate-480 was not required for the acylation step in HB polymerisation, while C319-H508 formed the catalytic dyad. Additionally, the class II synthase from *P. aeruginosa* has been examined using epoxide hydrolase from mice as a model [40]. The putative catalytic residues cysteine-296, aspartate-452, histidine-453, and histidine-480 were replaced by site-directed mutagenesis. Mutations to cysteine-296 and aspartate-452 abolished enzyme activity. Interestingly, mutation to histidine-480 which aligns with the conserved base catalyst in α/β hydrolases did not impact *in vivo* enzyme activity and only

reduced *in vitro* activity to 41% of the wildtype. In contrast H453Q strongly reduced both *in vivo* and *in vitro* activity to 24% and 7% of the wildtype respectively, indicating histidine-453 may functionally replace histidine-480 in class II synthases [40]. This study also replaced the active site cysteine-296 with a serine residue and found the synthase remained active, although at a reduced level [40].

Synthesis of PHB has also been suggested to proceed in a manner analogous to some type III polyketide synthases. Rather than needing to bring two thiol groups from different synthase units into a dimer, this model requires only one active site cysteine. The PHB chain is extended by repeated acylation of the same cysteine with a non-covalent binding step necessary for extension of the polymer. To test this model, a class III C149S-PhaEC mutant exhibiting a slowed reaction rate was used to catch non-covalently bound (HB)nCoA (n = 2 or 3) in the process of chain elongation. The model of PHB chain elongation by repeated acylation of cysteine-149 was supported by the detection of (HB)nCoA after rapid initiation and quenching of the reaction [53].

In all structural models the proposed catalytic triad is located adjacent to the enzyme core and the putative active site cysteine is always found within the strand-nucleophile-helix motif common to α/β hydrolases. Overall, the catalytic mechanism of α/β hydrolases, in particular lipases, has provided a useful model for examining the catalytic residues of PHA synthases. The mutational studies of class I-III PHA synthases from *R. eutropha, P. aeruginosa,* and *A. vinosum* respectively have provided strong support in favour of this model. The interfacial activation of lipases at lipid-water interfaces could be analogous to the activation of polyester synthase catalysis at the polyester-water interface of the growing PHA granule. This view is

supported by the increased activity of attached polyester synthase from *R. eutropha* compared to the soluble enzyme [54]. Upon binding of the substrate and extension of the PHA polymer, the soluble polyester synthase converts into an amphipathic molecule [4]. This change leads to self-assembly of the PHA granules with the hydrophobic PHA in the core surrounded by active polyester synthase on the surface.

4.3) Random mutagenesis

Polyester synthases have been subjected to directed evolution experiments to enhance enzyme activity, alter substrate specificity, and change the molecular weight of the PHA product [42, 55-59]. Altering the properties of polyester synthases allows for more efficient production of specific tailor-made biopolyesters.

In vitro and *in vivo* evolution of PHA synthases from *Aeromonas punctata* by random mutagenesis has been performed to identify point mutations which enhance PHA synthase activity [55, 56]. The first approach used PCR-mediated random mutagenesis targeting a limited region of the *A. punctata* FA440 *phaC* gene. This synthase produces a random co-polyester of 3-hydroxybutyrate and 3-hydroxyhexanoate [P(3HB-*co*-3HHx)], which has favourable toughness and flexibility compared to PHB homopolyester. Two mutations, N149S and D171G, were found to exhibit a 56% and 21% increase in activity towards 3HB-CoA, respectively. *In vivo* this increase in specific activity corresponded to an enhanced accumulation of the random co-polyester by 6.5 fold and 3 fold, respectively. Interestingly, both mutants showed an increase in the 3HHx fraction of the polymer -- up to 18% and 16% respectively compared to the wild-type (10%) [56]. Neither of these mutations is found in conserved regions of the *phaC* gene. The synergistic effect of both mutations was examined

by expressing a double mutant (N149S, D171G) in *R. eutropha*. The mutant showed enhanced incorporation (18.5%) of longer 3-hydroxyalkanoate monomers when octanoate was used as a carbon source and a very high molecular weight (M_w = 3.68 x 10^4) of P(3HB) homopolymer when grown on a fructose carbon source [59].

A second approach used the *E. coli* XL1-Red mutator strain to generate *in vivo* random mutants of the PHA synthase gene from *A. punctata*. Four mutants which displayed enhanced *in vivo* and *in vitro* activity were selected from the 200,000 mutants generated. The single mutation F518I showed a five-fold increase in PHA synthase activity but led to only a 20% increase in PHA accumulation compared to the wildtype. A second mutation, V214G, displayed a two-fold increase in specific activity but only a 7% increase in PHA accumulation [55]. All mutants synthesised PHA with increased molecular weight averages, but the molar fractions of PHA monomers were not significantly affected.

Improved class II synthases have also been achieved by random mutagenesis. *In vitro* evolution of *Pseudomonas* sp. 61–3 PHA synthase I identified E130D as a positive mutant with ten-fold higher accumulation of PHB in *E. coli* harbouring the mutant PHA synthase compared to 0.1 weight % for the wildtype synthase. Additionally, *in vitro* activity tests revealed the mutant PhaC had a higher activity towards various 3-hydroxyacyl-CoAs of up to ten carbons in length [60]. Another mutation (S477R) led to increased average molecular weights of PHB homopolymers -- up to six-fold over the wildtype enzyme -- and a substrate preference shift towards smaller monomer units [57]. Combinations of beneficial mutations such as E130D with S325T, S325C, and Q481L resulted in a synergistic effect on *in vivo* PHA production, *in vitro* enzyme activity, and substrate specificity [57, 60].

Saturation mutagenesis of the PHA synthase from *R. eutropha* was carried out on the glycine-4 residue. The N-terminal mutation G4D increased PhaC levels *in vivo,* thereby enhancing the PHB content of cells by 23 percentage points [58]. Further mutagenesis to a putative amphipathic α-helix region (D70-E88) enhanced activity of the synthase *in vitro*. The mutations Y75P and A81P produced an activity of 137% and 105% of the wildtype respectively. The double mutant Y75P/A81P had a synergetic effect, enhancing *in vitro* synthase activity to 162% of the wildtype using a total cellular protein extract [42]. The authors suggest disruption to the α-helix by proline may impair regulatory protein-protein interactions with the PHA synthase.

Although many beneficial mutations to PHA synthases of various classes have been characterised, the functional roles of the mutated residues have yet to be determined. Only mutations to the PHA synthase from *R. eutropha* have a suggested mechanism of action [42, 58], demonstrating the importance of understanding protein structure. Ultimately, the resolution of three-dimensional structure will be a crucial step in understanding these structure-function relationships.

4.4) Substrate specificity

PHA synthases have different substrate specificities which determine the monomer composition of the polyester produced; this in turn determines the properties of the resulting material. Altering the substrate specificity of the enzyme is an important tool for the production of useful tailor-made biopolyesters. The substrate specificities of polyester synthases from *R. eutropha* and *A. vinosum* have been studied *in vitro* using analogs of PHB

with varying chain lengths, branching, hydroxyl group chain position, and thioesters [61]. These polyester synthases were seen to be highly specific *in vitro*.

Metabolic engineering to provide a range of 3-hydroxy fatty acid CoA thioesters has been used to study the *in vivo* substrate range of PHA synthases in recombinant *E. coli* [62-65]. In contrast to the specific *in vitro* specificity, *in vivo* the class I PHA synthase from *R. eutropha* displayed a broad substrate specificity, even accepting MCL 3-hydroxy fatty acid CoA esters as substrates [62, 63]. It has also been shown that growing *R. eutropha* on 3-mercaptopropionic acid as the carbon source produced a co-polymer of 3-hydroxybutyric acid and 3-mercaptopropionic acid linked by thioester bonds [66]. Additionally, the increasing variety of PHA monomers detected in bacterially synthesized polyesters is further evidence that PHA synthases possess an extremely broad substrate specificity [4].

Lastly, mutagenesis has been used to alter the substrate specificity of PHA synthases. Initially, the substrate specificity of class II PhaC from *P. putida* was altered by localized semi random mutagenesis [67]. Later, alanine-510 of the *R. eutropha* polyester synthase was found to have a role in substrate specificity [68], and altering the serine-477 residue of the *Pseudomonas* sp. 61–3 PHA synthase enhanced its incorporation of short-chain length 3HA-CoA [57]. Additionally, a chimeric synthase with 26% of the N-terminal region from *Aeromonas caviae* and 74% of the C-terminal region from *R. eutropha* maintained the advantageous properties of both enzymes: broad substrate specificity and high enzyme activity, respectively. The chimeric synthase accumulated a higher amount of PHA (50 wt %) which consisted of 2 mol % 3-hydroxyhexanoate [69].

5) *In vivo* substrate provision for polyester synthases

Formation of PHA inclusions is initiated by provision of 3-hydroxyacyl CoA thioesters to a PHA synthase. Upon uptake of a suitable carbon source, anabolic and/or catabolic reactions convert the carbon compound into a hydroxyacyl CoA thioester **[Figure 2.5]**. The synthase uses these thioesters as substrates, catalyzing formation of the PHA polyester with concomitant release of CoA [70, 71]. Understanding the pathways that lead to biosynthesis of the CoA thioester precursors enables metabolic engineering of bacteria to produce tailor-made PHAs. Provision of different carbon sources affects the type and composition of PHA, resulting in polyesters with varied properties including tensile strength and melting point [72]. However, *in vivo* substrate specificity can only be determined experimentally by analysing the chemical composition of PHAs produced through cultivation on various carbon sources. One such screen observed variation in the composition of PHAs derived from 10 different carbon sources using the *Thiocapsa pfennigii* PHA synthase expressed recombinantly in *P. putida* [73].

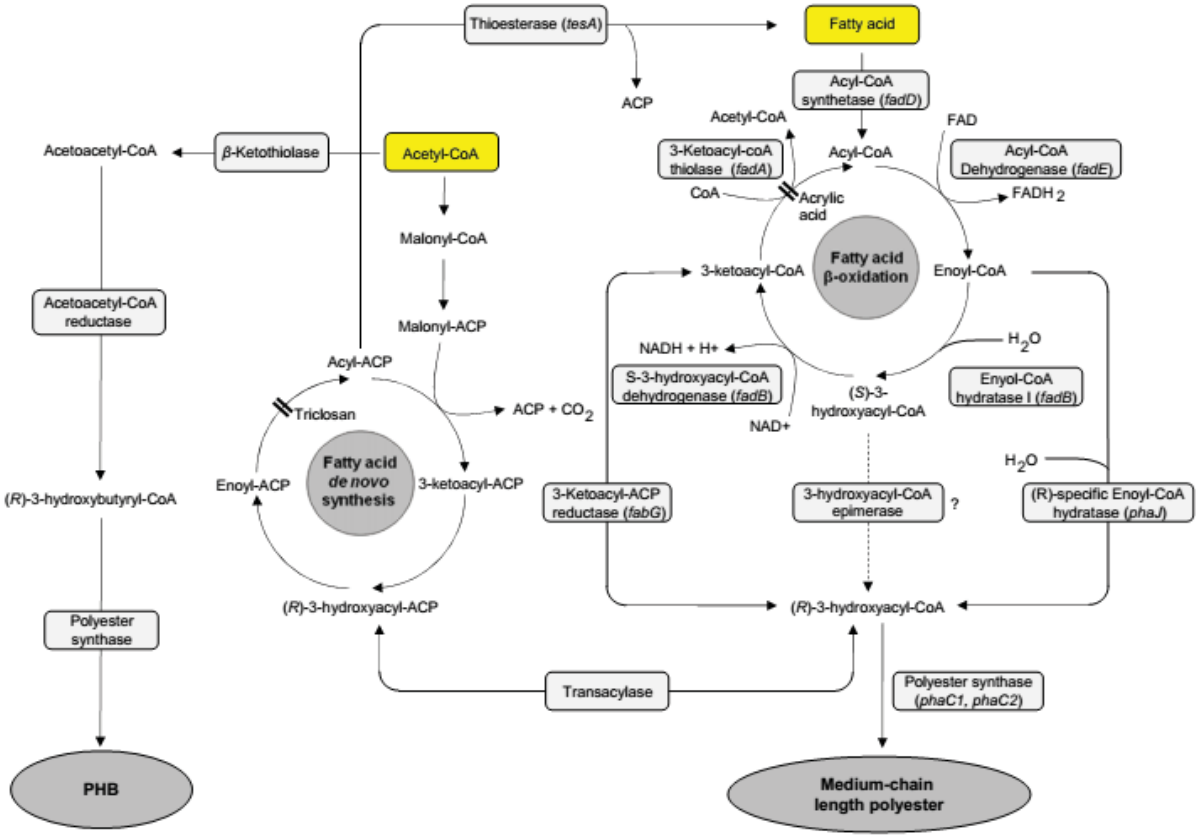

Figure 2.5 *Metabolic pathways of PHA production. (Modified from Rehm 2007 [111].)*

5.1) Short-chain-length polyester biosynthesis

Production of PHAscl of 3-5 carbon atoms is best represented by *R. eutropha's* synthesis of poly-3-hydroxybutyrate (P3HB). In *R. eutropha,* generation of thioester precursors from glucose is initiated by the enzyme PhaA, a β-ketothiolase which catalyzes the condensation of two acetyl-CoA molecules from the glycolysis pathway into acetoacetyl-CoA. The NADPH-dependent acetoacetyl-CoA reductase PhaB then reduces the acetoacetyl-CoA molecules to *(R)*-3-hydroxybutyrl-CoA, which the PHA synthase uses to produce poly-3-hydroxybutyrate (P3HB) [74-77]. However, use of octanoate and dodecanoate fatty acids as a carbon source

instead of glucose results in alternative PHAs composed of 3-hydroxyoctanoate (3HO) and 3-hydroxydodecanoate (3HDD) in addition to P3HB [62].

5.2) Medium-chain-length polyester biosynthesis

In pseudomonads, synthesis of PHA_{MCL} of 6-14 carbon atoms involves the fatty acid *de novo* biosynthesis pathway. *P. putida* encodes the (R)-3-hydroxydecanoyl-ACP:CoA transacylase enzyme PhaG, which links fatty acid *de novo* biosynthesis to PHA biosynthesis. PhaG is only required for PHA synthesis when gluconate or other non-related carbon sources are provided [78]. Such carbon sources are oxidized to acetyl-CoA and enter the fatty acid *de novo* biosynthesis pathway, but PhaG diverts intermediates of the pathway toward PHA biosynthesis. *P. aeruginosa*'s PHA biosynthetic pathways are more diverse, possibly due to the presence of the protein Rh1A, which plays a role in surfactant synthesis and PHA production. Synthesis of rhamnolipids and PHA is closely related in *P. aeruginosa,* as fatty acid derivatives are used as substrates in both pathways [79]. However, it was shown that PhaC can only use CoA fatty acids as substrates, and thus activity of the PhaG transacylase is required for PHA_{MCL} production from sugar carbon sources [80]. The sigma factor RpoN also appears to be involved in PHA biosynthesis gene regulation [81, 82].

6) The fatty acid β-oxidation pathway provides precursors from fatty acids

Fatty acid *β*-oxidation is a general metabolic pathway in eukaryotes and prokaryotes involved in the catabolism of fatty acids. In *E. coli*, genes involved in *β*-oxidation fatty acid degradation are encoded by the *fad* operon, which is negatively regulated by *fadR*.

Free fatty acids enter the *β*-oxidation pathway upon ligation to CoA, generating acyl-CoA thioesters; this process is mediated by the acyl-CoA synthetase FadD [83]. The 4-step fatty acid *β*-oxidation cycle generates various CoA thioester intermediates and ultimately produces acetyl-CoA **[Figure 2.5]**.

In the first step, the acyl-CoA thioesters produced by FadD are oxidised to enoyl-CoA by a FAD-dependent reaction with acyl-CoA dehydrogenase FadE; this is reportedly the rate-limiting step in the pathway [84]. The remaining 3 steps in the pathway are catalysed by the multienzyme complex FadBA, which is composed of two subunits in $\alpha_2\beta_2$ quaternary structure [85, 86].

The FadBA multienzyme complex encoded by the *fadBA* operon is thought to possess five enzymatic activities: enoyl-CoA hydratase (*fadB*), NADH-dependent (S)-3-hydroxyacyl-CoA dehydrogenase (*fadB*), *cis*-Δ_3-*trans*-Δ_2-enoyl-CoA isomerase, 3-hydroxyacyl-CoA epimerase and 3-ketoacyl-CoA thiolase (*fadA*) [87]. The crystal structure of the *fadAB* homolog *foaAB* from *Pseudomonas fragi* revealed that the α-dimer alone exhibits 2-enoyl-CoA hydratase and 3-hydroxyacyl-CoA dehydrogenase activity, involved in the catalytic conversion of enoyl-CoA and (*S*)-hydroxyacyl-CoA respectively. The 3-ketoacyl-CoA thiolase activity is mediated by contact between the α and β subunits, and is involved in the catalytic conversion of 3-ketoacyl-CoA to acetyl-CoA [88].

A relationship between *β*-oxidation and PHA_{MCL} synthesis is well known and extensively described in literature. Analysis of the PHA_{MCL} co-monomer composition from *P. putida* grown on fatty acids with ^{13}C-labeled substrates indicated the majority of the co-monomer was generated from *β*-oxidation [89]. Additionally, genes encoding enzymes involved in *β*-

oxidation and PHA$_{MCL}$ biosynthesis in *P. putida* KT2440 were both highly expressed when grown on fatty acid [90].

Acyl-CoA intermediates synthesised by the FadBA multienzyme complex, namely enoyl-CoA, (*S*)-3-hydroxyacyl-CoA and 3-ketoacyl-CoA, serve as major precursors for PHA$_{MCL}$ synthesis by class-II PHA synthases. However, due to the specificity of PHA synthases for (*R*)-3-hydroxyacyl-CoA thioesters, these intermediates cannot directly be utilised by the polyester synthase and must be converted to their (*R*)-3-hydroxyacyl-CoA moiety.

Enzymes involved in the conversion of *β*-oxidation intermediates have been extensively cloned and characterised in both PHA-producing and non- PHA-producing organisms. These enzymes include the (*R*)-specific enoyl-CoA hydratase (PhaJ) and the 3-ketoacyl-ACP reductase (FabG), involved in the conversion of enoyl-CoA and 3-ketoacyl-CoA respectively [91, 92]. The putative 3-hydroxyacyl-CoA epimerase encoded by the *fadBA* operon is thought to link the conversion of (*S*)-3-hydroxyacyl-CoA into (*R*)-3-hydroxyacyl-CoA; however, this has yet to be fully elucidated [87]. Disruption of the *β*-oxidation pathway and/or amplification of genes involved with the conversion of *β*-oxidation intermediates have been employed to study the flux of carbon towards PHA synthesis [32, 93, 94]. For example, disruption of *fadA* in *P. putida* KCTC1639 increased the pool of available *β*-oxidation intermediates which could be channelled towards PHA synthesis, leading to an increase in PHA$_{MCL}$ containing a higher percentage of longer-chain-length fatty acids [95].

6.1) Alternative β-oxidation fatty acid enzymes

In eukaryotes, multiple enzymes exist for each step of the *β*-oxidation pathway, and different sets degrade short, medium and long chain fatty acids [96]. Similarly, some prokaryotes encode multiple enzyme sets. For example, *P. putida* has several sets of *fad* genes, contributing to its metabolic diversity [97]. Likewise, the genome of *R. eutropha* H16 contains many genes potentially involved in *β*-oxidation, including 50 enoyl-CoA hydratases and 46 acyl-CoA dehydrogenases [96].

In *E. coli*, several *β*-oxidation pathway genes have been identified and characterised in literature. The *E. coli* genes *yfcX* and *yfcY* show significant homology to *fadB* and *fadA* respectively, and probably encode an alternative *β*-oxidation pathway utilized under anaerobic conditions [91]. YfcX can substitute for FadB in the PHA_{MCL} production pathway, and displays multienzyme activity similar to FadB's hydratase and dehydrogenase activity [98].

In addition to YfcX, 5 additional homologs *paaG, paaF, bhbD, sceH* and *ydbU* displaying high homology to *fadB* have been identified in the *E. coli* genome and have been suggested to play a role in PHA_{MCL} biosynthesis in a *fadB* mutant background [98]. MaoC from *E. coli* is an enoyl-CoA hydratase showing 34% protein sequence homology to the *P. aeruginosa* (*R*)-specific hydratase PhaJ1. MaoC is suggested to provide a link between fatty acid *β*-oxidation and PHA synthesis in *E. coli* by the catalytic conversion of enoyl-CoA in a *fadB* mutant. MaoC was required to channel (*R*)-3-hydroxyacyl-CoA into PHA biosynthesis, as PHA_{MCL} accumulation was severely affected in a *maoC* knockout mutant. This was further confirmed by plasmid based complementation with MaoC [99].

6.2) Inhibition of fatty acid β-oxidation

In both PHA-negative and PHA-producing organisms, FadB and/or FadA defective strains have been extensively used to study the link between the *β*-oxidation pathway and PHA synthesis. Disruption of the *β*-oxidation pathway results in a pool of *β*-oxidation intermediates that can be shunted towards PHA biosynthesis by specific hydratases, epimerases, and reductases. For example, production of PHA$_{MCL}$ in PHA-negative *E. coli* was successfully established by heterologously expressing a class-II PHA synthase in a *β*-oxidation pathway defective background [98].

FadB and/or FadA defective strains are normally created by a genetic approach; however, chemical inhibition with acrylic acid or Cerulenin has also been effectively employed [91]. Acrylic acid has been proven to be a powerful tool for disruption of the *β*-oxidation pathway by inhibiting FadA. Acrylic acid exposure of recombinant *P. fragi* or PHA-negative *R. eutropha* expressing *P. aeruginosa phaC1* results in an increase in PHA$_{MCL}$ accumulation [87]. Chemical inhibition of FadB with Cerulenin is also possible in recombinant *E. coli* [91].

Disruption of the *β*-oxidation pathway in PHA-producing organisms leads to synthesis of PHA$_{MCL}$ consisting largely of long-chain-length fatty acids. *P. putida* KT2440 typically produces PHA$_{MCL}$ consisting of 3-hydroxydecanoate (HHx), 3-hydroxyoctanoate (HO), 3-hydroxydecanoate (HD) and 3-hydroxydodecanoate (HDD) monomers when grown on dodecanoate as a sole carbon source, in which HHD will represent a small fraction of the overall composition. A significant shift in co-monomer composition towards the longer-chain-length fatty acid HHD was seen in a *β*-oxidation- impaired *P. putida* KT2440 *fadBA* mutant, validating the role of *fadA* and *fadB* in *β*-oxidation for the degradation of fatty acids [100].

Similar results were observed in a *P. putida* KCTC1639 *fadA* knockout [95]. Another study in *P. putida* KT2440 knockout mutants grown on dodecanoate resulted in co-monomers consisting of HD and HDD; it was suggested that these may be related to a secondary *β*-oxidation pathway or unknown isozymes or epimerases [101].

Disruption of *β*-oxidation regulator genes can also cause accumulation of PHA$_{MCL}$. The *fadR* repressor protein in *E. coli* regulates *fadBA* genes and some *fadBA* homologs such as *yfcXY*, blocking their transcription during growth on fatty acids [91]. Disruption of *fadR* results in the constitutive expression of *fad* genes, leading to a strong increase in accumulation of PHA$_{MCL}$ [65].

6.3) Putative 3-Hydroxyacyl-CoA epimerase

A 3-hydroxyacyl-CoA epimerase enzyme is thought to link the *β*-oxidation and PHA synthesis pathways by converting the *β*-oxidation intermediate (*S*)-3-hydroxyacyl-CoA into its corresponding *(R)*-enantiomer. However, a specific epimerase involved in PHA$_{MCL}$ biosynthesis has not been identified, yet. The multienzyme complex FadBA has epimerase activity *in vitro* [86] and may fill this role. However, a study investigating the putative epimerase function of recombinant *P. oleovorans* FadBA failed to demonstrate epimerase function *in vivo* [87]. Altogether, the source of 3-hydroxyacl-CoA epimerase activity linking the β-oxidation and PHA synthesis pathways remains unclear.

6.4) (R)-specific enoyl-CoA hydratases

The conversion of enoyl-CoA to (*R*)-3-hydroxyacyl-CoA is catalyzed by (*R*)-specific enoyl-CoA hydratases. A monofunctional (*R*)-specific enoyl-CoA hydratase was first identified in *A. caviae*

FA440 [92]. Since then further hydratases have been identified in other PHA producing organisms such as *P. aeruginosa, P. oleovorans, P. putida, R. rubrum,* and *R. eutropha* [102]. Homologous sequences have also been identified and characterised in non-PHA-producing organisms, such as MaoC in *E. coli* [99, 102].

In *P. aeruginosa,* four (*R*)-specific enoyl-CoA hydratases (PhaJ1 - PhaJ4) have been identified and characterised. All four PhaJs can supply (*R*)-3HA-CoA monomers for PHA synthesis when heterologously expressed with PhaC in *E. coli* [92]. PhaJ1 demonstrates substrate specificity towards short-chain-length enoyl-CoAs of C4-C6, while PhaJ2-PhaJ4 exhibit a longer chain specificity of C6-C12 [92].

PhaJ, like many other (*R*)-specific enoyl CoA hydratases, possesses a highly conserved hydratase 2 domain. The crystal structure of the *A. caviae* (*R*)-specific enoyl CoA hydratase revealed that the enzyme is a homodimer, with each monomer composed of five antiparallel β-sheets and five α-helices forming a "hot dog" fold [103, 104]. A binding pocket of highly conserved residues determines its specificity for C4-C6 substrates; however this specificity can be altered, as demonstrated by site directed mutagenesis [104]. Many recently identified *PhaJ* homologs also contain an MaoC-like domain (pfam01575) [102].

6.5) β-ketoacyl-CoA reductase

FabG from *P. aeruginosa* is an NADH-dependent *β*-ketoacyl-CoA reductase which converts the last *β*-oxidation intermediate 3-ketoacyl-CoA into (*R)*-3-hydroxyacyl-CoA. It has been extensively studied in recombinant *E. coli* carrying the class II PHA synthase PhaC1 from *P. aeruginosa*. The function of FabG in *β*-oxidation was demonstrated by heterologous

expression of *fab*G in *E. coli fabB* and *fabA* knockout mutants. Expression of FabG in an *E. coli fadR fadB* mutant did not significantly increase accumulation of PHA$_{MCL}$ when grown on fatty acids as a sole carbon source; this was expected, as a *fabB* knockout would have disrupted the pathway generating the 3-ketoacyl-CoA substrate for FabG [32]. However, expression in a fadR *fadA* mutant had the opposite effect: the *fadA* knockout resulted in a larger pool of 3-ketoacyl-CoA for FabG to convert to (*R)*-3-hydroxyacyl-CoA, and a significant increase in PHA$_{MCL}$ accumulation occurred [32].

More recently, overexpression of *fadG* in *P. putida* KCTC1639 was found to reduce PHA accumulation, which is in contrast to previous results. This lower PHA accumulation was possibly due to FabG's ability to catalyse the reverse reaction of (*R)*-3-hydroxyacyl-CoA to 3-ketoacyl-CoA [105].

6.6) Thioesterase

Accumulation of PHA$_{MCL}$ in recombinant *E. coli* grown on fatty acids has been extensively demonstrated. However, PHA$_{MCL}$ is not able to accumulate when sugars are the sole carbon source [106]. Thioesterases play an important role in PHA$_{MCL}$ production when carbon sources unrelated to the fatty-acid *β*-oxidation pathway are used.

The thiolase protein family contains two classes: degradative and synthetic thiolases. Degradative thiolases convert ketoacyl-CoA into acyl-CoA in the *β*-oxidation pathway. Synthetic thiolases catalyze the conversion of the fatty acid *de* novo biosynthesis intermediate product acyl-ACP into its corresponding fatty acid. Synthetic thiolases thus provide a direct link between fatty acid *de novo* biosynthesis and *β*-oxidation [106, 107]. Overexpression of the

native thioesterase-I gene *tesA* in a *β*-oxidation defective *fadR fadB E. coli* mutant harbouring *P. oleovorans phaC1* was capable of accumulating PHA_{MCL} when grown on gluconate with 3-hydroxyoctanoate as the main monomer constituent [91, 106]. In addition, an acyl-ACP thioesterase from the plant *Umbellularia californica* can mediate PHA_{MCL} production from gluconate in recombinant *E. coli* [91].

7) Polyester inclusions: self-assembly & structure

7.1 Self-assembly of polyester particles

Formation of PHA granules both *in vivo* and *in vitro* is mediated by the PHA synthase, which catalyzes the synthesis of water-soluble (*R*)-3-hydroxyacyl-CoA monomers into water-insoluble high molecular weight polyesters. Throughout this synthesis process, the PHA synthase remains covalently attached to the growing polyester chain. Substrate is continually incorporated until metabolic or spatial constraints terminate polymerization [108]. Though the exact mechanism of PHA granule formation remains unknown, to date two models have been proposed: the micelle model, and the budding model.

7.1a Micelle model

The micelle model is supported by the formation of PHA granules in vitro using only purified PHA synthase and substrate [54]. In this model, the amphipathic nature of the synthase as it forms the hydrophobic polyester allows self-aggregation into a micelle-like structure [109]. According to this model, nascent PHA granules formed *in vivo* are further coated with constituents other than the PHA synthase [110].

7.1b Budding model

The budding model considers the presence of the lipid membrane that has been observed surrounding isolated PHA granules. In this model, soluble PHA synthase exists close to the inner cell membrane, and the polymerization reaction occurs in the intra-membrane space, where the elongated PHA chains accumulate into a granule surrounded by a phospholipid monolayer, which eventually buds from the membrane into the cytoplasm [110, 111] **[Figure 2.6]**. However, since experimental evidence for the existence of a lipid layer *in vivo* is still lacking, it is conceivable that the lipids are a contaminant from the process of isolating the hydrophobic granules from lysed cells.

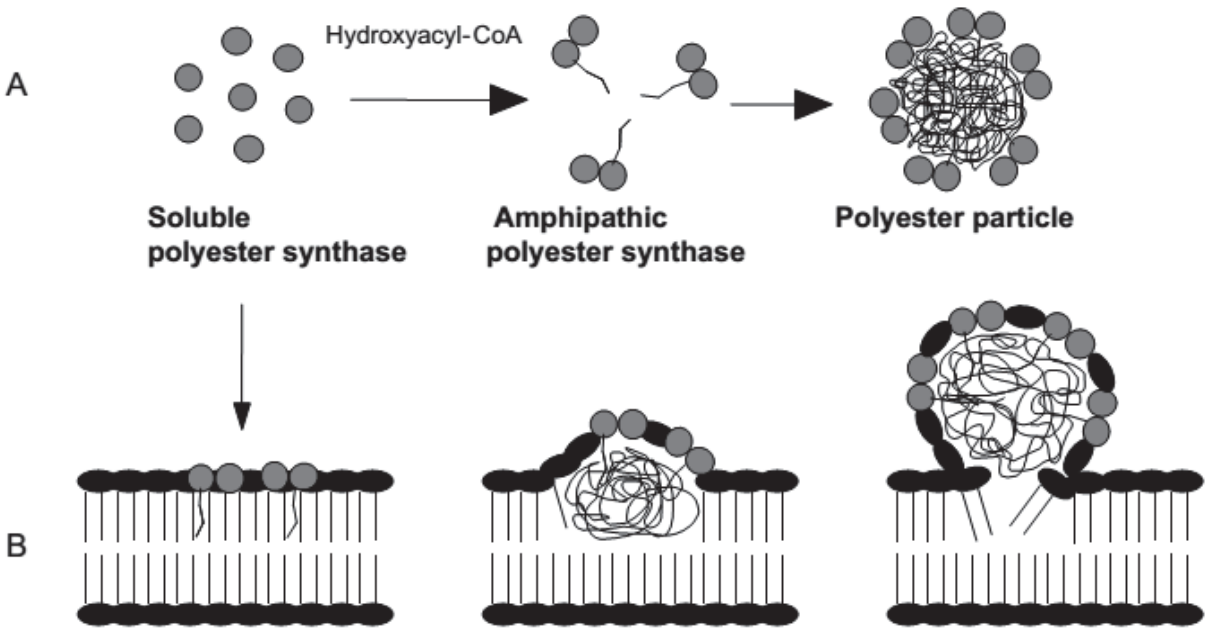

***Figure* 2.6** *Models for polyester bead self-assembly. (a) Micelle model and (b) Budding model. (Reproduced from Rehm 2007 [111].)*

7.1c Location of Granule Formation

The primary evidence for the budding model of PHA inclusion formation is the observation of granules forming at cell poles. Jendorssek *et al.* examined early-stage PHA granule distribution in different strains using transmission electron microscopy (TEM) and confocal laser scanning fluorescence microscopy (CLSM) of cells stained with the fluorescent lipophilic dye Nile Red, or using CLSM coupled with fluorescence from a phasin-EGFP fusion. These experiments showed that the granules were located close to the cytoplasmic membrane, at or near the cell poles [112, 113]. Independently, Peters and Rehm demonstrated that newly emerging PHA granules formed at the cell poles via fluorescence microscopy (FM) using a PHA synthase-GFP fusion [114].

However, Tian *et al.* observed via TEM of *R. eutropha* H16 cells that newly emerging granules arose only from the center of the cell, at unknown dark-staining “mediation elements”, which might serve as scaffolding initiation sites for PHB granule formation [115]. Mumtaz *et al.* also observed centrally-located, dark staining mediation elements at early-stage PHBV inclusion formation in *Comamonas sp.* EB172 [116].

Recent experiments with *Pseudomonas putida* KT2442 showed the nucleoid-associated phasin protein PhaF drives intracellular segregation of PHA granules, ensuring their equal distribution among daughter cells [117]. Later, Pfeiffer *et al.* discovered a similar phenomenon in *R. eutropha* H16: coordination between PhaM, the phasin PhaP5, and the PHB synthase PhaC1 determines the number, size, subcellular localization, and distribution of PHB granules to daughter cells [118].

Taken together, along with the finding that PHA granule location at cell poles was dependent on nucleoid structure in recombinant *E coli* [114], these studies suggest that nucleoid structures may be the "central mediation elements" to which PHA granules are anchored via phasin or phasin-like proteins. However, this anchoring is unnecessary for the initiation of PHA granule assembly, as granules can form not only in recombinant host strains lacking phasin proteins, but also in *in vitro* systems containing only PHA synthase and substrate [54].

7.2 Structure of PHA granules and the granule associated proteins

PHA granules consist of a hydrophobic polyester core coated with proteins and lipids. (However, as discussed above, the presence of lipids in native granules is currently unclear; for example, membrane composition and presence varied with PHA types, strains, and imaging approaches [119].) It has been reported that water molecules exist in the PHA core *in vivo*, acting as plasticizers to prevent crystallization [120]. Major constituent proteins have been identified and designated to four categories: PHA synthases, depolymerases, phasins, and regulatory proteins.

7.2.1 Depolymerases

The depolymerases attached to PHA granules are intracellular enzymes responsible for PHA degradation via thiolysis [121]. Studies of PHA depolymerases are limited, but in *R. eutropha* several have been discovered and are designated PhaZ1-PhaZ [122, 123]. Presence of the PhaZ1 depolymerase on the surface of native PHA granules was demonstrated by Western blot with anti-PhaZ1 antibodies [124]. Another granule-associated protein, the 3-hydroxybutyrate oligomer hydrolase PhaY, is involved in depolymerisation [125].

7.2.2 Phasins

Phasins are low-molecular-weight proteins ranging from 11-25 kDa, and are the most abundantly produced granule-associated proteins, representing as much as 5% of total cellular protein [126, 127]. The four phasin homologs identified in *R. eutropha* are designated *phaP1* – *phaP4* [124]. PhaP1 is the most extensively characterised phasin protein and is known to form a triangular trimer [128].

Phasins are non-covalently associated with PHA granules through hydrophobic interactions with the polyester core and are nonessential for PHA accumulation. However, gene deletion experiments in *R. eutropha* showed absence of phasin lowers the rate of PHB production, reducing yield up to 50% compared to wild-type [129]. Phasins appear to play a role in controlling granule size and number, as cells defective in phasin production tend form a single large bead which occupies most cell space, rather than many small granules as seen in wild-type cells [126]. Phasins in *P. putida* KT2442 and *R. eutropha* H16 have also been implicated in localizing PHA granules to the nucleoid, thus mediating distribution of granules among daughter cells [117, 118].

7.2.3 Regulatory proteins

According to mutagenesis studies performed in *R. eutropha*, both granule synthesis and phasin (PhaP) production are tightly controlled by the transcriptional regulator PhaR [129]. Experiments in *R. eutropha* and *P. denitrificans* suggest the following autoregulation model. Under non-PHA accumulating conditions, cytoplasmic PhaR binds to the *phaP* promoter and inhibits its transcription. However, once PHA accumulation begins, PhaR binds to the hydrophobic surfaces of newly formed PHA granules, causing the cytoplasmic concentration of

PhaR to drop. The *phaP* gene is thus derepressed, and PhaP protein begins to accumulate on the PHA granules. After the granules have reached maximum size, their surface is completely covered with PhaP phasins, preventing additional binding of PhaR. This results in an increase of cytoplasmic PhaR, which binds to the *phaP* promoter region and prevents transcription [108, 129, 130].

PhaR and other regulatory proteins bind non-covalently to the PHA granules [131]. It has been recently suggested PhaR may also play a role in other metabolic pathways, acting as a global PHA-repressor [108]. Other bead-associated proteins with regulatory functions have also been reported, such as PhaF from pseudomonads [131].

8) Production of tailor-made functionalized biopolyester nanoparticles

The properties of biodegradability, biocompatibility, and production from renewable carbon sources make PHA a desirable alternative to petrochemical-based plastics. Imperial Chemical Industries (ICI) first investigated *Azotobacter sp., Methylobacterium sp.* and *Ralstonia eutropha* as PHB production strains in the 1980s [132, 133]. High yields and low substrate cost led to commercial use of *R. eutropha* to produce "Biopol" for shampoo bottles, films, coatings and packaging materials [133]. In the quest for cheaper production and varied material properties, PHA biosynthesis genes have been cloned and expressed in alternative hosts such as *E. coli* and *Pseudomonas sp.* bacteria [76, 77, 134], *Arabidopsis thaliana* plants [26], *Spodopter frugiperda* insect cells [135], and *Saccharomyces cerevisiae* yeasts [136]. This expanded commercial interest led to an increased range of products and applications [137]

Isolation of PHA from host cells involves lysing the biomass, filtering the cell lysate to remove cellular debris, and precipitating the PHA with cold methanol or ethanol. PHA_{MCL} is soluble in acetone, allowing separation of PHA_{MCL} and PHA_{SCL} if required [138]. Cell lysis typically involves either enzymes such as lysozyme, or harsh solvents such as chloroform or methylene chloride; both methods can be used together to improve purity [139-141]. However, the aggressive chemicals used can cause polyester and protein degradation, and use of solvents can generate high production costs. Therefore the method chosen will depend on the purity and properties required of the end-product.

Despite much effort to develop economical large-scale production, PHAs are still more expensive to produce than oil-based plastics. Therefore, use of PHAs is primarily limited to specialty areas requiring their unique properties. For example, the biodegradability and biocompatibility of PHAs led to their use in a wide-range of medical applications such as cardiovascular patches and stents, bone and tissue scaffolds, and drug delivery via implants, tablets, and microparticles [142, 143]. In 2007 the FDA approved suture material made of PH4B (TephaFLEX® Absorbable Suture) [144] and recently PHB polymers have been used for regeneration of nerve cells [145, 146].

One interesting feature of PHA is its natural production as nano-/micro-scale spherical granules. Nano-/micro-particles have a wide-range of applications in molecular biology and medicine, including drug and gene delivery, fluorescent labelling, separation of biological molecules and cells, and tissue engineering [147]. Particles/beads can be made from a wide range of materials, including proteins, polymers, and inorganic compounds [148]. Proteins or chemicals can be incorporated into the particle to enable different functionalities, such as a

drug core with a polymer coating for slow release properties [17, 143, 149]. The production of bioseparation resins consisting of recombinant proteins chemically conjugated to synthesized polymer beads is a multi-billion-dollar industry for biomedical research and pharmaceutical production.

In most cases, production of functionalized polymeric particles requires a minimum three-step process: 1) the polymer must be produced and purified, 2) the active ingredient, often a protein, must be produced and purified, and 3) the two components must be assembled, usually via chemical crosslinking or emulsification. Each of these processes can be costly, prone to variability, and require use and removal of toxic agents.

Recently, a method was developed that exploits the natural process of PHA granule formation to produce functionalized nano-/micro-beads. Genetic fusions of target proteins to PHA-associated proteins such as phasins or synthases result in PHA particles naturally displaying the target protein on their surface **[Figure 2.8.1]**. This *in vivo* method for synthesizing functionalized particles has the clear advantage of one-step production, as the PHA beads and functional proteins are produced and crosslinked together in the same cell. However, the purification process for these beads needs to be gentler than the current commercial PHA extraction process to retain functionality [150-152]. The vast range of fusion proteins that can be produced in this way creates numerous applications for these PHA particles **[Figure 2.8.2]**. Some of these applications are discussed below.

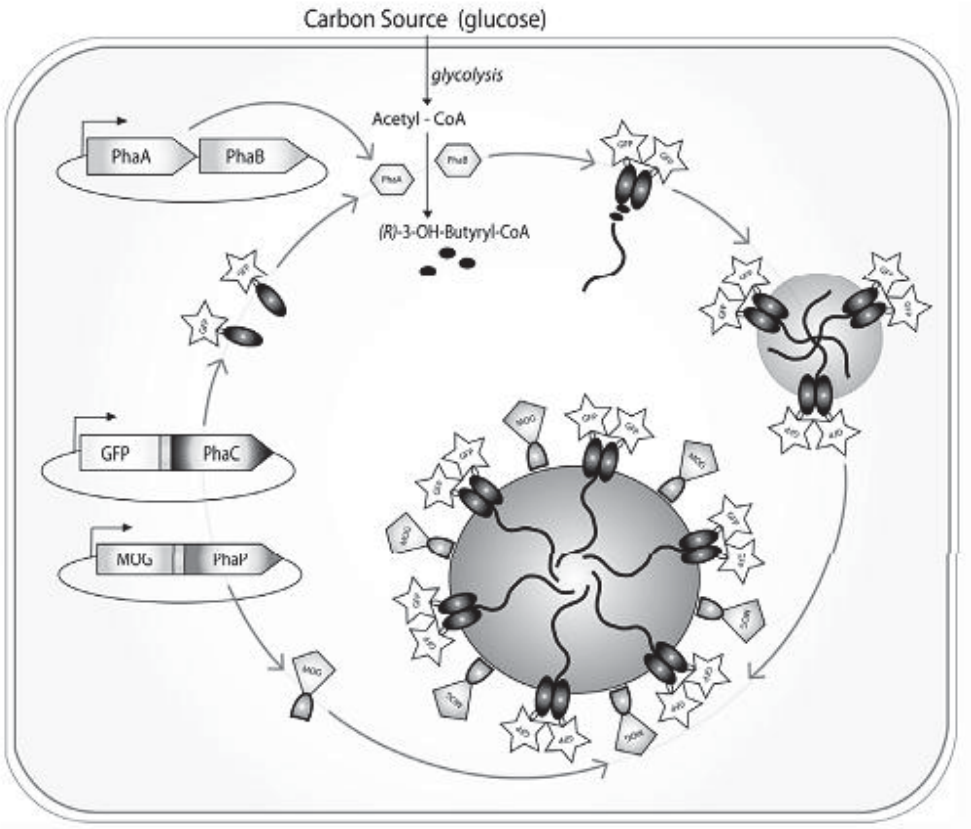

Figure 2.8.1 *Formation of functionalized biopolyester granules from recombinant fusion proteins. (Reproduced from Draper and Rehm 2012 [185].)*

8.1) Bioseparation

PHB beads displaying the ZZ domain of Protein A from *Staphylococcus aureus* as the result of N-terminal fusion to PhaC have demonstrated a robust bioseparation power for purifying IgG from serum samples, with a binding capacity similar to commercial protein-A sepharose [153, 154]. Initially generated in recombinant *E. coli*, similar beads were recently produced in recombinant *Lactococcus lactis* [155]. Intriguingly, the *L. lactis* produced beads were significantly smaller and had a higher binding capacity for IgG.

Similarly, a fusion of streptavidin to PhaC recombinantly expressed in *E. coli* generated PHB beads capable of binding biotin. The streptavidin-displaying beads were able to purify biotinylated antibodies and DNA [152].

Recently, PHB beads capable of removing endotoxin from a liquid sample were developed. A fusion of human lipopolysaccharide binding protein (hLBP) to PhaP was produced in the yeast *Pichia pastoris* GS115, and the resulting rhLBP-PhaP fusion protein was immobilized *in vitro* on PHB particles via the natural hydrophobic interaction between PhaP and PHB. PHB beads thus coated could separate endotoxin from liquid samples with an efficiency of over 90% [156].

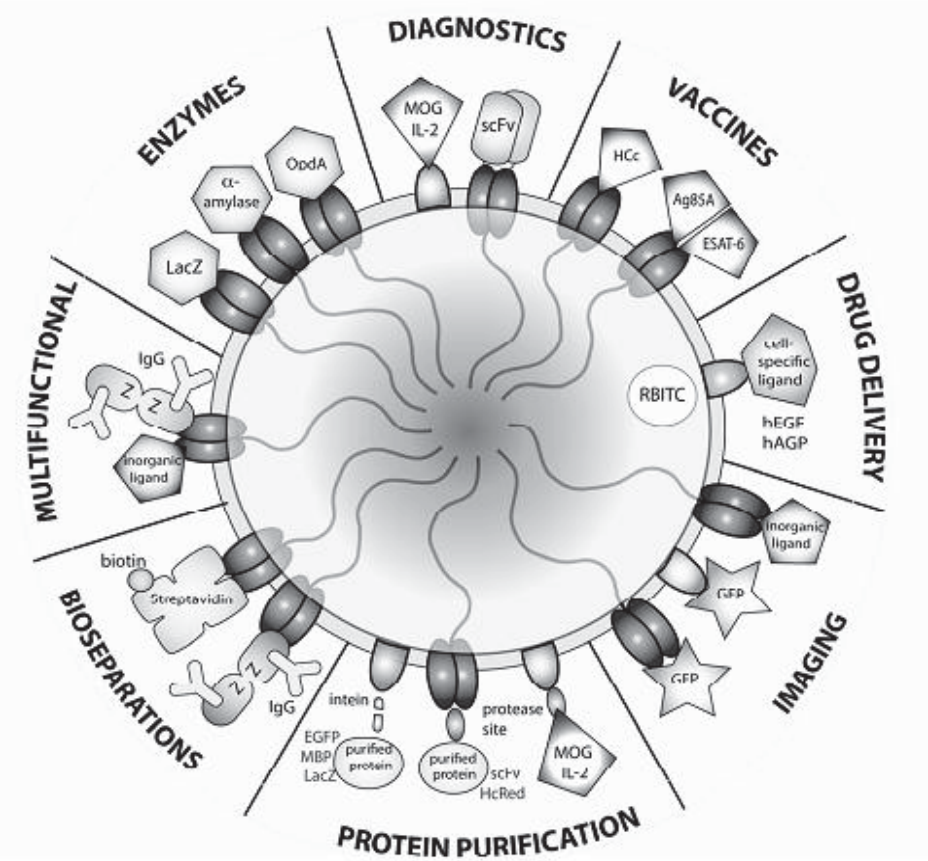

Figure* 2.8.2Experimentally demonstrated applications of functionalized biobeads. (Modified from Draper and Rehm 2012 [185].)*

8.2) Drug delivery

While polymers such as polylactic acid (PLA) and poly(lactic-co-glycolic acid) (PLGA) have been used for drug delivery for many years, PHA has received less interest. Release of antibiotics from PHBV rods or microparticles has been investigated [157, 158], and recently an alternative production host, *Bacillus cereus* SPV, was used to produce PHA which was processed into microspheres containing gentamicin [159].

Several experiments have demonstrated sustained chemical release from PHA particles. In one study, nanoparticles made of PHB, PHBHHx, or PLA were loaded with rhodamine B isothiocyanate (RBITC) *in vitro* and targeted to macrophages; results showed RBITC was released for at least 20 days and macrophage viability was maintained [143]. Likewise, PHA nanoparticles loaded with the phosphoinositide-3-kinases (PI3Ks) inhibitor TGX221 blocked proliferation of cancer cell lines, suggesting a potential application for PHB particles in cancer therapy [160]. A recent study showed promising drug release profiles using microspheres comprising PHB, cellulose acetate phthalate, and the anti-cancer drug 5-fluorouracil (5-FU) [161]. Animal studies have confirmed sustained drug delivery *in vivo*: PHBHHx nanoparticles loaded with an insulin phospholipid complex showed long-lasting insulin release in STZ diabetic rats [162].

Targeted drug delivery has also been investigated. The cell-specific ligands human epidermal growth factor (hEGF) and mannosylated human 1-acid glycoprotein (hAGP) were recombinantly expressed as PhaP fusions and bound *in vitro* to separately generated rhodamine B isothiocyanate (RBITC)-loaded PHBHHx nanoparticles. These beads were taken

up by macrophages and targeted to hepatocellular carcinoma cells both *in vitro* and *in vivo*, demonstrating the viability of functionalized PHA beads as a drug-delivery system [163].

8.3) Protein purification

PHA bead-based protein purification strategies have utilized fusions of the protein of interest to the PHA bead-associated phasin, regulatory, or synthase proteins.

In the system developed by Banki *et al.*, a phasin-intein-target protein fusion is expressed in PHA-producing *E coli* [164]. The phasin acts as a PHA affinity tag, anchoring the fusion protein to the PHA granule as it forms *in vivo*. The intein functions as self-cleaving tag to release target protein from the PHA granules after isolation. Maltose binding protein (MBP) and *β*-galactosidase (LacZ) were successfully purified by this method [164]. A similar strategy was used to purify *β*-galactosidase from *R. eutropha* [165].

A slightly different approach used PhaP as an *in vitro* PHA granule affinity tag: a PhaP-intein-target protein fusion recombinantly expressed in *E coli* could be captured by manufactured PHA beads [166]. This method was recently shown to function using the regulatory protein PhaR instead of PhaP [167].

In 2011, Grage *et al.* developed an alternative method by fusing the target protein to PhaC, separated by an enterokinase cleavage site. This method was used to purify functional HcRed (a fluorescent protein), and anti-β-galactosidase single chain variable fragment (scFv) proteins. The use of PhaC synthase as affinity tag avoids the leakage shortcoming of previous approaches; the PhaC synthase remains covalently attached to the PHB particle, whereas the

weaker attachment of PhaP/PhaR via hydrophobic interactions can result in contamination of the purified protein with the affinity partner [168].

8.4) Enzyme immobilization

In the fields of pharmaceutical and fine chemical synthesis enzymes are becoming the catalytic agent of choice [169]. Immobilization of enzymes onto a solid support facilitates separation from the product, often enhances stability, and allows for reuse of the expensive reaction catalyst [169-171]. The drawbacks to immobilization include some loss of enzyme activity and the high cost of enzyme purification and chemical immobilization [169, 170]. The loss in activity is counterbalanced by increased stability and ease of reuse [169].

The first immobilization of a functional enzyme onto PHA granules was demonstrated by fusion of the β-galactosidase gene *lacZ* to the PHA synthase from *P. aeruginosa* PAO1 [172]. The enzyme beads were highly functional and stable in storage for several months, comparable to free β-galactosidase.

Enhanced enzymatic properties of thermostable α-amylase (BLA) were achieved by fusion to the N-terminus of PhaC from *R. eutropha* [173]. Immobilized BLA had a K_m of 5 M and a V_{max} of 506 mU/mg of bead protein, similar to the free enzyme. However, the temperature optimum for the immobilized enzyme increased from 55 °C to 75 °C and it remained stable up to 85 °C. The pH optimum was also shifted from pH 5.6 to 8.0. These changes gave the PHA-immobilized BLA superior properties for use in starch liquification processes.

Recently, the organophosphorus pesticide hydrolase (OpdA) from *Agrobacterium radiobacter* was fused to the C-terminus of the *R. eutropha* PhaC via a designed linker [174]. OpdA PHA

granules isolated from *E. coli* displayed functional enzyme with k_{cat} reduced 16.5 fold to 139 s^{-1} and K_m increased 1.6 fold to $2.5x10^{-4}$ compared to free OpdA. Additionally, OpdA beads degraded organophosphorus pesticides in the demanding environmental conditions of wool scour effluent, demonstrating their applicability in bioremediation. Additionally, a single genetic fusion of the PhaA-PhaB-PhaC PHA synthesis pathway was shown to produce PHA granules in *E. coli*, demonstrating the ability to construct PHA beads recapitulating an entire enzymatic pathway [175].

Although these examples show the ability of PHA granules to display functional enzymes, the potential relevance of enzyme immobilization to PHA granules for pharmaceutical and fine chemical synthesis is yet to be realized.

8.5) Diagnostics

PHB beads have been used for flow cytometry based diagnostics. Hybrid genes encoding either the mouse interleukin-2 (IL2) or the myelin oligodendrocyte glycoprotein (MOG) fused via an enterokinase site to the phasin PhaP were produced in recombinant PHB-producing *E. coli*. The resulting beads could be used to detect anti-IL2 or anti-MOG antibodies using fluorescence-activated cell sorting (FACS); additionally, these beads retained functionality up to a year in storage [176].

Another approach developed multifunctional beads: co-expression of PhaC-GFP and MOG-PhaP fusions generated fluorescent beads recognized by anti-MOG and anti-GFP antibodies [150]. Such beads could be used for imaging and testing of diagnostic antibodies.

The recent success in producing PHB beads expressing a functional single-chain antibody variable fragment (scFv) in *E. coli* [177] also has clear implications for diagnostics, suggesting that tailor-made diagnostic beads displaying antibody fragments against target antigens could be produced to order.

8.6) Imaging

Fluorescent PHB granules have been created by many groups, utilizing both PhaC and PhaP fusions to fluorescent proteins such as GFP and YFP [114, 164, 166, 178].

Many of the PHB beads exhibiting bioseparation or diagnostic functions can also be used for imaging, especially if combined with an imaging agent such as fluorescence or inorganic contrast agents. Multifunctional beads displaying the MOG antigen combined with GFP have already been produced [150]. Additionally, PHB beads displaying binding sites for both antibodies and inorganic gold or silica particles were recently developed [179]. Antibody-mediated targeted delivery of an inorganic contrast agent by these beads could be used for bioimaging in medical applications.

8.7) Vaccine delivery

Over the past few decades, there has been increased interest in developing biodegradable nano-/micro-particles as vaccine delivery vehicles. Particulate vaccines target antigen-presenting cells and enhance cellular immune responses. Size and surface properties greatly influence the outcome of vaccination [180]. A range of polymers such as PLA and PLGA are often used, but the use of PHAs had not been investigated until recently.

PHB beads displaying hepatitis C core antigen (HCc) [181] and mycobacterial antigens antigen-85A (Ag85A) and 6 kDa early secretory antigenic target (ESAT6) [182, 183] were recently demonstrated to act as safe and effective vaccines in mice. Initially, genetic fusions of these antigens to the PhaC synthase of *R. eutropha* were expressed recombinantly in *E. coli* [183], generating PHB vaccine particles naturally coated in the target antigen. However, the potential presence of endotoxin contaminants in *E. coli*-produced beads limited their potential as human vaccines. Thus, *L. lactis* was used as an alternative production host [181, 182] due to its lack of endotoxin, previous use as a production host for recombinant proteins, and history of safe use for a range of human foods and products [184]. Antigen-specific cellular immune responses [181-183] and protection against tuberculosis [182] were observed in mice immunized with these PHB vaccine beads. These results suggest that PHB beads represent an emerging field for vaccinology.

9) Conclusion

The formation of biopolyesters in both naturally PHA-producing and recombinant bacteria has been extensively investigated. Many of the proteins involved in PHA synthesis, from synthases to regulators, have been cloned and characterized. The generation of PHA precursor molecules through multiple biosynthesis pathways has also been extensively investigated by many groups. Metabolic and genetic engineering approaches have demonstrated the ability to produce tailor-made biopolymers with unique material properties. However, despite much effort, biopolyesters remain more expensive to produce than conventional petroleum-based plastics. Thus, commercial use of biopolyesters is currently limited to high value niche

applications which benefit from their unique properties, such as biomedical products requiring biocompatible and biodegradable materials.

Recently, the natural production of PHA granules as nano-/micro-scale beads coated with functional proteins has been exploited to produce functionalized beads. Similar functional beads are currently employed as bioseparation resins and represent a multi-billion-dollar industry; however their production is a costly multi-step process typically involving both chemical synthesis and recombinant protein production. In contrast, the one-step bacterial manufacture of functional PHA granules suitable for bioseparation, bioremediation, enzymatic catalysis, diagnostics, targeted drug delivery, and vaccine delivery provides an attractive alternative to conventional bead technologies. This new technology has great promise for cost-effective production of tailor-made functional nano-/micro-particles.

10) Acknowledgements

This work was supported by grants from Massey University and Polybatics Ltd.

11) References

1. Anderson, A.J., G.W. Haywood, and E.A. Dawes, *Biosynthesis and composition of bacterial poly(hydroxyalkanoates).* International journal of biological macromolecules, 1990. **12**: p. 102-5.

2. Rehm, B.H.A., *Bacterial polymers: biosynthesis, modifications and applications.* Nature reviews. Microbiology, 2010. **8**: p. 578-92.

3. Lemoigne, M., *É'tudes sur l'autolyse microbienne acidification par formation d'acide-oxybutyrique.* Annales de l'Institut Pasteur, 1925. **39**: p. 144-173.

4. Rehm, B.H.A., *Polyester synthases: natural catalysts for plastics.* The Biochemical journal, 2003. **376**: p. 15-33.

5. Steinbüchel, A. and H.E. Valentin, *Diversity of bacterial polyhydroxyalkanoic acids.* FEMS Microbiology Letters, 1995. **128**: p. 219-228. 6. Kessler, B., et al., *Production of microbial polyesters: fermentation and downstream processes.* Advances in Biochemical Engineering / Biotechnology, 2001. **71**: p. 159-182.

7. Reusch, R., T. Hiske, and H. Sadoff, *Cellular incorporation of poly-β-hydroxybutyrate into plasma membranes of Escherichia coli and Azotobacter vinelandii alters native membrane structure.* Canadian Journal of Microbiology/Revue Canadienne de Microbiologie, 1987. **33**: p. 435-444.

8. Reusch, R.N., *Poly-β-hydroxybutyrate/calcium polyphosphate complexes in eukaryotic membranes.* Proceedings of the Society for Experimental Biology and Medicine, 1989. **191**: p. 377-381.

9. Reusch, R.N. and H.L. Sadoff, *Putative structure and function of a poly-β-hydroxybutyrate/calcium polyphosphate channel in bacterial plasma membranes.* Proceedings of the National Academy of Sciences, USA, 1988. **85**: p. 4176-4180.

10. Reusch, R.N., A.W. Sparrow, and J. Gardiner, *Transport of poly-β-hydroxybutyrate in human plasma.* Biochimica et Biophysica Acta - Lipids and Lipid Metabolism, 1992. **1123**: p. 33-40.

11. Seebach, D. and M.G. Fritz, *Detection, synthesis, structure, and function of oligo(3-hydroxyalkanoates): Contributions by synthetic organic chemists.* International Journal of Biological Macromolecules, 1999. **25**: p. 217-236.

12. Reusch, R.N., *Biological complexes of poly-β-hydroxybutyrate.* FEMS Microbiology Letters, 1992. **103**: p. 119-129.

13. Reusch, R.N., E.M. Bryant, and D.N. Henry, *Increased poly-(R)-3-hydroxybutyrate concentrations in streptozotocin (STZ) diabetic rats.* Acta Diabetologica, 2003. **40**: p. 91-94.

14. Rathberger, K., et al., *Comparative synthesis and hydrolytic degradation of poly (L-malate) by myxomycetes and fungi.* Mycological Research, 1999. **103**: p. 513-520.

15. Holler, E., et al., *Biological and biosynthetic properties of poly-L-malate.* FEMS Microbiology Letters, 1992. **103**: p. 109-118.

16. Portilla-Arias, J.A., et al., *Ionic complexes of biosynthetic poly(malic acid) and poly(glutamic acid) as prospective drug-delivery systems.* Macromolecular Bioscience, 2007. **7**: p. 897-906.

17. Huang, Z.W., et al., *New functional degradable and bio-compatible nanoparticles based on poly(malic acid) derivatives for site-specific anti-cancer drug delivery.* International Journal of Pharmaceutics, 2012. **423**: p. 84-92.

18. Portilla-Arias, J., et al., *Nanoconjugate platforms development based in poly(B,L-Malic Acid) methyl esters for tumor drug delivery.* Journal of Nanomaterials, 2010.

19. Lambov, N., et al., *Biodegradable cross-linked prodrug of bronchial dilator vephylline .1. Mechanism of the release.* Journal of Controlled Release, 1997. **45**: p. 193-197.

20. Yoncheva, K., et al., *Development and characterization of cross-linked poly(malate) microspheres with dipyridamole.* International journal of pharmaceutics, 2001. **226**: p. 31-37.

21. Liu, F., et al., *Production of poly-β-hydroxybutyrate on molasses by recombinant Escherichia coli.* Biotechnology Letters, 1998. **20**: p. 345-348.

22. Ramsay, J.A., M.-C.A. Hassan, and B.A. Ramsay, *Hemicellulose as a potential substrate for production of poly(β-hydroxyalkanoates).* Canadian Journal of Microbiology, 1995. **41**: p. 262-266.

23. Füchtenbusch, B., D. Wullbrandt, and A. Steinbüchel, *Production of polyhydroxyalkanoic acids by Ralstonia eutropha and Pseudomonas oleovorans from an oil remaining from biotechnological rhamnose production.* Applied Microbiology and Biotechnology, 2000. **53**: p. 167-172.

24. John, M.E. and G. Keller, *Metabolic pathway engineering in cotton: Biosynthesis of polyhydroxybutyrate in fiber cells.* Proceedings of the National Academy of Sciences, USA, 1996. **93**: p. 12768-12773.

25. Nakashita, H., et al., *Production of biodegradable polyester by a transgenic tobacco.* Bioscience, Biotechnology, and Biochemistry, 1999. **63**: p. 870-874.

26. Nawrath, C., Y. Poirier, and C. Somerville, *Targeting of the polyhydroxybutyrate biosynthetic pathway to the plastids of Arabidopsis thaliana results in high levels of polymer accumulation.* Proceedings of the National Academy of Sciences, USA, 1994. **91**: p. 12760-12764.

27. Sudesh, K. and T. Iwata, *Sustainability of Biobased and Biodegradable Plastics.* CLEAN - Soil, Air, Water, 2008. **36**(5-6): p. 433-442. 28. Ruth, K., et al., *Efficient production of (R)-3-hydroxycarboxylic acids by biotechnological conversion of polyhydroxyalkanoates and their purification.* Biomacromolecules, 2006. **8**: p. 279-286.

29. Kozhevnikov, I.V., et al., *Cloning and molecular organization of the polyhydroxyalkanoic acid synthase gene (phaC) of Ralstonia eutropha strain B5786.* Applied Biochemistry and Microbiology, 2010. **46**: p. 140-147.

30. Fukui, T. and Y. Doi, *Cloning and analysis of the poly(3-hydroxybutyrate-co-3-hydroxyhexanoate) biosynthesis genes of Aeromonas caviae.* Journal of bacteriology, 1997. **179**: p. 4821-30.

31. Bhubalan, K., et al., *Characterization of the highly active polyhydroxyalkanoate synthase of Chromobacterium sp. strain USM2.* Applied and environmental microbiology, 2011. **77**: p. 2926-33.

32. Ren, Q., et al., *FabG, an NADPH-Dependent 3-Ketoacyl Reductase of Pseudomonas aeruginosa, Provides Precursors for Medium-Chain-Length Poly-3-Hydroxyalkanoate Biosynthesis in Escherichia coli.* Journal of Bacteriology, 2000. **182**: p. 2978-2981.

33. Matsusaki, H., et al., *Cloning and molecular analysis of the Poly(3-hydroxybutyrate) and Poly(3-hydroxybutyrate-co-3-hydroxyalkanoate) biosynthesis genes in Pseudomonas sp. strain 61-3.* Journal of bacteriology, 1998. **180**: p. 6459-67.

34. Solaiman, D.K.Y. and R.D. Ashby, *Genetic characterization of the poly(hydroxyalkanoate) synthases of various Pseudomonas oleovorans strains.* Current microbiology, 2005. **50**: p. 329-33.

35. Liebergesell, M., B. Schmidt, and A. Steinbüchel, *Isolation and identification of granule-associated proteins relevant for poly(3-hydroxyalkanoic acid) biosynthesis in Chromatium vinosum D.* FEMS microbiology letters, 1992. **78**: p. 227-32.

36. Liebergesell, M. and A. Steinbüchel, *Cloning and nucleotide sequences of genes relevant for biosynthesis of poly(3-hydroxybutyric acid) in Chromatium vinosum strain D.* European journal of biochemistry / FEBS, 1992. **209**: p. 135-50.

37. Lu, Q., et al., *Genetic and biochemical characterization of the poly(3-hydroxybutyrate-co-3-hydroxyvalerate) synthase in Haloferax mediterranei.* Journal of bacteriology, 2008. **190**: p. 4173-80.

38. McCool, G.J. and M.C. Cannon, *Polyhydroxyalkanoate inclusion body-associated proteins and coding region in Bacillus megaterium.* Journal of bacteriology, 1999. **181**: p. 585-92.

39. Hyakutake, M., et al., *Polyhydroxyalkanoate (PHA) synthesis by class IV PHA synthases employing Ralstonia eutropha PHB(-)4 as host strain.* Bioscience, biotechnology, and biochemistry, 2011. **75**: p. 1615-7.

40. Amara, A.A. and B.H.A. Rehm, *Replacement of the catalytic nucleophile cysteine-296 by serine in class II polyhydroxyalkanoate synthase from Pseudomonas aeruginosa-mediated synthesis of a new polyester: identification of catalytic residues.* The Biochemical journal, 2003. **374**: p. 413-21.

41. Jia, Y., et al., *Lipases provide a new mechanistic model for polyhydroxybutyrate (PHB) synthases: characterization of the functional residues in Chromatium vinosum PHB synthase.* Biochemistry, 2000. **39**: p. 3927-36.

42. Zheng, Z., et al., *Mutation on N-terminus of polyhydroxybutyrate synthase of Ralstonia eutropha enhanced PHB accumulation.* Applied microbiology and biotechnology, 2006. **72**: p. 896-905.

43. Rehm, B.H.A., et al., *Molecular characterization of the poly(3-hydroxybutyrate) (PHB) synthase from Ralstonia eutropha: in vitro evolution, site-specific mutagenesis and development of a PHB synthase protein model.* Biochimica et biophysica acta, 2002. **1594**: p. 178-90.

44. Wodzinska, J., et al., *Polyhydroxybutyrate Synthase: Evidence for Covalent Catalysis.* Journal of the American Chemical Society, 1996. **118**: p. 6319-6320.

45. Gerngross, T.U., et al., *Immunocytochemical analysis of poly-beta-hydroxybutyrate (PHB) synthase in Alcaligenes eutrophus H16: localization of the synthase enzyme at the surface of PHB granules.* Journal of bacteriology, 1993. **175**: p. 5289-93.

46. Liebergesell, M., et al., *Purification and characterization of the poly(hydroxyalkanoic acid) synthase from Chromatium vinosum and localization of the enzyme at the surface of poly(hydroxyalkanoic acid) granules.* European journal of biochemistry / FEBS, 1994. **226**: p. 71-80.

47. Griebel, R.J., Z. Smith, and J.M. Merrick, *Metabolism of poly-beta-hydroxybutyrate. I. Purification, composition, and properties of native poly-beta-hydroxybutyrate granules from Bacillus megaterium.* Biochemistry, 1968. **7**: p. 3676-81.

48. Griebel, R.J. and J.M. Merrick, *Metabolism of poly- -hydroxybutyrate: effect of mild alkaline extraction on native poly- -hydroxybutyrate granules.* Journal of bacteriology, 1971. **108**: p. 782-9.

49. Gerngross, T.U., et al., *Overexpression and purification of the soluble polyhydroxyalkanoate synthase from Alcaligenes eutrophus: evidence for a required posttranslational modification for catalytic activity.* Biochemistry, 1994. **33**: p. 9311-20.

50. Hoppensack, A., B.H.A. Rehm, and A. Steinbüchel, *Analysis of 4-phosphopantetheinylation of polyhydroxybutyrate synthase from Ralstonia eutropha: generation of beta-alanine auxotrophic Tn5 mutants and cloning of the panD gene region.* Journal of bacteriology, 1999. **181**: p. 1429-35.

51. Tian, J., A.J. Sinskey, and J. Stubbe, *Detection of intermediates from the polymerization reaction catalyzed by a D302A mutant of class III polyhydroxyalkanoate (PHA) synthase.* Biochemistry, 2005. **44**: p. 1495-503.

52. Jia, Y., et al., *Mechanistic studies on class I polyhydroxybutyrate (PHB) synthase from Ralstonia eutropha: class I and III synthases share a similar catalytic mechanism.* Biochemistry, 2001. **40**: p. 1011-9.

53. Li, P., S. Chakraborty, and J. Stubbe, *Detection of covalent and noncovalent intermediates in the polymerization reaction catalyzed by a C149S class III polyhydroxybutyrate synthase.* Biochemistry, 2009. **48**: p. 9202-11.

54. Gerngross, T.U. and D.P. Martin, *Enzyme-catalyzed synthesis of poly[(R)-(-)-3-hydroxybutyrate]: formation of macroscopic granules in vitro.* Proceedings of the National Academy of Sciences of the United States of America, 1995. **92**: p. 6279-83.

55. Amara, A.A., A. Steinbüchel, and B.H.A. Rehm, *In vivo evolution of the Aeromonas punctata polyhydroxyalkanoate (PHA) synthase: isolation and characterization of modified PHA synthases with enhanced activity.* Applied microbiology and biotechnology, 2002. **59**: p. 477-82.

56. Kichise, T., S. Taguchi, and Y. Doi, *Enhanced accumulation and changed monomer composition in polyhydroxyalkanoate (PHA) copolyester by in vitro evolution of Aeromonas caviae PHA synthase.* Applied and environmental microbiology, 2002. **68**: p. 2411-9.

57. Matsumoto, K.i., et al., *In vivo and in vitro characterization of Ser477X mutations in polyhydroxyalkanoate (PHA) synthase 1 from Pseudomonas sp. 61-3: effects of beneficial mutations on enzymatic activity, substrate specificity, and molecular weight of PHA.* Biomacromolecules, 2006. **7**: p. 2436-42.

58. Normi, Y.M., et al., *Characterization and properties of G4X mutants of Ralstonia eutropha PHA synthase for poly(3-hydroxybutyrate) biosynthesis in Escherichia coli.* Macromolecular bioscience, 2005. **5**: p. 197-206.

59. Tsuge, T., et al., *Combination of N149S and D171G mutations in Aeromonas caviae polyhydroxyalkanoate synthase and impact on polyhydroxyalkanoate biosynthesis.* FEMS microbiology letters, 2007. **277**: p. 217-22.

60. Matsumoto, K.i., et al., *Synergistic effects of Glu130Asp substitution in the type II polyhydroxyalkanoate (PHA) synthase: enhancement of PHA production and alteration of polymer molecular weight.* Biomacromolecules, 2005. **6**: p. 99-104.

61. Yuan, W., et al., *Class I and III polyhydroxyalkanoate synthases from Ralstonia eutropha and Allochromatium vinosum: characterization and substrate specificity studies.* Archives of biochemistry and biophysics, 2001. **394**: p. 87-98.

62. Antonio, R.V., A. Steinbüchel, and B.H.A. Rehm, *Analysis of in vivo substrate specificity of the PHA synthase from Ralstonia eutropha: formation of novel copolyesters in recombinant Escherichia coli.* FEMS microbiology letters, 2000. **182**: p. 111-117.

63. Dennis, D., et al., *Formation of poly(3-hydroxybutyrate-co-3-hydroxyhexanoate) by PHA synthase from Ralstonia eutropha.* Journal of biotechnology, 1998. **64**: p. 177-86.

64. Qi, Q., B.H.A. Rehm, and A. Steinbüchel, *Synthesis of poly(3-hydroxyalkanoates) in Escherichia coli expressing the PHA synthase gene phaC2 from Pseudomonas aeruginosa: comparison of PhaC1 and PhaC2.* FEMS microbiology letters, 1997. **157**: p. 155-62.

65. Qi, Q., A. Steinbüchel, and B.H.A. Rehm, *Metabolic routing towards polyhydroxyalkanoic acid synthesis in recombinant Escherichia coli (fadR): inhibition of fatty acid beta-oxidation by acrylic acid.* FEMS microbiology letters, 1998. **167**: p. 89-94.

66. Lütke-Eversloh, T., et al., *Identification of a new class of biopolymer: bacterial synthesis of a sulfur-containing polymer with thioester linkages.* Microbiology (Reading, England), 2001. **147**: p. 11-9.

67. Sheu, D.-S. and C.-Y. Lee, *Altering the substrate specificity of polyhydroxyalkanoate synthase 1 derived from Pseudomonas putida GPo1 by localized semirandom mutagenesis.* Journal of bacteriology, 2004. **186**: p. 4177-84.

68. Tsuge, T., et al., *Mutation effects of a conserved alanine (Ala510) in type I polyhydroxyalkanoate synthase from Ralstonia eutropha on polyester biosynthesis.* Macromolecular bioscience, 2004. **4**: p. 963-70.

69. Matsumoto, K.i., et al., *Chimeric enzyme composed of polyhydroxyalkanoate (PHA) synthases from Ralstonia eutropha and Aeromonas caviae enhances production of PHAs in recombinant Escherichia coli.* Biomacromolecules, 2009. **10**: p. 682-5.

70. Anderson, A.J. and E.A. Dawes, *Occurrence, metabolism, metabolic role, and industrial uses of bacterial polyhydroxyalkanoates.* Microbiological reviews, 1990. **54**: p. 450-472.

71. Steinbüchel, A., *Polyhydroxyalkanoic acids*, in *Biomaterials*, D. Byrom, Editor 1991, MacMillan. p. 123-213.

72. Steinbüchel, A., et al., *Biosynthesis of polyesters in bacteria and recombinant organisms.* Polymer Degradation and Stability, 1998. **59**: p. 177-182.

73. Valentin, H., A. Schönebaum, and A. Steinbüchel, *Identification of 5-hydroxyhexanoic acid, 4-hydroxyheptanoic acid and 4-hydroxyoctanoic acid as new constituents of bacterial polyhydroxyalkanoic acids.* Journal Of Bacteriology, 1996. **46**: p. 261-267.

74. Peoples, O.P. and A.J. Sinskey, *Poly-β-hydroxybutyrate biosynthesis in Alcaligenes eutrophus H16. Characterization of the genes encoding β-ketothiolase and acetoacetyl-CoA reductase.* Journal of Biological Chemistry, 1989. **264**: p. 15293-15297.

75. Peoples, O.P. and A.J. Sinskey, *Poly-beta-hydroxybutyrate (PHB) biosynthesis in Alcaligenes eutrophus H16. Identification and characterization of the PHB polymerase gene (phbC).* J Biol Chem, 1989. **264**(26): p. 15298-303.

76. Schubert, P., A. Steinbüchel, and H.G. Schlegel, *Cloning of the Alcaligenes eutrophus genes for synthesis of poly-beta-hydroxybutyric acid (PHB) and synthesis of PHB in Escherichia coli.* Journal of bacteriology, 1988. **170**: p. 5837-5847.

77. Slater, S.C., W.H. Voige, and D.E. Dennis, *Cloning and expression in Escherichia coli of the Alcaligenes eutrophus H16 poly-beta-hydroxybutyrate biosynthetic pathway.* Journal of bacteriology, 1988. **170**: p. 4431-4436.

78. Fiedler, S., A. Steinbuchel, and B.H.A. Rehm, *PhaG-mediated synthesis of Poly(3-hydroxyalkanoates) consisting of medium-chain-length constituents from nonrelated carbon sources in recombinant Pseudomonas fragi.* Appl Environ Microbiol, 2000. **66**(5): p. 2117-24.

79. Soberón-Chávez, G., M. Aguirre-Ramírez, and R. Sánchez, *The Pseudomonas aeruginosa RhlA enzyme is involved in rhamnolipid and polyhydroxyalkanoate production.* Journal of industrial microbiology & biotechnology, 2005. **32**: p. 675-677.

80. Rehm, B.H.A., N. Krüger, and A. Steinbüchel, *A new metabolic link between fatty acid de novo synthesis and polyhydroxyalkanoic acid synthesis.* Journal of Biological Chemistry, 1998. **273**: p. 24044-24051.

81. Hoffmann, N. and B.H.A. Rehm, *Regulation of polyhydroxyalkanoate biosynthesis in Pseudomonas putida and Pseudomonas aeruginosa.* Fems Microbiology Letters, 2004. **237**: p. 1-7.

82. Hoffmann, N. and B.H.A. Rehm, *Nitrogen-dependent regulation of medium-chain length polyhydroxyalkanoate biosynthesis genes in pseudomonads.* Biotechnology letters, 2005. **27**: p. 279-282.

83. Hume, A.R., J. Nikodinovic-Runic, and K.E. O'Connor, *FadD from Pseudomonas putida CA-3 Is a True Long-Chain Fatty Acyl Coenzyme A Synthetase That Activates Phenylalkanoic and Alkanoic Acids.* Journal Of Bacteriology, 2009. **191**: p. 7554-7565.

84. Lu, X., et al., *Enhanced production of poly(3-hydroxybutyrate-co-3-hydroxyhexanoate) via manipulating the fatty acid beta-oxidation pathway in E-coli.* Fems Microbiology Letters, 2003. **221**: p. 97-101.

85. Pawar, S. and H. Schulz, *The structure of the multienzyme complex of fatty acid oxidation from Escherichia coli.* The Journal of Biological Chemistry, 1981. **256**: p. 3894-3899.

86. Pramanik, A., et al., *Five different enzymatic activities are associated with the multienzyme complex of fatty acid oxidation from Escherichia coli.* Journal Of Bacteriology, 1978. **137**: p. 469-473.

87. Fiedler, S., A. Steinbüchel, and B.H.A. Rehm, *The role of the fatty acid beta-oxidation multienzyme complex from Pseudomonas oleovorans in polyhydroxyalkanoate biosynthesis: molecular characterization of the fadBA operon from P. oleovorans and of the enoyl-CoA hydratase genes phaJ from P. oleovorans* Archives of Microbiology, 2002. **178**: p. 149-160.

88. Ishikawa, M., et al., *Reconstitution, morphology and crystallization of a fatty acid beta-oxidation multienzyme complex from Pseudomonas fragi.* Biochemical Journal, 1997. **328**: p. 815-820.

89. Eggink, G., P. Dewaard, and G.N.M. Huijberts, *Formation of novel poly(hydroxyalkanoates) from long-chain fatty-acids.* Canadian Journal of Microbiology, 1995. **41**: p. 14-21.

90. Wang, Q. and C.T. Nomura, *Monitoring differences in gene expression levels and polyhydroxyalkanoate (PHA) production in Pseudomonas putida KT2440 grown on different carbon sources.* Journal of Bioscience and Bioengineering, 2010. **110**: p. 653-659.

91. Park, S.J., J.i. Choi, and S.Y. Lee, *Engineering of Escherichia coli fatty acid metabolism for the production of polyhydroxyalkanoates.* Enzyme and Microbial Technology, 2005. **36**: p. 579-588.

92. Tsuge, T., et al., *Molecular characterization and properties of (R)-specific enoyl-CoA hydratases from Pseudomonas aeruginosa: metabolic tools for synthesis of polyhydroxyalkanoates via fatty acid beta-oxidation.* International Journal of Biological Macromolecules, 2003. **31**: p. 195-205.

93. Chung, A., et al., *Microbial production of 3-hydroxydodecanoic acid by pha operon and fadBA knockout mutant of Pseudomonas putida KT2442 harboring tesB gene.* Applied Microbiology and Biotechnology, 2009. **83**: p. 513-519.

94. Snell, K.D., et al., *YfcX enables medium-chain-length poly(3-hydroxyalkanoate) formation from fatty acids in recombinant Escherichia coli fadB strains.* Journal Of Bacteriology, 2002. **184**: p. 5696-5705.

95. Vo, M.T., et al., *Utilization of fadA knockout mutant Pseudomonas putida for overproduction of medium chain-length-polyhydroxyalkanoate.* Biotechnology Letters, 2007. **29**: p. 1915-1920.

96. Brigham, C.J., et al., *Elucidation of beta-Oxidation Pathways in Ralstonia eutropha H16 by Examination of Global Gene Expression.* Journal Of Bacteriology, 2010. **192**: p. 5454-5464.

97. Escapa, I.F., et al., *Disruption of beta-oxidation pathway in Pseudomonas putida KT2442 to produce new functionalized PHAs with thioester groups.* Applied Microbiology and Biotechnology, 2011. **89**: p. 1583-1598.

98. Park, S.J., S.Y. Lee, and S. Yup Lee, *New FadB homologous enzymes and their use in enhanced biosynthesis of medium-chain-length polyhydroxyalkanoates in FadB mutant Escherichia coli.* Biotechnology and Bioengineering, 2004. **86**: p. 681-686.

99. Park, S.J. and S.Y. Lee, *Identification and characterization of a new enoyl coenzyme A hydratase involved in biosynthesis of medium-chain-length polyhydroxyalkanoates in recombinant Escherichia coli.* Journal Of Bacteriology, 2003. **185**: p. 5391-5397.

100. Ouyang, S.P., et al., *Production of polyhydroxyalkanoates with high 3-hydroxydodecanoate monomer content by fadB and fadA knockout mutant of Pseudomonas putida KT2442.* Biomacromolecules, 2007. **8**: p. 2504-2511.

101. Ma, L., et al., *Production of two monomer structures containing medium-chain-length polyhydroxyalkanoates by beta-oxidation-impaired mutant of Pseudomonas putida KT2442.* Bioresource Technology, 2009. **100**: p. 4891-4894.

102. Kawashima, Y., et al., *Characterization and Functional Analyses of R-Specific Enoyl Coenzyme A Hydratases in Polyhydroxyalkanoate-Producing Ralstonia eutropha.* Applied and Environmental Microbiology, 2012. **78**: p. 493-502.

103. Hisano, T., et al., *Crystal structure of the (R)-specific enoyl-CoA hydratase from Aeromonas caviae involved in polyhydroxyalkanoate biosynthesis.* Journal of Biological Chemistry, 2003. **278**: p. 617-624.

104. Tsuge, T., et al., *Alteration of chain length substrate specificity of Aeromonas caviae R-enantiomer-specific enoyl-coenzyme A hydratase through site-directed mutagenesis.* Applied and Environmental Microbiology, 2003. **69**: p. 4830-4836.

105. Vo, M.T., et al., *Comparative effect of overexpressed phaJ and fabG genes supplementing (R)-3-hydroxyalkanoate monomer units on biosynthesis of mcl-polyhydroxyalkanoate in Pseudomonas putida KCTC1639.* Journal of Bioscience and Bioengineering, 2008. **106**: p. 95-98.

106. Klinke, S., et al., *Production of medium-chain-length poly(3-hydroxyalkanoates) from gluconate by recombinant Escherichia coli.* Applied and Environmental Microbiology, 1999. **65**: p. 540-548.

107. Hiltunen, J.K. and Y.M. Qin, *Beta-Oxidation - strategies for the metabolism of a wide variety of acyl-CoA esters.* Biochimica Et Biophysica Acta-Molecular and Cell Biology of Lipids, 2000. **1484**: p. 117-128.

108. Grage, K., et al., *Bacterial Polyhydroxyalkanoate Granules: Biogenesis, Structure, and Potential Use as Nano-/Micro-Beads in Biotechnological and Biomedical Applications.* Biomacromolecules, 2009. **10**: p. 660-669.

109. Stubbe, J. and J. Tian, *Polyhydroxyalkanoate (PHA) homeostasis: the role of the PHA synthase.* Natural Product Reports, 2003. **20**: p. 445.

110. Thomson, N. and E. Sivaniah, *Synthesis , properties and uses of bacterial storage lipid granules as naturally occurring nanoparticles.* Soft Matter, 2010: p. 4045-4057.

111. Rehm, B.H.A., *Biogenesis of microbial polyhydroxyalkanoate granules: a platform technology for the production of tailor-made bioparticles.* Current Issues in Molecular Biology, 2007. **9**: p. 41-62.

112. Jendrossek, D., *Fluorescence microscopical investigation of poly(3-hydroxybutyrate) granule formation in bacteria.* Biomacromolecules, 2005. **6**: p. 598-603.

113. Jendrossek, D., O. Selchow, and M. Hoppert, *Poly(3-hydroxybutyrate) granules at the early stages of formation are localized close to the cytoplasmic membrane in Caryophanon latum.* Applied and environmental microbiology, 2007. **73**: p. 586-93.

114. Peters, V. and B.H.A. Rehm, *In vivo monitoring of PHA granule formation using GFP-labeled PHA synthases.* FEMS microbiology letters, 2005. **248**: p. 93-100.

115. Tian, J., A.J. Sinskey, and J. Stubbe, *Kinetic Studies of Polyhydroxybutyrate Granule Formation in Wautersia eutropha H16 by Transmission Electron Microscopy Kinetic Studies of Polyhydroxybutyrate Granule Formation in Wautersia eutropha H16 by Transmission Electron Microscopy.* Society, 2005. **187**.

116. Mumtaz, T., et al., *Visualization of Core-Shell PHBV Granules of Wild Type Comamonas sp. EB172 In Vivo under Transmission Electron Microscope.* International Journal of Polymer Analysis and Characterization, 2011. **16**: p. 228-238.

117. Galán, B., et al., *Nucleoid-associated PhaF phasin drives intracellular location and segregation of polyhydroxyalkanoate granules in Pseudomonas putida KT2442.* Molecular microbiology, 2011. **79**: p. 402-18.

118. Pfeiffer, D. and D. Jendrossek, *Interaction between poly(3-hydroxybutyrate) granule-associated proteins as revealed by two-hybrid analysis and identification of a new phasin in Ralstonia eutropha H16.* Microbiology (Reading, England), 2011. **157**: p. 2795-807.

119. Sudesh, K., et al., *Surface structure, morphology and stability of polyhydroxyalkanoate inclusions characterised by atomic force microscopy.* Polymer Degradation and Stability, 2002. **77**: p. 77-85.

120. Horowitz, D.M. and J.K.M. Sanders, *Amorphous, Biomimetic Granules of Polyhydroxybutyrate: Preparation, Characterization, and Biological Implications.* Journal of the American Chemical Society, 1994. **116**.

121. Uchino, K., T. Saito, and D. Jendrossek, *Poly(3-hydroxybutyrate) (PHB) depolymerase PhaZa1 is involved in mobilization of accumulated PHB in Ralstonia eutropha H16.* Applied and environmental microbiology, 2008. **74**: p. 1058-63.

122. Saegusa, H., et al., *Cloning of an intracellular poly[D(-)-3-hydroxybutyrate] depolymerase gene from Ralstonia eutropha H16 and characterization of the gene product*, 2001. p. 94-100.

123. York, G.M., et al., *Ralstonia eutropha H16 encodes two and possibly three intracellular Poly[D-(-)-3-hydroxybutyrate] depolymerase genes.* Journal of bacteriology, 2003. **185**: p. 3788-94.

124. Pötter, M. and A. Steinbüchel, *Poly(3-hydroxybutyrate) granule-associated proteins: impacts on poly(3-hydroxybutyrate) synthesis and degradation.* Biomacromolecules, 2005. **6**: p. 552-60.

125. Haruhisa, S., S. Mari, and S. Terumi, *Cloning of an intracellular D(-)-3-hydroxybutyrate-oligomer hydrolase gene from Ralstonia eutropha H16 and identification of the active site serine residue by site-directed mutagenesis.* Journal of Bioscience and Bioengineering, 2002. **94**(2): p. 106-112.

126. Hanley, S.Z., et al., *Re-evaluation of the primary structure of Ralstonia eutropha phasin and implications for polyhydroxyalkanoic acid granule binding.* FEBS letters, 1999. **447**: p. 99-105.

127. Wieczorek, R., et al., *Analysis of a 24-kilodalton protein associated with the polyhydroxyalkanoic acid granules in Alcaligenes eutrophus . These include : Analysis of a 24-Kilodalton Protein Associated with the Polyhydroxyalkanoic Acid Granules in Alcaligenes eutrophus.* Microbiology, 1995. **177**.

128. Neumann, L., et al., *Binding of the major phasin, PhaP1, from Ralstonia eutropha H16 to poly(3-hydroxybutyrate) granules.* Journal of bacteriology, 2008. **190**: p. 2911-9.

129. York, G.M., J. Stubbe, and A.J. Sinskey, *The Ralstonia eutropha PhaR Protein Couples Synthesis of the PhaP Phasin to the Presence of Polyhydroxybutyrate in Cells and Promotes Polyhydroxybutyrate Production* Society, 2002.

130. Pötter, M., et al., *Regulation of phasin expression and polyhydroxyalkanoate (PHA) granule formation in Ralstonia eutropha H16.* Microbiology (Reading, England), 2002. **148**: p. 2413-26.

131. Rehm, B.H.A., *Genetics and biochemistry of polyhydroxyalkanoate granule self-assembly: The key role of polyester synthases.* Biotechnology letters, 2006. **28**: p. 207-13.

132. Byrom, D., *Polymer synthesis by micro- organisms: technology and economics.* Trends in biotechnology, 1987. **5**: p. 246-250.

133. Luzier, W.D., *Materials derived from biomass/biodegradable materials.* Proceedings of the National Academy of Sciences of the United States of America, 1992. **89**: p. 839-842.

134. Steinbüchel, A. and P. Schubert, *Expression of the Alcaligenes eutrophus poly(β-hydroxybutyric acid)-synthetic pathway in Pseudomonas sp.* Archives of Microbiology, 1989. **153**: p. 101-104.

135. Williams, M.D., et al., *Production of a polyhydroxyalkanoate biopolymer in insect cells with a modified eucaryotic fatty acid synthase . These include : Production of a Polyhydroxyalkanoate Biopolymer in Insect Cells with a Modified Eucaryotic Fatty Acid Synthase.* Microbiology, 1996. **62**.

136. Leaf, T.A., et al., *Saccharomyces cerevisiae expressing bacterial polyhydroxybutyrate synthase produces poly-3-hydroxybutyrate.* Microbiology, 1996. **142**(5): p. 1169-1180.

137. Chen, G.-Q., *A microbial polyhydroxyalkanoates (PHA) based bio- and materials industry.* Chemical Society reviews, 2009. **38**: p. 2434-2446.

138. Yao, J., et al., *Production of polyhydroxyalkanoates by Pseudomonas nitroreducens.* Antonie van Leeuwenhoek, 1999. **75**: p. 345-349.

139. Chen, G., et al., *Industrial scale production of poly(3-hydroxybutyrate-co-3-hydroxyhexanoate).* Applied Microbiology and Biotechnology, 2001. **57**: p. 50-55.

140. Choi, J.-i. and S.Y. Lee, *Efficient and Economical Recovery of Poly (3-Hydroxybutyrate) from Recombinant Escherichia coli by Simple Digestion With Chemicals.* Biotechnology and bioengineering, 1999. **62**: p. 546-553.

141. Furrer, P., S. Panke, and M. Zinn, *Efficient recovery of low endotoxin medium-chain-length poly([R]-3-hydroxyalkanoate) from bacterial biomass.* Journal of microbiological methods, 2007. **69**: p. 206-213.

142. Williams, S.F. and D.P. Martin, *Applications of PHAs in Medicine and Pharmacy*, in *Biopolymers Online*2005, Wiley-VCH Verlag GmbH & Co. KGaA.

143. Xiong, Y.-C., et al., *Application of polyhydroxyalkanoates nanoparticles as intracellular sustained drug-release vectors.* Journal of Biomaterials Science Part A, 2010. **21**: p. 127-140.

144. Martin, D.P. and S.F. Williams, *Medical applications of poly-4-hydroxybutyrate: a strong flexible absorbable biomaterial.* Biochemical Engineering Journal, 2003. **16**: p. 97-105.

145. Hazari, A., et al., *A resorbable nerve conduit as an alternative to nerve autograft in nerve gap repair.* British journal of plastic surgery, 1999. **52**: p. 653-657.

146. Wang, L., et al., *Differentiation of human bone marrow mesenchymal stem cells grown in terpolyesters of 3-hydroxyalkanoates scaffolds into nerve cells.* Biomaterials, 2010. **31**: p. 1691-1698.

147. Salata, O.V., *Applications of nanoparticles in biology and medicine.* Journal of Nanobiotechnology, 2004. **2**: p. doi:10.1186/1477-3155-2-3.

148. Peek, L.J., C.R. Middaugh, and C. Berkland, *Nanotechnology in vaccine delivery.* Advanced drug delivery reviews, 2008. **60**: p. 915-928.

149. Mailänder, V., and K. Landfester, *Interaction of Nanoparticles with Cells.* Biomacromolecules, 2009. **10**: p. 2379-2400.

150. Atwood, J.A. and B.H.A. Rehm, *Protein engineering towards biotechnological production of bifunctional polyester beads.* Biotechnology letters, 2009. **31**: p. 131-137.

151. Jahns, A.C. and B.H.A. Rehm, *Tolerance of the Ralstonia eutropha class I polyhydroxyalkanoate synthase for translational fusions to its C terminus reveals a new mode of functional display.* Applied and environmental microbiology, 2009. **75**: p. 5461-5466.

152. Peters, V. and B.H.A. Rehm, *Protein engineering of streptavidin for in vivo assembly of streptavidin beads.* Journal of biotechnology, 2008. **134**: p. 266-274.

153. Brockelbank, J.A., V. Peters, and B.H.a. Rehm, *Recombinant Escherichia coli strain produces a ZZ domain displaying biopolyester granules suitable for immunoglobulin G purification.* Applied and environmental microbiology, 2006. **72**: p. 7394-7.

154. Lewis, J.G. and B.H.A. Rehm, *ZZ polyester beads: an efficient and simple method for purifying IgG from mouse hybridoma supernatants.* Journal of immunological methods, 2009. **346**: p. 71-4.

155. Mifune, J., K. Grage, and B.H.A. Rehm, *Production of functionalized biopolyester granules by recombinant Lactococcus lactis.* Appl Environ Microbiol, 2009. **75**(14): p. 4668-75.

156. Li, J., et al., *Endotoxin removing method based on lipopolysaccharide binding protein and polyhydroxyalkanoate binding protein PhaP.* Biomacromolecules, 2011. **12**: p. 602-8.

157. Sendil, D., et al., *Antibiotic release from biodegradable PHBV microparticles.* Journal of controlled release : official journal of the Controlled Release Society, 1999. **59**: p. 207-217.

158. Gurselt, I., et al., *In vitro antibiotic release from poly(3-hydroxybutyrate-co-3-hydroxyvalerate) rods.* Journal of microencapsulation. **19**: p. 153-64.

159. Francis, L., et al., *Controlled Delivery of Gentamicin Using Poly(3-hydroxybutyrate) Microspheres.* International journal of molecular sciences, 2011. **12**: p. 4294-4314.

160. Lu, X.-Y., et al., *Sustained release of PI3K inhibitor from PHA nanoparticles and in vitro growth inhibition of cancer cell lines.* Applied microbiology and biotechnology, 2011. **89**: p. 1423-33.

161. Chaturvedi, K., A.R. Kulkarni, and T.M. Aminabhavi, *Blend Microspheres of Poly (3-hydroxybutyrate) and Cellulose Acetate Phthalate for Colon Delivery of 5-Fluorouracil.* Industrial and Engineering Chemistry Research, 2011. **50**: p. 10414-10423.

162. Peng, Q., et al., *A rapid-acting, long-acting insulin formulation based on a phospholipid complex loaded PHBHHx nanoparticles.* Biomaterials, 2012. **33**: p. 1583-8.

163. Yao, Y.-C., et al., *A specific drug targeting system based on polyhydroxyalkanoate granule binding protein PhaP fused with targeted cell ligands.* Biomaterials, 2008. **29**: p. 4823-4830.

164. Banki, M.R., T.U. Gerngross, and D.W. Wood, *Novel and economical purification of recombinant proteins: Intein-mediated protein purification using in vivo polyhydroxybutyrate (PHB) matrix association.* Protein Science, 2005: p. 1387-1395.

165. Barnard, G.C., et al., *Integrated Recombinant Protein Expression and Purification Platform Based on Ralstonia eutropha Integrated Recombinant Protein Expression and Purification Platform Based on Ralstonia eutropha.* Society, 2005. **71**: p. 5735-5742.

166. Wang, Z., et al., *A novel self-cleaving phasin tag for purification of recombinant proteins based on hydrophobic polyhydroxyalkanoate nanoparticles.* Lab on a chip, 2008. **8**: p. 1957-62.

167. Zhang, S., Z.H. Wang, and G.Q. Chen, *Microbial polyhydroxyalkanote synthesis repression protein PhaR as an affinity tag for recombinant protein purification.* Microbial cell factories, 2010. **9**: p. 28.

168. Grage, K., V. Peters, and B.H.A. Rehm, *Recombinant protein production by in vivo polymer inclusion display.* Applied and environmental microbiology, 2011. **77**: p. 6706-6709.

169. Novick, S.J. and J.D. Rozzell, *Immobilization of Enzymes by Covalent Attachment*, in *Microbial Enzymes and Biotransformations*2005. p. 247-271.

170. Katchalski-Katzir, E., *Immobilized enzymes--learning from past successes and failures.* Trends in biotechnology, 1993. **11**: p. 471-478.

171. Sheldon, R.A., *Enzyme Immobilization: The Quest for Optimum Performance.* Advanced Synthesis & Catalysis, 2007. **349**: p. 1289-1307.

172. Peters, V. and B.H.A. Rehm, *In vivo enzyme immobilization by use of engineered polyhydroxyalkanoate synthase.* Applied and environmental microbiology, 2006. **72**.

173. Rasiah, I.A. and B.H.A. Rehm, *One-step production of immobilized alpha-amylase in recombinant Escherichia coli.* Appl Environ Microbiol, 2009. **75**(7): p. 2012-6.

174. Blatchford, P.A., et al., *Immobilization of organophosphohydrolase OpdA from Agrobacterium radiobacter by overproduction at the surface of polyester inclusions inside engineered Escherichia coli.* Biotechnology and bioengineering, 2011. **In press**: p. doi 10.1002/bit.24402.

175. Mullaney, J.A. and B.H.A. Rehm, *Design of a single-chain multi-enzyme fusion protein establishing the polyhydroxybutyrate biosynthesis pathway.* Journal of Biotechnology, 2010. **147**: p. 31-6.

176. Bäckström, B.T., J.A. Brockelbank, and B.H.A. Rehm, *Recombinant Escherichia coli produces tailor-made biopolyester granules for applications in fluorescence activated cell sorting: functional display of the mouse interleukin-2 and myelin oligodendrocyte glycoprotein.* BMC biotechnology, 2007. **7**: p. 3.

177. Grage, K. and B.H.A. Rehm, *In vivo production of scFv-displaying biopolymer beads using a self-assembly-promoting fusion partner.* Bioconjugate chemistry, 2008. **19**: p. 254-62.

178. Peters, V., D. Becher, and B.H.A. Rehm, *The inherent property of polyhydroxyalkanoate synthase to form spherical PHA granules at the cell poles: the core region is required for polar localization.* Journal of biotechnology, 2007. **132**: p. 238-45.

179. Jahns, A.C., R.G. Haverkamp, and B.H.A. Rehm, *Multifunctional inorganic-binding beads self-assembled inside engineered bacteria.* Bioconjugate chemistry, 2008. **19**: p. 2072-80.

180. Soppimath, K.S., et al., *Biodegradable polymeric nanoparticles as drug delivery devices.* Journal of controlled release: official journal of the Controlled Release Society, 2001. **70**: p. 1-20.

181. Parlane, N.A., et al., *Production of a particulate hepatitis C vaccine candidate by an engineered Lactococcus lactis strain.* Applied and environmental microbiology, 2011. **77**: p. 8516-8522.

182. Parlane, N.A., et al., *Vaccines displaying mycobacterial proteins on biopolyester beads stimulate cellular immunity and induce protection against tuberculosis.* Clinical and vaccine immunology, 2012. **19**: p. 37-44.

183. Parlane, N.A., et al., *Bacterial polyester inclusions engineered to display vaccine candidate antigens for use as a novel class of safe and efficient vaccine delivery agents.* Applied and environmental microbiology, 2009. **75**: p. 7739-44.

184. Villatoro-Hernandez, J., R. Montes-de-Oca-Luna, and O.P. Kuipers, *Expert opinion on Biological therapy*, 2011. p. 261-267.

185. Draper, J. and B.H.A. Rehm, *Engineering bacteria to manufacture functionalized polyester beads.* Bioengineered Bugs, 2012. **3**(4).

Chapter 3

Molecules **2014**, *19*, 1-x manuscripts; doi:10.3390/molecules190x0000x

OPEN ACCESS

molecules

ISSN 1420-3049

www.mdpi.com/journal/molecules

Review

3. Polyhydroxyalkanoate Synthase Fusions as a Strategy for Oriented Enzyme Immobilisation

David O. Hooks [1], Mark Venning-Slater [1], Jinping Du [1] and Bernd H. A. Rehm [1,2,*]

[1] Institute of Fundamental Sciences, Massey University, Private Bag 11222, Palmerston North, 4442, New Zealand; E-Mails: d.o.hooks@massey.ac.nz (D.O.H.); m.venningslater@massey.ac.nz (M.V.-S.); j.du@massey.ac.nz (J.D.)

[2] MacDiarmid Institute for Advanced Materials and Nanotechnology, Kelburn Parade, Wellington, 6140, New Zealand

* Author to whom correspondence should be addressed; E-Mail: b.rehm@massey.ac.nz; Tel.: +64 6 350 5515 ext84704

Received: 16 May 2014; in revised form: 19 June 2014 / Accepted: 19 June 2014 / Published: June 2014

Abstract: Polyhydroxyalkanoate (PHA) is a carbon storage polymer produced by certain bacteria in unbalanced nutrient conditions. The PHA forms spherical inclusions surrounded by granule associate proteins including the PHA synthase (PhaC). Recently, the intracellular formation of PHA granules with covalently attached synthase from *Ralstonia eutropha* has been exploited as a novel strategy for oriented enzyme immobilisation. Fusing the enzyme of interest to PHA synthase results in a bifunctional protein able to produce PHA granules and immobilise the active enzyme of choice to the granule surface. Functionalised PHA granules can be isolated from the bacterial hosts, such as *Escherichia coli*, and maintain enzymatic activity in a wide variety of assay conditions. This approach to oriented enzyme immobilisation has produced higher enzyme activities and product levels than non-oriented immobilisation techniques such as protein inclusion based particles. Here, enzyme immobilisation via PHA synthase fusion is reviewed in terms of the genetic designs, the choices of enzymes, the control of enzyme orientations, as well as their current and potential applications.

Keywords: Ralstonia eutropha; polyhydroxyalkanoate synthase; enzyme immobilisation

1. Oriented Enzyme Immobilisation

Enzymes can be viewed as industrial catalysts and have applications ranging from fine chemical synthesis to environmental bioremediation [1,2]. In general, enzymes have high activity under chemically mild conditions (low temperature, atmospheric pressure, near-neutral pH) and high specificity for their substrates. Despite these advantages, industrial use of enzymes can be hindered by lack of stability, the challenge of separation from product, and difficulty recycling the soluble enzyme. For multimeric enzymes the stability problem is even more pronounced as dissociation of the subunits at low concentrations is the first step in deactivation of the enzyme and leads to additional contamination of the final product. Immobilisation of enzymes overcomes these drawbacks. Immobilising an enzyme enhances performance under harsh conditions (temperature, pH, etc) and increases stability [3]. Immobilisation also allows simple separation of the catalyst from the product and facilitates re-use. Three broad categories of enzyme immobilisation exist: attachment to a solid support, encapsulation within a carrier, and carrier-free cross-linking [4]. In some techniques, the activity of the enzyme can be enhanced and its selectivity altered. If performed with care, immobilisation can also prevent subunit dissolution and keep the local concentration of enzyme high [5].

In addition to the increase in stability and recyclability, immobilisation provides the opportunity to co-localise multiple enzymes creating a synthetic multienzyme complex (MEC) that mimics structures found in nature and allows for more complex, multistep reaction *in vitro* [6]. Further, oriented immobilisation has been considered important for higher catalytic activity, optimal electron exchange between the redox enzymes and

support material, and activation of hydrophobic active sites for hydrophobic substrates [7]. In the case of redox enzymes, the enzyme active site needs to be in close proximity to the carrier so the transfer of electrons can occur. In other cases, such as the immobilisation of subtilisin, the active site may need to be fully exposed to the solute to allow efficient access by the substrate [8]. Using particular attachment sites can alter an enzyme's properties including enhanced stability [3]. Finally, oriented enzyme immobilisation is also thought to be crucial for the optimal function and miniaturisation of biosensors [7]. This review covers the advances made in a particular *in vivo* enzyme immobilisation technique using the natural properties of bacterial polyhydroxyalkanoate (PHA) inclusion formation to generate oriented display of enzymes attached to a solid support.

2. Polyhydroxyalkanoate Biobeads

PHAs, also referred to as bioplastics or biopolyesters, are naturally occurring polyesters composed of (*R*)-3-hydroxy fatty acids. Many bacteria and some archaea are able to produce PHAs under carbon-excess and nitrogen-limiting conditions [9]. These polyesters are stored as water-insoluble inclusions inside the cells and serve as energy and carbon storage polymers [10–12].

Formation of the most common short chain-length PHAs, such as polyhydroxybutyrate, requires three key enzymes. The β-ketothiolase (PhaA) catalyses the condensation of acetyl-CoA, acetoacetyl-CoA reductase (PhaB) reduces the condensation product acetoacetyl-CoA into PHA precursor molecule (*R*)-3-hydroxybutyryl-CoA, and the PHA synthase (PhaC)

polymerises the precursor molecule into PHA [13,14]. The PHA biosynthesis pathway from the PHA inclusion model organism *Ralstonia eutropha* has been successfully transferred to and established in recombinant bacteria like Gram-negative *Escherichia coli,* as well as Gram-positive organisms such as *Corynebacterium glutamicum* and *Lactococcus lactis* [15–17]. In these recombinant systems, PhaA and PhaB are produced as soluble proteins. The PhaC is under the control of an inducible T7 promoter and the expressed enzyme remains covalently attached to the growing PHA chain.

As the PHA synthase (PhaC) remains covalently attached to the polyester core of the inclusions, it is considered as an important tag for anchoring target proteins on the surface of PHAs and to produce functionalised biobeads. This is achieved by first constructing fusions of the PhaC to proteins of interest. Production of these fusion proteins in recombinant bacteria (either natural or engineered PHA producers) leads to the formation of functionalised PHA biobeads. A significant advantage to this approach is the elimination of a chemical attachment step of the free enzyme to a support material. This crosslinking step is often expensive or difficult and results in a random orientation of enzymes to the support material surface. In contrast, the PhaC fusions anchor the protein of interest in a defined orientation to the biopolyester surface *in vivo* meaning the protein of interest is being immobilised prior to isolation. Other ways to get oriented enzyme display have been reviewed, including site-directed mutagenesis [18].

3. *In Vivo* Immobilisation and Surface Display

In natural producers of PHB, phasins (PhaP) can comprise up to 5% of the intracellular proteins making them the most abundant granule-associated protein [19]. The potential for PhaP to be used as the anchor protein for recombinant enzyme immobilisation and display was demonstrated by the fusion of β-galactosidase to PhaP via a self-cleaving intein [20]. PHA biobeads were separated from lysed cells by gradient centrifugation and the β-galactosidase was cleaved using a DTT-containing solution. The purified β-galactosidase had a specific activity of 53 U/μmol, comparable to other purification methods [20]. Additionally, recombinant human tissue plasminogen activator (rPA) was fused to PhaP with a thrombin cleavage site as the linker [21]. As rPA is a serine protease with multiple disulfide bonds, recombinant expression is difficult. In the fibrin degradation assay, rPA was found to be active both when attached to the biobeads and after cleavage into solution with thrombin [21].

PhaC can be divided into Classes I to IV based on quaternary structure and composition of the PHA synthesised. Not only Class I but also Class II PhaC has been demonstrated capable of immobilising enzymes on PHA biobeads. Both Class I and Class II PhaC consist of only one subunit. However Class I PhaC produces short-chain-length PHA, while Class II PhaC yields medium-chain-length PHA [10].

In 2006 β-galactosidase was successfully immobilised on PHA beads using a PHA-negative mutant of *Pseudomonas aeruginosa* and by fusing this enzyme N-terminally to Class II PHA synthase from *P. aeruginosa* [22]. Further studies switched to an engineered

E. coli PHA producing system using N- and/or C- terminal fusions to Class I PhaC from *R. eutropha* in order to immobilise a series of technical enzymes [23–26].

A variety of enzymes ranging from oxidoreductase (NemA), hydrolase (for example, β-galactosidase, LacZ [EC 3.2.1.23]; α-amylase, BLA [EC 3.2.1.1]; and organophosphohydrolase, OpdA [EC 3.1.8.1]), lyase (*N*-acetylneuraminic acid aldolase, NanA [EC 4.1.3.3]), to isomerase (*N*-acetylglucosamine 2-epimerase, Slr1975 [EC 5.1.3.8]) were successfully immobilised to PHA biobeads [23–26]. These enzymes differed in quaternary structures from monomer (BLA), dimer (OpdA, Slr1975) to tetramer (NanA, LacZ), and ranged in monomer size from about 33 kDa (NanA) to 116 kDa (LacZ) [27–31]. In addition, two of the immobilised enzymes (BLA and OpdA) are secreted in their original hosts. Enzymes originated from a variety of hosts such as Gram-positive bacterium *Bacillus licheniformis* (BLA); as well as Gram-negative bacteria *E. coli* (LacZ, NemA, NanA), *Agrobacterium radiobacter* (OpdA) and the cyanobacterium *Synechocystis* sp. (Slr1975).

Immobilisation of enzymes to PHA biobeads by fusion to either PhaP or PhaC has been shown to be viable. PhaP attaches to the PHA biobead through hydrophobic interactions whereas PhaC is stabilised by a covalent attachment to the PHA polymer itself. Additionally, the use of PhaP as an anchoring protein requires an extra gene which is strictly unnecessary for the recombinant production of PHA biobeads. Elimination of PhaP allows for PhaC to coat the outer surface of the PHA biobeads. Possibly due to its weaker interaction with the PHA biobead, PhaP is used when isolation of soluble enzyme is desired [20,21]. For enzyme immobilisation, PhaC has been seen as the anchoring protein

of choice, especially if harsh reaction conditions and multiple recycles are required [24–26].

4. *In Vitro* Immobilisation and Surface Display

In addition to the *in vivo* approach, PHA biobeads can also be produced *in vitro* [32,33]. This method involves first expressing and purifying the PhaC-fusion protein from a recombinant host then PHB nanoparticles (diameter 200 nm) are formed from pure PHB. Finally, the PhaC-fusion protein, PHB nanoparticles, and the PhaC substrate 3-hydroxybutyryl-coenzyme A (3-HB-CoA) are mixed together. PhaC polymerises the 3-HB-CoA forming a fusion protein-PHB hybrid molecule. The growing hydrophobic PHB chain is pushed towards the hydrophobic PHB nanoparticle with the fusion protein facing the aqueous environment. So far, this approach has only been used to immobilise the targeting peptide RGD4C [32] and green fluorescent protein (GFP) [33] but the same principle could apply to enzyme immobilisation in the future. The RGD4C tagged biobeads were shown to be targeted to MDA-MB 231 breast cancer cells *in vitro* and able to deliver the lipophilic dye Nile Red as a model drug [32]. The advantages of an *in vitro* approach to PHA biobeads are control over biobead purity as well as size which can be modulated by the amount of 3-HB-CoA added to the emulsion. The disadvantages are the increase in complexity and production costs when compared to the one-step *in vivo* immobilisation of fusion protein.

5. Orientation of Biobead Immobilised Enzymes

The orientation of an enzyme crosslinked to a support material is critical for its functionality/activity *i.e.* the ability to bind and convert a substrate. For example, structural analysis of a lipase from *Thermomyces lanuginosus* (TLL) showed that the enzyme possesses an alpha-helical surface loop lid (a common structure of lipases) that governs access of reaction media to the hydrophobic active site [34–36]. TLL, like most lipases, is activated at the oil/water interface which induces the lid to open providing access to the active site of the enzyme. Immobilisation of TLL to a hydrophobic support by utilising this interfacial activation, orientates the enzyme so that it is stabilised in its open conformation and leads to hyperactive levels of activity [37,38].

As described above, the enzymes fused to PhaC are displayed on the surface of PHA beads. PhaC dictates a homogenous orientation of its fusion partner at the surface of the beads which, if properly engineered, provides maximum interaction with substrate, hence leading to high specific activity of the immobilised enzyme. Additionally, the non-porous nature of the PHA beads avoids the problem of substrate diffusion by enabling convective interactions. Due to the co-translation of enzyme-PhaC fusions, enzymes are orientated in one of two directions, depending on whether the fusion occurs at the N- or C-terminus (Figure 3.1). For example, a variant of a thermostable α-amylase from *B. licheniformis* has been fused by its C-terminus to PhaC which led to the successful production and isolation of PHA beads that exhibit enzyme activity [23]. Furthermore, in two separate studies, a chromium (VI) reductase (NemA) from *E. coli* and an organophosphate hydrolase from *A. radiobacter* (OpdA) have been fused to PhaC via their N-termini, respectively, and have

also resulted in the isolation of enzymatically active PHA beads [24,26]. However, there is evidence that orientation via fusion at either terminus can affect enzyme activity. PHA beads were produced that displayed an *N*-acetylneuraminic acid aldolase (NanA) from *E. coli* that was fused by either its N- or C-terminus [25]. Under optimal conditions it was shown that fusion protein which had NanA fused at its C-terminus to PhaC (NanA-PhaC) produced beads that exhibited superior NanA activity compared to beads formed from PhaC-NanA. This study also demonstrated the possibility of fusing two enzymes to the PhaC termini simultaneously using NanA and an *N*-acetylglucosamine 2-epimerase (Slr1975) from *Synechocystis* sp. strain PCC 6803. Although beads displaying single enzymes exhibited higher activity, functional dual-enzyme beads could still be obtained, highlighting the potential for immobilising enzymes of the same pathway in close proximity.

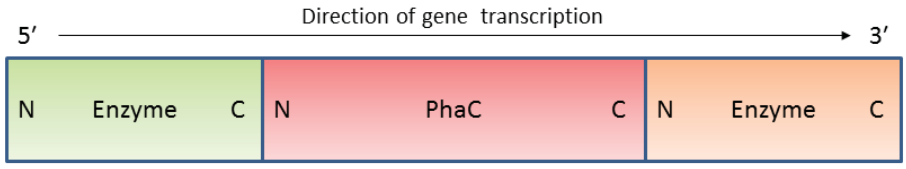

Figure 3.1. Potential sites of enzyme attachment utilising gene fusions to PHA synthase. N,N-terminus; C,C-terminus.

6. Quaternary Structures of Immobilised Enzymes

Enzymes used in industry encompass a range of quaternary structures, and the correct conformation of these structures is critical in the display of enzyme activity. Therefore, an enzyme immobilisation system must have a strong bond between enzyme and support while allowing flexibility for the enzyme to fold correctly, *i.e.*, to form its functional quaternary structure. Various enzymes have been immobilised using the PHA immobilisation system and have retained activity, demonstrating the versatility of this system.

A modified thermostable α-amylase (BLA) from *B. licheniformis* was immobilised and displayed on PHA beads [23]. BLA is a monomeric enzyme with a molecular mass of approximately 55 kDa [29]. Interestingly, the BLA-PHA beads were thermostable retaining activity after incubation at 85 °C for 5 h [23]. The OpdA quaternary structure can be deduced from an extensively studied homologue from *Brevundimonas diminuta* (a.k.a *Pseudomonas diminuta*) which has been shown to be dimeric [28]. NanA has been shown to be homotetrameric where each subunit consists of an α/β-barrel domain and three α-helices extending from the C-terminus [31]. Although comparisons with free NanA enzymes were not within the scope of this study, NanA-PhaC and PhaC-NanA beads demonstrated aldolase activity with NanA-PhaC exhibiting superior activity at 590 U/g dry bead weight [25]. In addition, NanA was also fused to PhaC in conjunction with the dimeric enzyme *N*-acetylglucosamine 2-epimerase (Slr1975) from *Synechocystis* sp. strain PCC 6803 to yield beads displaying both enzymes [25]. The structure of a homologous epimerase has been resolved [30]. Interestingly, only NanA-PhaC-Slr1975 beads displayed activity,

suggesting limits on the placement of enzyme functions within the PhaC fusion protein. However, Slr1975-PhaC-NanA beads did form, demonstrating the robustness of the PhaC enzyme in exhibiting its own enzyme activity and bead forming ability.

PHA beads have been shown to be capable of displaying active enzymes with varying quaternary structures, and also in different combinations. Being able to fuse enzyme functions to both the N and C-termini of PhaC, as single and dual enzyme functions, demonstrates the versatility and potential of PHA beads in enzyme applications.

7. The Initial Proof of Concept of PHA Synthase Mediated Enzyme Immobilisation

As mentioned above, the first proof for PHA synthase mediated enzyme immobilisation was obtained in 2006 [22]. β-galactosidase-displaying PHA beads were produced by fusing β-galactosidase from *E. coli* to the N-terminus of Class II PhaC from *P. aeruginosa*.

The PHA-negative mutant of *P. aeruginosa* PAO1 was complemented by plasmid pBBR1JO5-lacZphaC1 containing the LacZ-PhaC fusion protein encoding gene under *lac* promoter control. Cells were cultivated under conditions favouring PHA bead accumulation. Upon bead isolation, the β-galactosidase was demonstrated to be covalently immobilised on the bead surface and showed an activity of 68,000 MU on average, with a K_m of 630 μM and a V_{max} of 17.6 nmol/min using orthonitrophenyl-β-D-galactopyranoside as substrate. This result shed lights on protein engineering of PHA synthase as a platform technology for efficient covalent enzyme immobilisation.

8. Current Applications

PHA beads have been used to immobilise a variety of enzymes that can be used for a range of applications from food production to the synthesis of fine chemicals. The successful display of a thermostable α-amylase (BLA) could be used in a wide variety of industries that require starch liquefaction including food processing, detergent manufacture, paper processing, and textiles [39–41]. Immobilised enzymes have a potential use in the bioremediation of toxic chemicals which would otherwise persist in the environment. Hexavalent chromium is a water-soluble toxin generated by a range of industries including pigment production, leather tanning, wood preservation, stainless steel manufacture, and nuclear technology [24,42]. PHA beads displaying pollutant detoxifying or degrading enzymes will likely enhance the residence time of the respective enzyme in the polluted environment while being fully biodegraded over time. In combination with either *Bacillus subtilis* glucose dehydrogenase or *Candida boidinii* formate dehydrogenase as a cofactor generating partner, PHA beads displaying NemA were able to transform toxic, water-soluble chromium (VI) to relatively non-toxic, water-insoluble chromium (III) [24]. Another bioremediation target is the build-up of certain pesticides. Organophosphate pesticides are highly toxic and intentionally used in farming, particularly in the developing world, and account for approximately 200,000 deaths per year and are considered as a significant global health problem by the World Health Organisation [43,44]. Due to such use there is the potential of contamination to water supplies. PHA beads displaying OpdA were able to effectively degrade the organophosphate insecticide coumaphos present in undiluted wool scour in less than two

hours [26]. Finally, PHA beads displaying enzymes have potential use in fine chemical synthesis. The NanA and Slr1975 enzymes can catalyse a reaction pathway involved in the synthesis of *N*-acetylneuraminic acid (Neu5Ac), a precursor of an antiviral used as a neuraminidase inhibitor for the treatment of influenza virus infections [45–47]. Both single enzyme and double-enzyme beads were successfully employed in the production of this fine chemical, and represent an alternative to chemical synthesis [25]. The successful display of active enzymes that exhibit a range of quaternary structure and activity illustrates the versatility of the PHA bead enzyme immobilisation system for research and industry.

9. Performance of PHA Bead Immobilized Enzymes

The initial fusion of LacZ to PhaC possessed immobilised LacZ with a binding affinity of 630 µM [22] which was high when compared with the method of attaching LacZ covalently to gold-coated devices [48]. Immobilisation of the α-amylase to PHA beads resulted in Michaelis-Menten kinetics with V_{max} at 506 mU/mg bead protein and a K_m of 5 µM [23] which is consistent with free α-amylase at 9.6 µM but less than measured for α-amylase attached to cellulose beads of 44 µM [40]. After three cycles of reaction the immobilised α-amylase retained 78% of its initial activity.

In the case of OpdA immobilisation, the K_m of covalently attached PhaC-OpdA protein was found to be 250 µM, about 1.6 times higher than free OpdA at 160 µM [26]. The apparent k_{cat} for attached PhaC-OpdA was 139 s^{-1}; 16 times lower than for free OpdA at 2300 s^{-1}. These values result in a second order rate constant (k_{cat}/K_m) of 5.5x10^5 $M^{-1}s^{-1}$ for

attached PhaC-OpdA and 1.4×10^7 $M^{-1}s^{-1}$ for free OpdA. The thermal properties were also assessed with attached PhaC-OpdA having slightly more thermal stability than free OpdA. An increase of 1.58 °C in apparent melting temperature and a slow decline in activity from 35–80 °C was seen in attached PhaC-OpdA compared to a rapid decline in activity for free OpdA at 55–70 °C. Both can perform in the demanding reaction environment of wool scour. Long-term stability was assessed in tap water at 25 °C with little loss in activity or difference between the attached and free OpdA observed after 11 days. After 5 months storage, 15% of the attached OpdA activity remained [26].

Immobilisation of NemA to PHA beads resulted in a substantial increase in the K_m for chromium VI to 95 µM compared to the free NemA at 1.7 µM. However, the K_m for NADH was essentially identical: 49 µM for attached NemA compared to 45 µM for free NemA [24]. Even though the immobilisation reduced the ability of NemA to transform chromium VI, the data indicated that it remained an efficient chromium VI reductase. Stability of the immobilised NemA was high, after nine months at 4 °C no reduction in enzyme activity was detectable [24].

Activity of Slr1975 fusion protein immobilised to PHA beads was measured at 1.8 U/mg and 0.58 U/mg depending on the arrangement of the fusion protein [25]. These values are lower than the previously reported activities of immobilised GlcNAc-2 epimerases which range from 3.4–29 U/mg protein [49,50]. During the same study, NanA was also immobilised to the PHA beads. The activity of NanA fusion protein was measured at 43 U/mg and 82 U/mg [49,50], again depending on the arrangement of the fusion protein. These values compared favourably with the previously reported activities of immobilised

NanA between 2.5–36 U/mg protein. Moreover, an alternative GFP fusion protein particle approach for immobilisation of NanA resulted in specific NanA activity of 76 mU/mg [51].

In general, the effect of immobilising an enzyme to the PHA beads is an increase in the K_m when compared to free enzyme. However, when compared to other immobilisation methods, the PHA system performs to approximately the same level in regard to the measured properties with some variation depending on the enzyme of interest. The direct comparison of specific enzymes immobilised to PHA beads and immobilised to GFP fusion protein particles is particularly relevant because of the similarity in fusion protein construction. In all three cases, NanA, α-amylase, and OpdA the performance under the same reaction conditions is less for the GFP fusion protein particles when compared to the equivalent PHA bead [51]. This is likely to be due to differences in the way the different particles form and the resultant orientation and surface exposure of the respective enzyme. In the PHA beads the enzyme is displayed on the bead surface which allows for active site access by the substrate. In the GFP fusion particles, the enzyme may be buried in a random orientation and with limited substrate access to the enzyme.

10. Potential Applications

The PHA synthase enzyme immobilisation system is amenable to functional fusions on both termini simultaneously [52], even with two different enzymes [25], or a protein functionality of choice (Figure 3.2). This creates an opportunity for a multistep catalysis reaction or biomolecular interaction to be established. In nature, many enzymes are known to operate in multi-enzyme complexes (MEC), for example tryptophan synthase, or

the pyruvate dehydrogenase complex. Display systems which allow the immobilisation of two or more enzymes can be useful as a model of biological enzyme complexes. MECs have high local concentration of intermediates, lessening reaction inefficiencies caused by diffusion.

This is especially valuable for highly reactive intermediates which degrade quickly. Of critical importance in a dual enzyme immobilisation system is the relative positioning of the enzymes and their level of interaction. In most dual immobilisation systems, steric hindrance prevents compact display. However, in the PHA system, the enzymes are brought together by the initial fusion, dimerisation of PhaC, and formation of a PHA bead with a surface display of the fusion protein. Further, there is some evidence suggesting the PhaC dual fusion partners are in close proximity [25,52]. The potential of the PHA

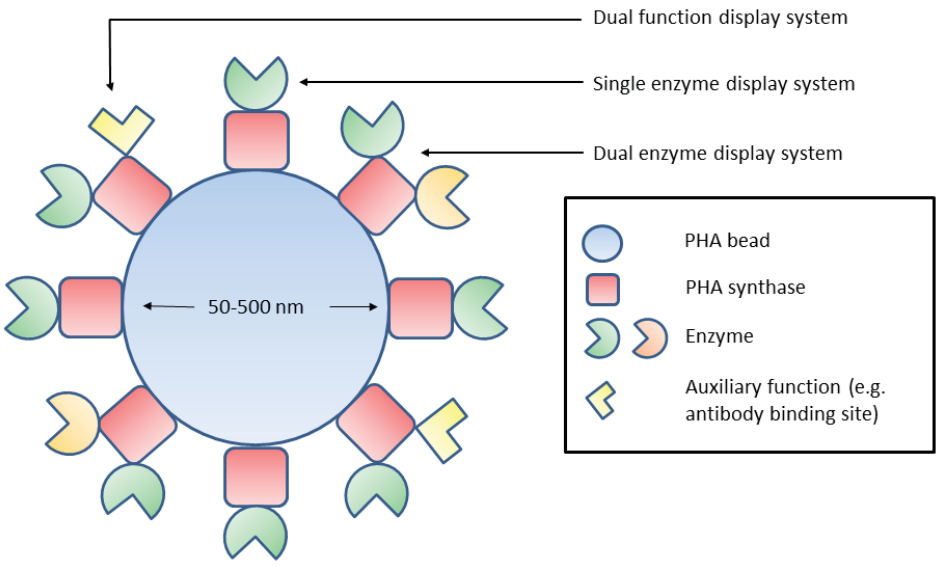

Figure 3.2. Potential applications of the PHA bead display system.

immobilisation system to enhance dual enzyme display could be further explored with the widely used model glucose oxidase/horse radish peroxidase (GOx/HRP) glucose detection system. Certain dual enzyme display approaches have been shown to enhance intermediate hydrogen peroxide conversion up to 250% compared with the equivalent amount of free enzyme in solution [53]. Other systems could include a main enzyme and a secondary helper enzyme which enhances enzymatic activity by regeneration of cofactors. An example of fine chemical synthesis by a dual enzyme system is D-hydantoinase/D-carboamylase (D-case) which mediates the formation of the optically pure antibiotic precursor, p-hydroxyphenylglycine (D-pHPG), from a racemic mixture of hydroxyphenylhydantoin [54]. In commercial preparation of D-pHPG, a chemical process is used for the second step due to the high oxidative sensitivity and low stability of D-case. A dual enzyme system immobilised to chitin had increased pH stability and activity at low temperatures [54]. Finally, the enzyme pair could work in tandem to produce a greater result than either could produce alone, such as the industrially useful enzyme laccase combined with HRP. This combination allows the breakdown of lignin to occur to a greater extent than each enzyme separately [55].

11. Discussion

The recent studies on the PHA biobead enzyme display technology have revealed the flexibility of the system. It is able to successfully express enzymes with different functional roles, varying quaternary structure, and potential applications. The K_m is often, but not always, higher for the immobilised enzyme than the free enzyme meaning lower substrate

binding affinity for the attached enzyme. In the case of immobilised OpdA, k_{cat} was also substantially reduced [26]. However, it is expected that immobilised enzymes would have weaker substrate affinities when compared to their free counterparts in solution. One of the main advantages of enzyme immobilisation is the ability to recycle the enzyme over multiple uses. The α-amylase displaying beads were able to be recycled over three reactions while the NanA and Slr1975 displaying beads were able to be used over five cycles each [23,25].

Additional research has included studying the function of enzymes displayed on PHA beads in comparison to enzymes immobilised to GFP fusion protein particles [51]. Samples were standardised based on the amount of fusion protein per reaction, and then subjected to a variety of treatments followed by the respective activity assay. Beads and particles displaying BLA, NanA, and OpdA were assessed. In all cases enzyme-bearing PHA beads catalysed higher rates of reaction, as well as achieved higher levels of product formation [51]. This difference in activity is possibly due to differences in the way in which PHA beads and GFP particles form, and the resultant display of the enzymes. As explained above, the PhaC is responsible for the formation of PHA beads, and remains covalently attached at the bead surface [12]. Therefore, any enzyme that is fused to PhaC is also displayed on the bead surface, and has ready access to substrate. Although no model for GFP particle formation has been proposed, evidence suggests that they are similar to inclusion bodies consisting of GFP fusion proteins that contain a fusion of GFP, an inactive variant of PhaC (PhaC(C319A)), and the relevant enzyme fused at the C-terminus. The inactive PhaC was also found to be replaceable by different polypeptides serving as linker

between engineered GFP and the fused target protein. Inclusion bodies are protein aggregates that have been commonly observed in bacteria that have been engineered to overproduce recombinant proteins [56]. They form through the aggregation of partially misfolded proteins that have been overproduced, which form proto-aggregates that aggregate further to form mature inclusion bodies [57,58]. Furthermore, structural analysis of inclusion bodies has identified native-like secondary structure of the constituent proteins and amyloid-like cross-molecular β-sheet formations indicating an ordered process of formation [56,59]. Although inclusion bodies exhibit an ordered structure the constituent proteins are displayed throughout the aggregate. In terms of enzyme-bearing GFP particles, this means there is little control on the placement and orientation of the enzyme fusions. As the assays were standardised on the amount of fusion protein, most of the fusion protein used in the GFP particle reaction was below the surface of the particle separated from substrate. Furthermore, it is also possible that the enzyme portion of the surface fusion proteins are still buried below the surface of the particles, or in an orientation that restricts movement, therefore, resulting in decreased activity. Moreover, if the formation of GFP particles abides by the current model of inclusion body formation not all of the fusion protein of the GFP particles will be correctly folded [56,58]. Therefore, only a fraction of the fusion protein in GFP particles will consist of active enzyme of which only a fraction will have access to substrate. Observing decreased enzyme activity of GFP particles in comparison to PHA beads indicates a favourable comparison to inclusion bodies, and that some enzyme molecules of the GFP fusion proteins are not optimally placed. Interestingly, GFP particles have been shown to

function comparably to PHA beads, and even to a higher extent, in terms of IgG binding capacity when fused to the IgG binding domain ZZ derived from protein A[60]. This could be due to differences in particle density, shape, surface area, the IgG binding sites in comparison to enzymes, and the ability of the ZZ-domain to rapidly fold after translation. However, despite this, enzyme activity comparisons based on fusion protein quantity highlights the importance of providing favourable conditions for enzyme protein folding, and for controlled enzyme placement and orientation.

12. Outlook

The PHA beads immobilisation method was proven to be versatile as a variety of functionally and structurally diverse enzymes could be actively immobilised. Compared to other immobilisation methods the enzymatic properties of the PHA beads were not always superior. However, very little was undertaken to optimise the immobilisation strategy, *i.e.*, improve the design of the PhaC fusion protein. For example LacZ had a higher K_m and Slr1975 had a lower activity but NanA had a higher activity than other NanA immobilisation techniques [22]. Direct experimental comparison of oriented PHA biobeads to GFP fusion particles revealed that enzymes immobilised to PHA beads consistently reached higher product formation rates [51]. This effect was observed for enzymes active as monomers, dimers, and tetramers indicating the advantages and flexibility of the PHA biobead system. The production levels of 1.5 g per litre of bacterial culture for at least some enzyme biobeads indicate a high level of volumetric productivity [24]. Attention to design of the fusion protein is needed as enzymes which may be functional when

expressed on one terminus of PhaC are sometimes not functional when fused to the other [25]. Future research in this field will include double enzyme fusions especially in high-value product lines such as biofuels, flavanoids, and optically pure pharmaceuticals.

Acknowledgments

This work was supported by the Institute of Fundamental Sciences at Massey University, New Zealand.

Author Contributions

DOH: writing and revision, MV-S: writing and revision, JD: writing, BHAR: revision.

Conflicts of Interest

The authors declare no conflict of interest.

References

1. Fernández-Fernández, M.; Sanromán, M.Á.; Moldes, D. Recent developments and applications of immobilized laccase. *Biotechnol. Adv.* **2013**, *31*, 1808–18025.
2. Muñoz Solano, D.; Hoyos, P.; Hernáiz, M.J.; Alcántara, a R.; Sánchez-Montero, J.M. Industrial biotransformations in the synthesis of building blocks leading to enantiopure drugs. *Bioresour. Technol.* **2012**, *115*, 196–207.
3. Mateo, C.; Palomo, J.M.; Fernandez-Lorente, G.; Guisan, J.M.; Fernandez-Lafuente, R. Improvement of enzyme activity, stability and selectivity via immobilization techniques. *Enzyme Microb. Technol.* **2007**, *40*, 1451–1463.
4. Sheldon, R.A.; van Pelt, S. Enzyme immobilisation in biocatalysis: Why, what and how. *Chem. Soc. Rev.* **2013**, *42*, 6223–6235.
5. Fernandez-Lafuente, R. Stabilization of multimeric enzymes: Strategies to prevent subunit dissociation. *Enzyme Microb. Technol.* **2009**, *45*, 405–418.
6. Jia, F.; Narasimhan, B.; Mallapragada, S. Materials-based strategies for multi-enzyme immobilization and co-localization: A review. *Biotechnol. Bioeng.* **2013**, *111*, 209–222.
7. Steen Redeker, E.; Ta, D.T.; Cortens, D.; Billen, B.; Guedens, W.; Adriaensens, P. Protein engineering for directed immobilization. *Bioconjug. Chem.* **2013**, *24*, 1761–1777.
8. Huang, W.; Wang, J.; Bhattacharyya, D.; Bachas, L.G. Improving the activity of immobilized subtilisin by site-specific attachment to surfaces. *Anal. Chem.* **1997**, *69*, 4601–4607.
9. Tan, G.-Y.; Chen, C.-L.; Li, L.; Ge, L.; Wang, L.; Razaad, I.; Li, Y.; Zhao, L.; Mo, Y.; Wang, J.-Y. Start a Research on Biopolymer Polyhydroxyalkanoate (PHA): A Review. *Polymers (Basel).* **2014**, *6*, 706–754.
10. Rehm, B.H.A. Polyester synthases: Natural catalysts for plastics. *Biochem. J.* **2003**, *376*, 15–33.
11. Rehm, B.H.A. Genetics and biochemistry of polyhydroxyalkanoate granule self-assembly: The key role of polyester synthases. *Biotechnol. Lett.* **2006**, *28*, 207–213.
12. Grage, K.; Jahns, A.C.; Parlane, N.; Palanisamy, R.; Rasiah, I.A.; Atwood, J.A.; Rehm, B.H.A. Bacterial polyhydroxyalkanoate granules: biogenesis, structure, and potential use as nano-/micro-beads in biotechnological and biomedical applications. *Biomacromolecules* **2009**, *10*, 660–669.
13. Normi, Y.M.; Hiraishi, T.; Taguchi, S.; Abe, H.; Sudesh, K.; Najimudin, N.; Doi, Y. Characterization and properties of G4X mutants of Ralstonia eutropha PHA synthase for poly(3-hydroxybutyrate) biosynthesis in Escherichia coli. *Macromol. Biosci.* **2005**, *5*, 197–206.
14. Satoh, Y.; Tajima, K.; Tannai, H.; Munekata, M. Enzyme-catalyzed poly(3-hydroxybutyrate) synthesis from acetate with CoA recycling and NADPH regeneration in Vitro. *J. Biosci. Bioeng.* **2003**, *95*, 335–341.
15. Jo, S.-J.; Maeda, M.; Ooi, T.; Taguchi, S. Production system for biodegradable polyester polyhydroxybutyrate by Corynebacterium glutamicum. *J. Biosci. Bioeng.* **2006**, *102*, 233–236.

16. Mifune, J.; Grage, K.; Rehm, B.H.A. Production of functionalized biopolyester granules by recombinant Lactococcus lactis. *Appl. Environ. Microbiol.* **2009**, *75*, 4668–4675.
17. Valappil, S.P.; Boccaccini, A.R.; Bucke, C.; Roy, I. Polyhydroxyalkanoates in Gram-positive bacteria: insights from the genera Bacillus and Streptomyces. *Antonie Van Leeuwenhoek* **2007**, *91*, 1–17.
18. Hernandez, K.; Fernandez-Lafuente, R. Control of protein immobilization: coupling immobilization and site-directed mutagenesis to improve biocatalyst or biosensor performance. *Enzyme Microb. Technol.* **2011**, *48*, 107–122.
19. Steinbuchel, A.; Aerts, K.; Babel, W.; Follner, C.; Liebergesell, M.; Madkour, M.H.; Mayer, F.; Pieper-Furst, U.; Pries, A.; Valentin, H.E. Considerations on the structure and biochemistry of bacterial polyhydroxyalkanoic acid inclusions. *Can. J. Microbiol.* **1995**, *41* (Suppl. 1), 94–105.
20. Barnard, G.C.; McCool, J.D.; Wood, D.W.; Gerngross, T.U. Integrated recombinant protein expression and purification platform based on Ralstonia eutropha. *Appl. Environ. Microbiol.* **2005**, *71*, 5735–5742.
21. Geng, Y.; Wang, S.; Qi, Q. Expression of active recombinant human tissue-type plasminogen activator by using *in vivo* polyhydroxybutyrate granule display. *Appl. Environ. Microbiol.* **2010**, *76*, 7226–7230.
22. Peters, V.; Rehm, B.H.A. *In vivo* enzyme immobilization by use of engineered polyhydroxyalkanoate synthase. *Appl. Environ. Microbiol.* **2006**, *72*, 1777–83.
23. Rasiah, I.A.; Rehm, B.H.A. One-step production of immobilized alpha-amylase in recombinant Escherichia coli. *Appl. Environ. Microbiol.* **2009**, *75*, 2012–2016.
24. Robins, K.J.; Hooks, D.O.; Rehm, B.H.A.; Ackerley, D.F. Escherichia coli NemA is an efficient chromate reductase that can be biologically immobilized to provide a cell free system for remediation of hexavalent chromium. *PLoS One* **2013**, *8*, e59200.
25. Hooks, D.O.; Blatchford, P.A.; Rehm, B.H.A. Bioengineering of bacterial polymer inclusions catalyzing the synthesis of N-acetylneuraminic acid. *Appl. Environ. Microbiol.* **2013**,*79*, 3116–3121.
26. Blatchford, P.A.; Scott, C.; French, N.; Rehm, B.H.A. Immobilization of organophosphohydrolase OpdA from Agrobacterium radiobacter by overproduction at the surface of polyester inclusions inside engineered Escherichia coli. *Biotechnol. Bioeng.* **2012**, *109*, 1101–1108.
27. Juers, D.H.; Jacobson, R.H.; Wigley, D.; Zhang, X.J.; Huber, R.E.; Tronrud, D.E.; Matthews, B.W. High resolution refinement of beta-galactosidase in a new crystal form reveals multiple metal-binding sites and provides a structural basis for alpha-complementation. *Protein Sci.* **2000**, *9*, 1685–1699.
28. Benning, M.M.; Shim, H.; Raushel, F.M.; Holden, H.M. High resolution X-ray structures of different metal-substituted forms of phosphotriesterase from Pseudomonas diminuta. *Biochemistry* **2001**, *40*, 2712–2722.
29. Hwang, K.Y.; Song, H.K.; Chang, C.; Lee, J.; Lee, S.Y.; Kim, K.K.; Choe, S.; Sweet, R.M.; Suh, S.W. Crystal structure of thermostable alpha-amylase from Bacillus licheniformis refined at 1.7 A resolution. *Mol. Cells* **1997**, *7*, 251–258.
30. Lee, Y.-C.; Wu, H.-M.; Chang, Y.-N.; Wang, W.-C.; Hsu, W.-H. The central cavity from the (alpha/alpha)6 barrel structure of Anabaena sp. CH1 N-acetyl-D-glucosamine 2-

epimerase contains two key histidine residues for reversible conversion. *J. Mol. Biol.* **2007**, *367*, 895–908.
31. Izard, T.; Lawrence, M.C.; Malby, R.L.; Lilley, G.G.; Colman, P.M. The three-dimensional structure of N-acetylneuraminate lyase from Escherichia coli. *Structure* **1994**, *2*, 361–369.
32. Kim, H.-N.; Lee, J.; Kim, H.-Y.; Kim, Y.-R. Enzymatic synthesis of a drug delivery system based on polyhydroxyalkanoate-protein block copolymers. *Chem. Commun. (Camb.)* **2009**, *7345*, 7104–7106.
33. Lee, J.; Jung, S.-G.; Park, C.-S.; Kim, H.-Y.; Batt, C. a; Kim, Y.-R. Tumor-specific hybrid polyhydroxybutyrate nanoparticle: surface modification of nanoparticle by enzymatically synthesized functional block copolymer. *Bioorg. Med. Chem. Lett.* **2011**, *21*, 2941–2944.
34. Derewenda, U.; Swenson, L.; Green, R.; Wei, Y.; Yamaguchi, S.; Joerger, R.; Haas, M.J.; Derewenda, Z.S. Current progress in crystallographic studies of new lipases from filamentous fungi. *Protein Eng.* **1994**, *7*, 551–557.
35. Berg, O.G.; Cajal, Y.; Butterfoss, G.L.; Grey, R.L.; Alsina, M.A.; Yu, B.Z.; Jain, M.K. Interfacial activation of triglyceride lipase from Thermomyces (Humicola) lanuginosa: kinetic parameters and a basis for control of the lid. *Biochemistry* **1998**, *37*, 6615–6627.
36. Fernandez-Lafuente, R. Lipase from Thermomyces lanuginosus: Uses and prospects as an industrial biocatalyst. *J. Mol. Catal. B Enzym.* **2010**, *62*, 197–212.
37. Bastida, A.; Sabuquillo, P.; Armisen, P.; Fernandez-Lafuente, R.; Huguet, J.; Guisan, J. A single step purification, immobilization, and hyperactivation of lipases via interfacial adsorption on strongly hydrophobic supports. *Biotechnol. Bioeng.* **1998**, *58*, 486–493.
38. Fernandez-Lafuente, R.; Armisén, P.; Sabuquillo, P.; Fernández-Lorente, G.; Guisán, J.M. Immobilization of lipases by selective adsorption on hydrophobic supports. *Chem. Phys. Lipids* **1998**, *93*, 185–197.
39. Bravo Rodríguez, V.; Jurado Alameda, E.; Martínez Gallegos, J.F.; Reyes Requena, A.; García López, A.I. Enzymatic hydrolysis of soluble starch with an alpha-amylase from Bacillus licheniformis. *Biotechnol. Prog.* **2006**, *22*, 718–722.
40. Shewale, S.D.; Pandit, A.B. Hydrolysis of soluble starch using Bacillus licheniformis alpha-amylase immobilized on superporous CELBEADS. *Carbohydr. Res.* **2007**, *342*, 997–1008.
41. Pandey, A.; Nigam, P.; Soccol, C.R.; Soccol, V.T.; Singh, D.; Mohan, R. Advances in microbial amylases. *Biotechnol. Appl. Biochem.* **2000**, *31*, 135–152.
42. Riley, R.G.; Zachara, J.M.; Wobber, F.J. *Chemical Contaminants on DOE Lands and Selection of Contaminant Mixtures for Subsurface Science Research*; U.S. Department of Energy, Office of Energy Research, Subsurface Science Program; Available to the public from the National Technical Information Service, U.S. Department of Commerce: Washington, DC, USA; Springfield, VA, USA, 1992.
43. Jeyaratnam, J. Acute pesticide poisoning: a major global health problem. *World Health Stat. Q.* **1990**, *43*, 139–144.

44. Isbister, G.K.; Mills, K.; Friberg, L.E.; Hodge, M.; O'Connor, E.; Patel, R.; Abeyewardene, M.; Eddleston, M. Human methyl parathion poisoning. *Clin. Toxicol. (Phila)* **2007**, *45*, 956–960.
45. Von Itzstein, M. The war against influenza: discovery and development of sialidase inhibitors. *Nat. Rev. Drug Discov.* **2007**, *6*, 967–974.
46. Rodríguez-Aparicio, L.B.; Ferrero, M.A.; Reglero, A. N-acetyl-D-neuraminic acid synthesis in Escherichia coli K1 occurs through condensation of N-acetyl-D-mannosamine and pyruvate. *Biochem. J.* **1995**, *308*, 501–505.
47. Luchansky, S.J.; Yarema, K.J.; Takahashi, S.; Bertozzi, C.R. GlcNAc 2-epimerase can serve a catabolic role in sialic acid metabolism. *J. Biol. Chem.* **2003**, *278*, 8035–8042.
48. Ball, J.C.; Puckett, L.G.; Bachas, L.G. Covalent immobilization of beta-galactosidase onto a gold-coated magnetoelastic transducer via a self-assembled monolayer: Toward a magnetoelastic biosensor. *Anal. Chem.* **2003**, *75*, 6932–6937.
49. Hu, S.; Chen, J.; Yang, Z.; Shao, L.; Bai, H.; Luo, J.; Jiang, W.; Yang, Y. Coupled bioconversion for preparation of *N*-acetyl-D-neuraminic acid using immobilized *N*-acetyl-D-glucosamine-2-epimerase and *N*-acetyl-D-neuraminic acid lyase. *Appl. Microbiol. Biotechnol.* **2010**, *85*, 1383–1391.
50. Wang, T.-H.; Chen, Y.-Y.; Pan, H.-H.; Wang, F.-P.; Cheng, C.-H.; Lee, W.-C. Production of N-acetyl-D-neuraminic acid using two sequential enzymes overexpressed as double-tagged fusion proteins. *BMC Biotechnol.* **2009**, *9*, 63.
51. Venning-Slater, M.; Hooks, D.O.; Rehm, B.H.A. *In vivo* self-assembly of stable green fluorescent protein fusion particles and their uses in enzyme immobilization. *Appl. Environ. Microbiol.* **2014**, *80*, 3062–3071.
52. Jahns, A.C.; Rehm, B.H.A. Tolerance of the Ralstonia eutropha class I polyhydroxyalkanoate synthase for translational fusions to its C terminus reveals a new mode of functional display. *Appl. Environ. Microbiol.* **2009**, *75*, 5461–5466.
53. Pescador, P.; Katakis, I.; Toca-Herrera, J.L.; Donath, E. Efficiency of a bienzyme sequential reaction system immobilized on polyelectrolyte multilayer-coated colloids. *Langmuir* **2008**, *24*, 14108–14114.
54. Aranaz, I.; Ramos, V.; De La Escalera, S.; Heras, A. Co-immobilization of d -hydantoinase and d -carboamylase on Chitin: Application to the Synthesis of p-hydroxyphenylglycine. *Biocatal. Biotransformation* **2003**, *21*, 349–356.
55. Crestini, C.; Melone, F.; Saladino, R. Novel multienzyme oxidative biocatalyst for lignin bioprocessing. *Bioorg. Med. Chem.* **2011**, *19*, 5071–5078.
56. García-Fruitós, E.; Vázquez, E.; Díez-Gil, C.; Corchero, J.L.; Seras-Franzoso, J.; Ratera, I.; Veciana, J.; Villaverde, A. Bacterial inclusion bodies: making gold from waste. *Trends Biotechnol.* **2012**, *30*, 65–70.
57. García-Fruitós, E.; Sabate, R.; de Groot, N.S.; Villaverde, A.; Ventura, S. Biological role of bacterial inclusion bodies: a model for amyloid aggregation. *FEBS J.* **2011**, *278*, 2419–2427.
58. Peternel, S.; Komel, R. Active Protein Aggregates Produced in Escherichia coli. *Int. J. Mol. Sci.* **2011**, *12*, 8275–8287.
59. Carrió, M.; González-Montalbán, N.; Vera, A.; Villaverde, A.; Ventura, S. Amyloid-like properties of bacterial inclusion bodies. *J. Mol. Biol.* **2005**, *347*, 1025–1037.

60. Jahns, A.C.; Maspolim, Y.; Chen, S.; Guthrie, J.M.; Blackwell, L.F.; Rehm, B.H.A. *In Vivo* Self-Assembly of Fluorescent Protein Microparticles Displaying Specific Binding Domains. *Bioconjug. Chem.* **2013**, *24*, 1314–1323.

Chapter 4

4. Bioengineering of bacterial polymer inclusions catalyzing the synthesis of *N*-acetyl neuraminic acid

David O. Hooks[1], Paul A. Blatchford[1,2], Bernd H. A. Rehm[1,#]

Institute of Molecular Biosciences, Massey University, Private Bag 11222, Palmerston North, New Zealand[1].

[2] Plant and Food Research, Fitzherbert Science Centre, Private Bag 11600, Palmerston North, New Zealand.
[#] Corresponding author - telephone: +64-6-350-5515, ext. 7890; fax: +64-6-350-2267; e-mail: b.rehm@massey.ac.nz.

Abstract

***N*-acetyl neuraminic acid is produced by alkaline epimerization of *N*-acetyl glucosamine to *N*-acetyl mannosamine then subsequent condensation with pyruvate catalyzed by free *N*-acetyl neuraminic acid aldolase. The high alkaline conditions of this process result in the degradation of reactants and products while the purification of free enzymes to be used for the synthesis reaction is a costly process. *N*-acetyl glucosamine 2-epimerase has been seen as an alternative to the alkaline epimerization process. In this study, these two enzymes involved in *N*-acetyl neuraminic acid production were immobilized to biopolyester beads *in vivo* in a one-step, cost-efficient production and isolation process. Beads with epimerase-only, aldolase-only, and combined epimerase/aldolase activity were recombinantly produced in *Escherichia coli*. The enzymatic activities were 32 U, 590 U, and 2.2 U/420 U per gram dry bead weight, respectively. Individual beads could convert 18% and 77% of initial GlcNAc and ManNAc, respectively, at high substrate concentrations and near-neutral pH demonstrating the application of this biobead technology to fine chemical synthesis. Beads establishing the entire *N*-acetyl neuraminic acid synthesis pathway were able to convert up to 22% of the initial *N*-acetyl glucosamine after a 50 h reaction time into *N*-acetyl neuraminic acid.**

Introduction

Derivatives of neuraminc acid frequently occur at the terminal position of cell-surface oligosaccharides (Traving & Schauer, 1998). This high level of exposure correlates with their biological role in cellular interaction, bacterial and viral infection, and immune-system recognition (Brusés & Rutishauser, 2001; Mahdavi et al., 2002; Schauer, 2004). In addition, a derivative of *N*-acetyl neuraminic acid (zanamivir) is used as a neurimidase inhibitor for the treatment of influenza virus (Von Itzstein, 2007). The biological roles and recent pharmaceutical interest in *N*-acetyl neuraminic acid (Neu5Ac) make industrial-scale production of this chemical desirable. *N*-acetyl neuraminic acid aldolase (NanA, EC 4.1.3.3) catalyzes the conversion of Neu5Ac to *N*-acetyl-D-mannosamine (ManNAc) and pyruvate (Rodríguez-Aparicio, Ferrero, & Reglero, 1995). Although the reverse reaction has an unfavorable equilibrium requiring a large excess of reactants, NanA is still the enzyme of choice as pyruvate is readily available as a substrate. *N*-acetyl glucosamine 2-epimerase (Slr1975, E.C. 5.1.3.8) is able to catalyze the conversion of *N*-acetyl-D-glucosamine (GlcNAc) to ManNAc with ATP required in catalytic amounts (Luchansky, Yarema, Takahashi, & Bertozzi, 2003). Immobilization of enzymes onto a solid support facilitates removal from the product, often enhances stability, and allows for reuse of the expensive reaction catalyst (Katchalski-Katzir, 1993; Novick & Rozzell, 2005; Sheldon, 2007). Usually enzymes are produced in a recombinant system, isolated, and attached to a solid support system. This type of approach has been applied to both aldolase and epimerase enzymes (Hu et al., 2010; Tzu-Hsien Wang et al., 2009). Alternatively, the production and immobilization of the enzymes can occur in a single step avoiding the potentially expensive attachment and simplifying enzyme isolation from the recombinant system. For example, NanA has been immobilized in a spore-display system which allows for one-step production (Xu et al., 2011).

Recently, the PhaC enzyme from *Ralstonia eutropha* has been used to immobilize an N-terminally fused thermostable α-amylase (Rasiah & Rehm, 2009) and an organophosphate hydrolase fused to the C-terminus of PhaC (Blatchford, Scott, French, & Rehm, 2012) to self-assembled polyester beads *in vivo*. The polyhydroxyalkanoate produced by PhaC aggregates to form spherical inclusions of 50 – 500 nm in diameter (Grage et al., 2009). Additionally, β-galactosidase has been successfully fused to the N-terminus of Class II PhaC from *P. aeruginosa* mediating recombinant production of β-galactosidase displaying polyester beads (Peters & Rehm, 2006). Expression of these proteins in a polyester (PHA=polyhydroxyalkanoate) production host led to a one-step, self-assembled, and cost-effective enzyme display biobead system.

In this study we utilized the previously identified properties of the PHA biobead system to enable efficient production, immobilization, and isolation of both NanA from *E. coli* and Slr1975 from *Synechocystis* sp. PCC 6803 on both individual and dual enzyme-displaying PHA beads. The aim of this study was to demonstrate enzymatic synthesis of Neu5Ac by the PHA enzyme-immobilization biobead system and the wider applicability of this platform technology to fine-chemical synthesis.

Materials and methods

Chemicals

GlcNAc (≥99% purity), ManNAc (≥98% purity), sodium pyruvate, and ATP were purchased from Sigma–Aldrich (St. Louis, MO). Neu5Ac was purchased from GlycoFineChem (New Zealand).

Bacteria, plasmids, and growth conditions

Escherichia coli XL1-Blue was grown at 37 °C, 200 rpm and *E. coli* BL21(DE3) at 25 °C, 200 rpm. When required ampicillin (75 μg/mL), chloramphenicol (50 μg/mL), and tetracycline (12.5 μg/mL) were added to the Luria-Bertani media. Bacterial strains and plasmids used in this study are in Table S41.

Plasmid construction

General cloning procedures and DNA isolation were performed as described elsewhere (Sambrook, Fritsch, & Maniatis, 1989). Primers were purchased from Integrated DNA Technologies (Coraville, IA) while *Taq* and Platinum *Pfx* polymerases were purchased from Invitrogen (Carlsbad, CA). The *slr1975* and *nanA* genes were synthesized by Genscript Corporation (Piscataway, NJ) and inserted in pUC57 vectors with flanking restriction endonuclease sites for subsequent cloning.

The construction of the plasmid pET14b:NanA-PhaC-l-Slr1975 was based upon the plasmid pET14b:ZZ-PhaC-l-GFP from previous studies (Jahns & Rehm, 2009). The plasmid pET14b:ZZ-PhaC-l-GFP was hydrolyzed with the *Xho*I and *Bam*HI restriction enzymes, cleaving the *gfp* region from the vector. The resulting backbone was ligated to the purified *slr1975* fragment. This gave rise to the plasmid pET14b:ZZ-PhaC-l-Slr1975. The plasmid pET14b:ZZ-PhaC-l-Slr1975 was hydrolyzed with the *Nde*I restriction enzyme, cleaving the *zz* region from the vector. The resulting backbone was purified and ligated to the purified *nanA* fragment (Fig. S4.1).

Additionally, the plasmid pET14b:ZZ-PhaC-l-Slr1975 was hydrolyzed with the *Nde*I restriction enzyme, cleaving the *zz* region from the vector, and re-ligated to produce the plasmid pET14b: PhaC-l-Slr1975.

The pET14b:NanA-PhaC construct was assembled by hydrolyzing the plasmid pET14b:AmyS-PhaC (Rasiah & Rehm, 2009) with the restriction enzymes *Xba*I and *Not*I and the resulting backbone was ligated with the *nanA* fragment to produce the plasmid pET14b:NanA-PhaC (Fig. S4.2).

The pET14b:PhaC-NanA construct was assembled by amplification of the *nanA* gene from pUC57:NanA adding *Xho*I and *Bam*HI restriction sites. The plasmid pET14b:PhaC-l-Slr1975 was hydrolyzed with the restriction enzymes *Xho*I and *Bam*HI and the resulting backbone was ligated with the *nanA* fragment to produce the plasmid pET14b:PhaC-NanA.

Additional plasmid constructs pET14b:Slr1975-PhaC and pET14b:Slr1975-PhaC-NanA were created in a similar manner although were not tested extensively past the initial immobilized enzyme screening process.

DNA sequencing was performed to confirm the expected plasmid sequence and was carried out by the Massey Genome Service (Palmerston North, New Zealand) on a capillary ABI3730 Genetic Analyzer (Applied Biosystems, Foster City, CA).

Overexpression of phaC genetic constructs

Cells of *E. coli* BL21/pMCS69 were transformed with pET14b plasmids containing the *nanA-phaC*, *phaC-nanA, phaC-l-slr1975*, or *nanA-phaC-l-slr1975* constructs. The plasmid pMCS69 contained the *phaA* and *phaB* genes that mediate the synthesis of the precursor (*R*)-3-hydroxybutyryl-coenzyme A (3HB-CoA) required for polyester synthesis. Cultures were grown at 37 °C until an OD of 0.3, gene expression was induced with 1 mM isopropyl-β-D-thiogalactopyranoside (IPTG), and the cultures transferred to 25 °C for an additional 48 h of growth. Cells were harvested by centrifugation (4,000 × *g*, 20 min).

Determination of PhaC functionality

Initial screening of PhaC functionality was performed by staining cell pellets with Nile Red and observing cells with fluorescence microscopy as previously described (Peters & Rehm, 2005). Ultimately, PHA production was quantified using gas-chromatography mass-spectrometry (GC/MS) after conversion of the PHA into 3-hydroxymethylester by acid-catalyzed methanolysis (Brandl, Gross, Lenz, & Fuller, 1988). GC/MS was performed by The New Zealand Institute for Plant & Food Research (Palmerston North, New Zealand).

PHA bead isolation

E. coli cell pellets containing polyester were resuspended in 50 mM potassium phosphate buffer (pH 7.5), mechanically disrupted using a constant cell disruption system at 20 kpsi with a one-shot head adapter (Constant Systems Ltd., Northants, U.K.), and the lysate was subjected to centrifugation (4,000 × *g*, 20 min, 4 °C) to sediment the PHA beads. Final separation of the beads from bacterial lysate was achieved by ultracentrifugation (150,000 × *g*, 2 h, 10 °C) on a glycerol gradient (Jahns, Haverkamp, & Rehm, 2008). Isolated PHA beads were stored at 4 °C in 50 mM potassium phosphate buffer (pH 7.5) supplemented with 20% v/v ethanol until required.

Protein analysis

Bead-associated proteins were analyzed by sodium dodecyl sulfate-polyacrylamide gel electrophoresis (SDS-PAGE) as described elsewhere (Laemmli, 1970). Protein bands of interest were excised from an SDS-PAGE gel and subjected to tryptic digest and mass spectrometry performed by the Centre for Protein Research (Otago, New Zealand).

Activity assays

Slr1975 epimerase activity was determined 37 °C in 1 mL of 50 mM potassium phosphate buffer (pH 7.5). Isolated beads were reacted with 20 mM of ManNAc (with 5 mM ATP and 10 mM $MgCl_2$) for 30 min and the resulting mixture centrifuged (6,000 × *g*, 4 min), an aliquot boiled at 100 °C for 5 min, and subjected to HPLC (Tzu-Hsien Wang et al., 2009). One unit was defined as the amount of Slr1975 needed to catalyze the production of 1 µmol GlcNAc per min. NanA aldolase activity was determined at 37 °C in 1 mL of 50 mM potassium phosphate buffer (pH 7.5). Isolated beads were reacted with 4 mM Neu5Ac for 10 min and the resulting mixture centrifuged (6,000 × *g*, 4 min), an aliquot boiled at 100 °C for 5 min, and subjected to HPLC (Xu et al., 2011). One unit of enzyme activity was defined as the amount of NanA needed to catalyze the production of 1 µmol pyruvate per min.

Synthesis of Neu5Ac

The reaction conditions for GlcNAc epimerization to ManNAc were 100 mM GlcNAc, 10 mM ATP, and 10 mM $MgCl_2$ at 50 °C for 20 h. PHA beads were present at 5 mg (wet bead mass) in 50 mM potassium phosphate buffer (pH 7.5). For the synthesis of Neu5Ac from ManNAc, 1 M sodium pyruvate and 400 mM ManNAc were reacted with 5 mg PHA beads in 50 mM potassium phosphate buffer (pH 7.5) at 50 °C for 44 h (Dawson, Noble, & Mahmoudian, 1996; Xu et al., 2011). Recycling reactions for PhaC-l-Slr1975 beads were identical to the reaction conditions described above. The conditions for NanA-PhaC bead recycling reactions were 250 mM pyruvate and 100 mM ManNAc for 20 h. The full biosynthesis of Neu5Ac from GlcNAc and pyruvate was initially carried out with 100 mM sodium pyruvate, 250 mM GlcNAc, 10 mM ATP, and 10 mM $MgCl_2$ at 50 °C for 44 h. PHA beads were present at 10 mg (wet bead weight) in 50 mM potassium

phosphate buffer (pH 7.5). The final conditions were as above except the reactions were carried out at 30 °C for 50 h using a GlcNAc starting concentration of 100 mM (27).

Analytical procedures

ManNAc, pyruvate, and Neu5Ac concentration were determined by a Dionex Summit HPLC system using two Phenomenex (Torrance, CA) RHM columns (300 × 7.8 mm) in series. Flow rate was 0.5 mL/min of 6 mM H_2SO_4 and the columns were maintained at 60 °C. Injection volume was 25 µL and the UV detector was set at 205 nm. Chromatographic data was analyzed with the Chromeleon software (v 6.3).

Neu5Ac was additionally determined by a resorcinol-based colorimetric assay. Briefly, 100 µL of 40 mM periodic acid was vortex mixed into 500 µL of sample and placed in an ice bath for 20 min. Then 1.25 mL of resorcinol solution (0.6 g resorcinol, 250 µL 100 mM $CuSO_4$, 45 mL 37% HCl, make to 100 mL with H_2O) was added, the samples were vortex mixed and returned to the ice bath for 5 min. Samples were boiled in a 100 °C oil bath for 15 min, 1.25 mL of tert-butanol added, and vortex mixed vigorously to achieve a single phase. Finally, samples were incubated for 3 min at 37 °C, cooled to room temperature, and absorbance at 630 nm was measured.

Results

Bioengineering toward the recombinant production of PHA beads displaying selected enzymes relevant to Neu5Ac synthesis

PhaC, a 64 kDa protein which forms a dimer, was used as an anchoring protein for the display of the 46 kDa dimeric Slr1975 from *Synechocystis* sp. PCC 6803 (T-H Wang & Lee, 2006) and the 33

kDa tetrameric NanA from *E. coli* on the surface of PHA beads. NanA was fused to the N-terminus of PhaC while Slr1975 was fused to the C-terminus via a glycine linker. Both single and double enzyme fusions encoding hybrid genes were constructed. The T7 promoter was used to induce high-level expression of the respective fusion proteins.

The fusion proteins NanA-PhaC, PhaC-l-Slr1975, and NanA-PhaC-l-Slr1975 all mediated the formation of PHA beads in the production host BL21(DE3)/pMCS69 as indicated by the Nile Red staining procedure (Fig. S4.3). GCMS analysis of the dried cells producing the respective PHA beads confirmed a high level of PHA production contributing to 45 – 47% of cellular dry weight (Table S4.2).

Proteins associated with isolated PHA beads were analyzed by SDS-PAGE. The theoretical molecular weights of NanA-PhaC, PhaC-l-Slr1975, and NanA-PhaC-l-Slr1975 were 97, 112, and 145 kDa, respectively and appear as the predominant protein with the respective apparent molecular weight (Fig. 4.1). The identity of each fusion protein was confirmed by tryptic peptide fingerprinting using MALDI-TOF MS/MS (Table S4.3).

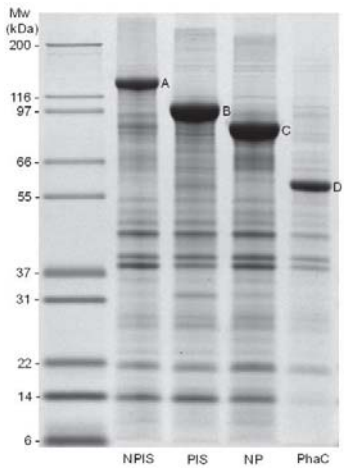

Figure 4.1: Protein profile of PHA beads as demonstrated by SDS-PAGE. Mw: Molecular weight standard Mark 13 ladder (Invitrogen, CA), NPlS: NanA-PhaC-l-Slr1975 (A), PlS: PhaC-l-Slr1975 (B), NP: NanA-PhaC (C), PhaC: PhaC (D). The letters A, B, C, and D correspond to the fusion protein of interest overproduced on their respective PHA beads.

Screening for successful enzyme immobilization of PhaC-fusion constructs

Reaction conditions for immobilized NanA were confirmed using PHA beads which formation was mediated by pET14b:PhaC-NanA. Neu5Ac production was measured using the resorcinol assay. PHA bead concentration could range between 1 – 15 mg/mL wet bead mass (Fig. S4.4) and the optimal temperature for NanA was found to be 50 °C (Fig. S5) agreeing with other reports (Xu et al., 2011). Enzyme activity was sensitive to trypsin treatment indicating successful enzyme immobilization on the bead surface (not shown). For PHA beads with imobilized PhaC-l-Slr1975, a reaction temperature between 37 - 50 °C had negligible impact on Neu5Ac production therefore all further production reactions were carried out at 50 °C (not shown). In addition, the immobilized

fusion proteins NanA-PhaC, PhaC-NanA, Slr1975-PhaC, PhaC-Slr1975, NanA-PhaC-l-Slr1975, and Slr1975-PhaC-NanA were screened for activity with the resorcinol assay. Slr1975-PhaC and Slr1975-PhaC-NanA were found not to possess epimerase activity and were not studied further (data not shown). Further, NanA-PhaC had superior yield to PhaC-NanA under the previously determined aldolase conditions, therefore PhaC-NanA was not studied further (not shown).

Activity assays of enzymes displayed on PHA beads

N-acetyl glucosamine 2-epimerase activity tests were used for beads displaying Slr1975 fusions. PhaC only beads served as negative control and showed some background activity which corresponded to 0.2 U/g dry bead mass. Beads displaying PhaC-Slr1975 had 32 U/g dry bead mass and beads displaying NanA-PhaC-l-Slr1975 had 2.2 U/g dry bead mass (Table 4.1). Beads displaying immobilized NanA fusions were subjected to *N*-acetyl neuraminic acid aldolase activity tests using Neu5Ac as a substrate. PhaC only beads had no detectable aldolase activity whereas beads displaying NanA-PhaC had 590 U/g dry bead mass. Beads displaying NanA-PhaC-l-Slr1975 had 420 U/g dry bead mass (Table 4.2). Specific enzyme activity was determined by quantifying bead protein concentration using densitometry from SDS-PAGE and known standards of BSA (Fig. S4.6) and calculating the fusion enzyme concentration present in each activity reaction.

Table 4.1: Specific epimerase activity of PHA beads with immobilized Slr1975

	Specific activity (mean ± S.D.)	
Fusion protein (n = 3)	Enzyme units per dry bead weight (U/g)	Enzyme units per protein weight (U/mg)
PhaC-Slr1975	32.3 ± 1.1	1.76 ± 0.38
NanA-PhaC-l-Slr1975	2.17 ± 0.18	0.58 ± 0.07
PhaC	0.20 ± 0.19	0.04 ± 0.04

Table 4.2: Specific aldolase activity of PHA beads with immobilized NanA

	Specific activity (mean ± S.D.)	
Fusion protein (n = 3)	Enzyme units per dry bead weight (U/g)	Enzyme units per protein weight (U/mg)
NanA-PhaC	585 ± 49	42.6 ± 6.9
NanA-PhaC-l-Slr1975	418 ± 53	81.9 ± 19
PhaC	n.d.	n.d.

Production of ManNAc by Slr1975 displaying beads

The enzymatic epimerization of GlcNAc to ManNAc was carried out at 50 °C and the reaction conditions were 100 mM GlcNAc, 10 mM $MgCl_2$, and 10 mM of ATP in 50 mM phosphate buffer (pH 7.5). Reactions were stopped after 20 h and a sample was taken to be measured by HPLC. For the PhaC-l-Slr1975 fusion, the concentration of ManNAc reached 21 mM (18% conversion), the likely equilibrium point of the reaction. The NanA-PhaC-l-Slr1975 fusion reached only 4 mM (4%

conversion) after 20 h while the PhaC beads had no detectable production of ManNAc (Table 3). The ability of the PhaC-l-Slr1975 beads to be recycled was tested over five cycles under conditions identical to those described above. After an initial yield of 22% ManNAc, the conversion rate slowly declined from 19% to 17% over the next four cycles (Fig. 4.2).

Table 4.3: Production of *N*-acetyl mannosamine and *N*-acetyl neuraminic acid using single bead systems

	Production (mean ± S.D.) [conversion percent]	
Fusion protein (n = 3)	ManNAc production (mM)	Neu5Ac production (mM)
NanA-PhaC	NA	282 ± 8.0 [77%]
PhaC-l-Slr1975	21.4 ± 1.0 [18%]	NA
NanA-PhaC-l-Slr1975	4.47 ± 0.10 [4%]	257 ± 11 [70%]
PhaC	n.d.	n.d.

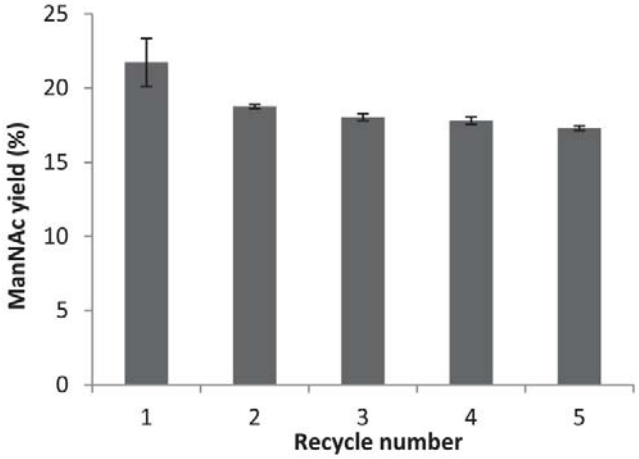

Figure 4.2: Recycling of PhaC-l-Slr1975 displaying PHA beads. Reaction conditions were 100 mM GlcNAc with 10 mM of both ATP and MgCl2 as cofactors. The reaction occurred at 50 °C for 20 h. Yield of ManNAc from GlcNAC was measured by HPLC. Error bars are ± one standard deviation, n = 3.

Production of Neu5Ac under optimal conditions using enzyme immobilized beads

The enzymatic synthesis of ManNAc (400 mM) and pyruvate (1 M) to Neu5Ac was carried out at 50 °C. The amount of PHA beads was 5 mg wet bead mass per mL (0.63 U/mL). After a 44 h reaction, the concentrations of ManNAc and Neu5Ac were measured using HPLC. NanA-PhaC and NanA-PhaC-l-Slr1975 beads were able to convert approximately 77% and 70% of the initial ManNAc to Neu5Ac, respectively. PhaC only beads showed no detectable production of Neu5Ac (Table 4.3). Recycling of the NanA-PhaC beads was tested under lower substrate concentrations (100 mM ManNAc and 250 mM pyruvate) and over a shorter timeframe (20 h). The initial reaction produced a yield of 73% Neu5Ac. However, in the second reaction, yield increased to 97% with subsequent reactions decreasing yield (Fig. 4.3). After four reaction cycles, the overall yield had decreased back to 70%.

Enzymatic synthesis of GlcNAc and pyruvate to Neu5Ac was initially performed at 50 °C using substrate concentrations of 250 mM and 100 mM, respectively. The cofactors of 10 mM $MgCl_2$ and 10 mM ATP were also added. Overall, each reaction contained 10 mg (wet bead mass) of PHA beads. The weight of wet beads added to the reaction were: PhaC only: 10 mg, NanA-PhaC-l-Slr1975: 10 mg, and NanA-PhaC + PhaC-l-Slr1975: 5 mg each. Samples were taken at 44 h and subjected to analysis by HPLC. PhaC only beads showed no detectable levels of ManNAc or Neu5Ac. NanA-PhaC + PhaC-l-Slr1975 showed some production of 41 mM ManNAc and 14 mM of Neu5Ac a 14% and 4.7% conversion of the starting GlcNAc concentration respectively. NanA-PhaC-l-Slr1975 had slight production of 6.0 mM of ManNAc and 5.1 mM of Neu5Ac a 2% and 1.7% conversion of the starting GlcNAc concentration respectively (Fig. 4. 4). Finally, the NanA-PhaC + PhaC-l-Slr1975 combination was tested further at conditions favoring the conversion of GlcNAc to ManNAc.

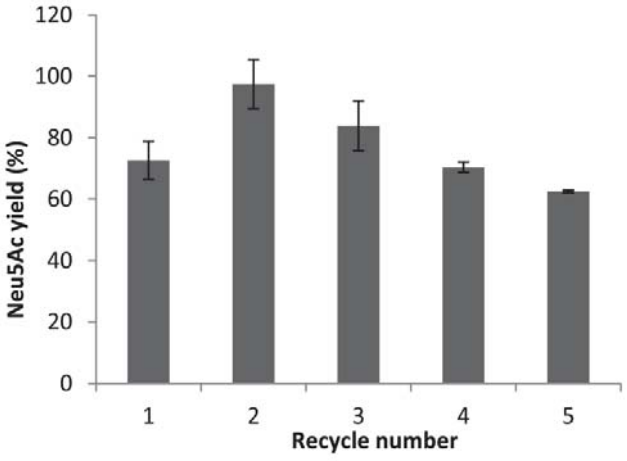

Figure 4.3: Recycling of NanA-PhaC displaying PHA beads. Reaction conditions were 100 mM ManNAc and 250 mM pyruvate at 50 °C for 20 h. Yield of Neu5Ac from ManNAc was measured by HPLC. Error bars are ± one standard deviation, n = 3.

The initial concentration of substrate was 100 mM of both pyruvate and GlcNAc with 10 mM of both $MgCl_2$ and ATP added. The weight of wet beads added were: NanA-PhaC: 2.5 mg and PhaC-l-Slr1975: 7.5 mg. The reaction was carried out at 30 °C for 50 h. While the PhaC-only control had no detectable production of ManNAc or Neu5Ac, the final yield of the two-bead system with respect to the starting GlcNAc concentration was 19% ManNAc and 22% Neu5Ac (Fig. 4.4).

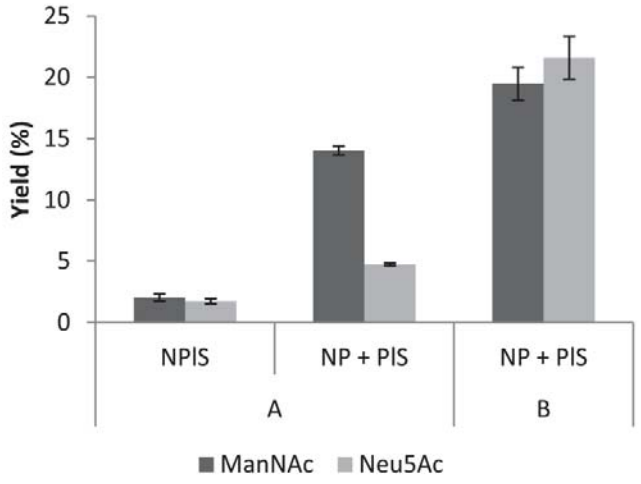

Figure 4.4: A: Production of Neu5Ac from 250 mM GlcNAc and 100 mM pyruvate over 44 h at 50 °C using 10 mg (wet weight) of NanA and Slr1975 displaying beads. NanA-PhaC + PhaC-l-Slr1975 beads, 5 mg (wet weight) of each, yielded 14% ManNAC and 4.7% Neu5Ac conversion of the starting GlcNAc concentration. NanA-PhaC-l-Slr1975 beads, 10 mg wet weight, yielded 2% ManNAc and 1.7% Neu5Ac conversion of the starting GlcNAc concentration. B: Production of Neu5Ac from 100 mM GlcNAc and 100 mM pyruvate over 50 h at 30 °C using 10 mg (wet weight) of NanA and Slr1975 displaying beads. NanA-PhaC + PhaC-l-Slr1975 beads, 2.5 mg and 7.5 (wet weight) respectively, yielded 19% ManNAC and 22% Neu5Ac conversion of the starting GlcNAc concentration. Error bars are ± one standard deviation, n = 3.

Discussion

Previous research has demonstrated that PHA beads are a useful platform for protein immobilization (Grage et al., 2009). Enzymes immobilized to PHA beads have shown high density display, high activity, enhanced stability, and improved kinetic properties (Rasiah & Rehm, 2009), suggesting a role for this technology in fine chemical synthesis. The one-step production and immobilization of the target enzymes NanA and Slr1975 offers significant advantages over previous multi-step immobilization techniques (e.g., Hu et al., 2010).

The PhaC fusion proteins were overproduced using the pET vector expression system in *E. coli* leading to a high level of protein production on the PHA bead surface as exhibited by the NanA-PhaC and PhaC-l-Slr1975 enzyme immobilizations of 4.5 µg/mg and 7.8 µg/mg wet bead weight, respectively (Figs. 4.1 and S4.3). In contrast, the NanA-PhaC-l-Slr1975 double fusion displayed 1.6 µg/mg wet bead weight (i.e., less fusion protein on the bead surface). It has been previously suggested the N-terminus of PhaC has an important interaction with its C-terminus (Jahns & Rehm, 2009). Therefore, the lower level of protein immobilization seen on the NanA-PhaC-l-Slr1975 PHA beads may be explained by the steric hindrance of this interaction due to attaching fusion partners on both termini of the PhaC enzyme.

The epimerase activity of PhaC-l-Slr1975 fusion protein was 1.8 U/mg protein compared to 0.58 U/mg for the NanA-PhaC-l-Slr1975 fusion protein (Table 4.1). Reported activities of immobilized GlcNAc-2 epimerases range from 3.4 – 29 U/mg protein (Hu et al., 2010; Tzu-Hsien Wang et al., 2009). The C-terminus of PhaC has been recognized as important for PhaC attachment to the bead surface (Jahns & Rehm, 2009) and disruption of the PhaC C-terminus may explain both the lower level of fusion protein attachment seen in the double fusion protein as well as its lower epimerase activity.

In contrast, the aldolase activity of NanA-PhaC was 43 U/mg protein compared with 82 U/mg for the NanA-PhaC-l-Slr1975 fusion protein (Table 4.2). The assembly of the tetrameric structure of NanA may be assisted by the lower levels of protein expression found on the NanA-PhaC-l-Slr1975 bead surface.

The equilibrium point for GlcNAc to ManNAc epimerization has been reported as 1:4 (Hu et al., 2010) matching with the observed 18% conversion of 100 mM GlcNAc after 20 h by the beads only displaying the epimerase. In contrast, the double enzyme bead was only able to convert 4% of the initial GlcNAc over the same reaction time (Table 4.3). The low reaction yield of the epimerase portion of the double fusion can be explained by its low activity measurement. Additionally, the PhaC-l-Slr1975 beads were able to produce this conversion rate over at least five reaction cycles showing these beads can retain their catalytic activity for sustained periods (100 h) at relatively high temperature (Fig. 4.2).

The production of Neu5Ac using high concentrations of ManNAc and pyruvate was particularly successful with the conversion rates of 77% and 70% from the aldolase only and double enzyme beads respectively (Table 4.3). Although the fusion protein for the double enzyme bead exhibits a higher aldolase activity than beads only displaying the aldolase, the abundance of fusion protein on the surface of the aldolase only beads means both beads have similar aldolase activities as a function of bead weight. As both beads have high aldolase activities, the activity of PHA-immobilized NanA compares favorably with previously reported activities of 2.5 – 36 U/mg protein (Hu et al., 2010; Tzu-Hsien Wang et al., 2009) and they perform similarly over the 44 h reaction. Recycling reactions showed that NanA-PhaC beads retain at least 70% conversion of ManNAc over four reaction cycles (Fig. 4.3). The increase in yield seen in the second reaction may be due to carry-over of reactants associated with the NanA enzyme to the next reaction.

Ultimately, the applicability of both systems to the production of Neu5Ac from GlcNAc and pyruvate was compared by equalizing the amount of enzyme beads added to the reaction on a per mass basis. As pyruvate is an inhibitor of Slr1975 its concentration must be kept below 100 mM (Lee, Yi, Lee, Takahashi, & Kim, 2004) even though it is driving the reaction towards Neu5Ac. Given these constraints, the production system composed of 5 mg aldolase only beads with 5 mg of epimerase only beads produced 14 mM of Neu5Ac (4.7% conversion of GlcNAc) while 10 mg of the double enzyme beads produced only 5.1 mM of Neu5Ac (1.7% conversion of GlcNAc). Despite the higher aldolase activity of the dual enzyme beads, a Neu5Ac production system composed of single enzyme immobilization is the more effective option (Fig. 4.4). Both the activity measurements of Slr1975-displaying beads and the low yield of ManNAc in the full biosynthesis pathway suggested the Slr1975-displaying bead was not performing optimally in the double bead system. Therefore, a further set of reaction conditions hypothesized to favor conversion of GlcNAc to ManNAc by Slr1975 was tested. The production system consisting single enzyme immobilizations (7.5 mg of PhaC-l-Slr1975 beads and 2.5 mg NanA-PhaC beads) was able to convert 22% of the starting GlcNAc to Neu5Ac (Fig. 4.4), this compares to the traditional approach utilizing alkaline epimerization and free NanA which has been reported to yield 33% *N*-acetyl neuraminic acid (Blayer, Woodley, Dawson, & Lilly, 1999).

Conclusion

This study demonstrated that NanA and Slr1975 can be successfully immobilized on the PHA biobead system by fusion to PhaC. Both NanA and Slr1975 retained enzymatic activity in both single and double fusions to PhaC and the resulting functionalized beads could be produced in a one-step, cost-efficient bacterial fermentation that is amenable to industrial-scale production

(Rehm, 2010). Recycling experiments showed the single-fusion beads could be recovered and reused several times before losing their initial yield potential and the overall biosynthesis pathway from GlcNAc to Neu5Ac was shown to perform at a relatively high level (22% yield) which may make the PHA biobead platform suitable for use as a biocatytic production system in fine-chemical synthesis.

Acknowledgements

This study was supported by the New Zealand Foundation for Research Science and Technology and the Institute of Molecular Biosciences at Massey University. DOH received a PhD scholarship from Massey University. The purchase of the Phenomenex RHM HPLC columns was funded by New Zealand Pharmaceuticals, Ltd (Palmerston North, New Zealand).

References

Amara, A. A., & Rehm, B. H. A. (2003). Replacement of the catalytic nucleophile cysteine-296 by serine in class II polyhydroxyalkanoate synthase from Pseudomonas aeruginosa-mediated synthesis of a new polyester: identification of catalytic residues. *Biochemical Journal*, *374*(Pt 2), 413–21. doi:10.1042/BJ20030431

Blatchford, P. A., Scott, C., French, N., & Rehm, B. H. A. (2012). Immobilization of organophosphohydrolase OpdA from Agrobacterium radiobacter by overproduction at the surface of polyester inclusions inside engineered Escherichia coli. *Biotechnology and Bioengineering*, *109*(5), 1101–8. doi:10.1002/bit.24402

Blayer, S., Woodley, J. M., Dawson, M. J., & Lilly, M. D. (1999). Alkaline biocatalysis for the direct synthesis of N-acetyl-D-neuraminic acid (Neu5Ac) from N-acetyl-D-glucosamine (GlcNAc). *Biotechnology and Bioengineering*, *66*(2), 131–6. Retrieved from http://www.ncbi.nlm.nih.gov/pubmed/10567071

Brandl, H., Gross, R. A., Lenz, R. W., & Fuller, R. C. (1988). Pseudomonas oleovorans as a Source of Poly(beta-Hydroxyalkanoates) for Potential Applications as Biodegradable Polyesters. *Applied and Environmental Microbiology*, *54*(8), 1977–82. Retrieved from http://www.pubmedcentral.nih.gov/articlerender.fcgi?artid=202789&tool=pmcentrez&rendertype=abstract

Brusés, J. L., & Rutishauser, U. (2001). Roles, regulation, and mechanism of polysialic acid function during neural development. *Biochimie*, *83*(7), 635–43. Retrieved from http://www.ncbi.nlm.nih.gov/pubmed/11522392

Dawson, M., Noble, D., & Mahmoudian, M. (1996). Process for the preparation of N-acetylneuraminic acid. *US Patent 6,156,544*. Washington, D.C.: U.S. Patent and Trademark Office. Retrieved from http://www.google.com/patents?hl=en&lr=&vid=USPAT6156544&id=fLMFAAAAEBAJ&oi=fnd&dq=Process+for+the+preparation+of+n-acetylneuraminic+acid&printsec=abstract

Draper, J., Du, J., Hooks, D. O., Lee, J. W., Parlane, N. A., & Rehm, B. H. A. (2013). Polyhyroxyalkanoate inclusions: polymer synthesis, self-assembly, and display technology. In B. H. A. Rehm (Ed.), *Bionanotechnology: Biological Self-assembly and Its Applications* (pp. 1–36). Norfolk: Caister Academic Press.

Grage, K., Jahns, A. C., Parlane, N., Palanisamy, R., Rasiah, I. A., Atwood, J. A., & Rehm, B. H. A. (2009). Bacterial polyhydroxyalkanoate granules: biogenesis, structure, and

potential use as nano-/micro-beads in biotechnological and biomedical applications. *Biomacromolecules*, *10*(4), 660–9. doi:10.1021/bm801394s

Hooks, D. O., Venning-Slater, M., Du, J., & Rehm, B. H. A. (2014). Polyhydroyxalkanoate synthase fusions as a strategy for oriented enzyme immobilisation. *Molecules (Basel, Switzerland)*, *19*(6), 8629–43. doi:10.3390/molecules19068629

Hu, S., Chen, J., Yang, Z., Shao, L., Bai, H., Luo, J., … Yang, Y. (2010). Coupled bioconversion for preparation of N-acetyl-D-neuraminic acid using immobilized N-acetyl-D-glucosamine-2-epimerase and N-acetyl-D-neuraminic acid lyase. *Applied Microbiology and Biotechnology*, *85*(5), 1383–91. doi:10.1007/s00253-009-2163-9

Jahns, A. C., Haverkamp, R. G., & Rehm, B. H. A. (2008). Multifunctional inorganic-binding beads self-assembled inside engineered bacteria. *Bioconjugate Chemistry*, *19*(10), 2072–80. doi:10.1021/bc8001979

Jahns, A. C., & Rehm, B. H. A. (2009). Tolerance of the Ralstonia eutropha class I polyhydroxyalkanoate synthase for translational fusions to its C terminus reveals a new mode of functional display. *Applied and Environmental Microbiology*, *75*(17), 5461–6. doi:10.1128/AEM.01072-09

Katchalski-Katzir, E. (1993). Immobilized enzymes--learning from past successes and failures. *Trends in Biotechnology*, *11*(11), 471–478. Retrieved from http://www.ncbi.nlm.nih.gov/pubmed/7764401

Laemmli, U. K. (1970). Cleavage of structural proteins during the assembly of the head of bacteriophage T4. *Nature*, *227*(5259), 680–685. doi:10.1038/227680a0

Lee, J.-O., Yi, J.-K., Lee, S.-G., Takahashi, S., & Kim, B.-G. (2004). Production of N-acetylneuraminic acid from N-acetylglucosamine and pyruvate using recombinant human renin binding protein and sialic acid aldolase in one pot. *Enzyme and Microbial Technology*, *35*(2-3), 121–125. doi:10.1016/j.enzmictec.2003.10.020

Luchansky, S. J., Yarema, K. J., Takahashi, S., & Bertozzi, C. R. (2003). GlcNAc 2-epimerase can serve a catabolic role in sialic acid metabolism. *Journal of Biological Chemistry*, *278*(10), 8035–42. doi:10.1074/jbc.M212127200

Mahdavi, J., Sondén, B., Hurtig, M., Olfat, F. O., Forsberg, L., Roche, N., … others. (2002). Helicobacter pylori SabA adhesin in persistent infection and chronic inflammation. *Science*, *297*(5581), 573. Retrieved from http://www.sciencemag.org/content/297/5581/573.short

Novick, S. J., & Rozzell, J. D. (2005). Immobilization of Enzymes by Covalent Attachment. In *Microbial Enzymes and Biotransformations* (Vol. 17, pp. 247–271). doi:10.1385/1-59259-846-3:247

Peters, V., & Rehm, B. H. A. (2005). In vivo monitoring of PHA granule formation using GFP-labeled PHA synthases. *FEMS Microbiology Letters*, *248*(1), 93–100. doi:10.1016/j.femsle.2005.05.027

Peters, V., & Rehm, B. H. A. (2006). In vivo enzyme immobilization by use of engineered polyhydroxyalkanoate synthase. *Applied and Environmental Microbiology*, *72*(3), 1777. doi:10.1128/AEM.72.3.1777

Rasiah, I. A., & Rehm, B. H. A. (2009). One-step production of immobilized alpha-amylase in recombinant Escherichia coli. *Applied and Environmental Microbiology*, *75*(7), 2012–6. doi:10.1128/AEM.02782-08

Rehm, B. H. A. (2010). Bacterial polymers: biosynthesis, modifications and applications. *Nature Reviews Microbiology*, *8*(8), 578–92. doi:10.1038/nrmicro2354

Rodríguez-Aparicio, L. B., Ferrero, M. A., & Reglero, A. (1995). N-acetyl-D-neuraminic acid synthesis in Escherichia coli K1 occurs through condensation of N-acetyl-D-mannosamine and pyruvate. *Biochemical Journal*, *308 (Pt 2*, 501–5. Retrieved from http://www.pubmedcentral.nih.gov/articlerender.fcgi?artid=1136953&tool=pmcentrez&rendertype=abstract

Sambrook, J., Fritsch, E., & Maniatis, T. (1989). *Molecular cloning: A laboratory manual.* Plainview, NY: Cold Spring Harbor Laboratory Press.

Schauer, R. (2004). Sialic acids: fascinating sugars in higher animals and man. *Zoology*, *107*(1), 49–64. doi:10.1016/j.zool.2003.10.002

Sheldon, R. A. (2007). Enzyme Immobilization: The Quest for Optimum Performance. *Advanced Synthesis and Catalysis*, *349*(8-9), 1289–1307. doi:10.1002/adsc.200700082

Traving, C., & Schauer, R. (1998). Structure, function and metabolism of sialic acids. *Cellular and Molecular Life Sciences*, *54*(12), 1330–49. Retrieved from http://www.ncbi.nlm.nih.gov/pubmed/9893709

Von Itzstein, M. (2007). The war against influenza: discovery and development of sialidase inhibitors. *Nature Reviews Drug Discovery*, *6*(12), 967–974. Retrieved from http://www.nature.com/nrd/journal/v6/n12/abs/nrd2400.html

Wang, T.-H., Chen, Y.-Y., Pan, H.-H., Wang, F.-P., Cheng, C.-H., & Lee, W.-C. (2009). Production of N-acetyl-D-neuraminic acid using two sequential enzymes

overexpressed as double-tagged fusion proteins. *BMC Biotechnology*, *9*, 63. doi:10.1186/1472-6750-9-63

Wang, T.-H., & Lee, W.-C. (2006). Expression and characterization of the N-acetyl-D-glucosamine 2-epimerase as a tagged protein for the conversion of N-acetyl-D-glucosamine to N-acetyl-D-Mannosamine. *Journal of the Chinese Institute of Chemical Engineers*, *37*(2), 131–137.

Xu, X., Gao, C., Zhang, X., Che, B., Ma, C., Qiu, J., … Xu, P. (2011). Production of N-acetyl-D-neuraminic acid by use of an efficient spore surface display system. *Applied and Environmental Microbiology*, *77*(10), 3197–201. doi:10.1128/AEM.00151-11

<u>Supplementary material for:</u> Bioengineering of bacterial polymer inclusions catalyzing the synthesis of *N*-acetyl neuraminic acid.

David O. Hooks, Paul A. Blatchford, Bernd H. A. Rehm

Institute of Fundamental Sciences, Massey University, Private Bag 11222, Palmerston North, New Zealand; telephone: +64-6-350-5515, ext. 7890; fax: +64-6-350-2267; e-mail: b.rehm@massey.ac.nz.

Strains and plasmids

Table S4.1: Bacterial strains and plasmids used in this study

Name	*Characteristics*	*Source*
Bacterial strains		
XLI-Blue	*recA1*, *endA1*, *gyrA96*, *thi-1*, *hsdR17*($r-_k$, $m+_k$), *supE44*, *relA1*, -, *lac*[*F'*, *proAB*, *lacI*^{q}, *lacZΔM15*, *Tn10*(*Tc*^{r})]	Stratagene
BL21(DE3)	F-, *ompT*, *hsdS*$_B$ (r_B- m_B-), *gal*, *dcm* (DE3)	Novagen
Plasmids		
pMCS69	pBBR1MCS derivative containing genes *pha*A and *pha*B of *R. eutropha* colinear to lac promoter, Cp^R	(Amara & Rehm, 2003)
pUC57:NanA	Ap^r, containing *nanA* on the pUC57 plasmid	Genscript Corporation
pUC57:l-Slr1975	Ap^r, containing *l-slr1975* on the pUC57 plasmid	Genscript Corporation
pET14b	Ap^r, T7 promoter	Novagen
pET14b:PhaC	Coding for PhaCwt	(Peters & Rehm, 2006)
pET14b:ZZ-PhaC-l-GFP	Containing *zz* fused to the 5' end of *phaC* and *gfp* fused to the 3' end of *phaC* via a linker sequence	(Jahns & Rehm, 2009)
pET14b:AmyS-PhaC	Containing *amyS* fused to the 5' end of *phaC*	(Rasiah & Rehm, 2009)
pET14b:NanA-PhaC	Containing *nanA* fused to the 5' end of *phaC*	This study
pET14b:PhaC-NanA	Containing *nanA* fused to the 3' end of *phaC*	This study
pET14b:PhaC-l-Slr1975	Containing *Slr1975* fused to the 3' end of *phaC* via a linker sequence	This study
pET14b:NanA-PhaC-l-Slr1975	Containing *nanA* fused to the 5' end of *phaC* and *Slr1975* fused to the 3' end of *phaC* via a linker sequence	This study

Plasmid construction

Figure S4.1: Construction of plasmids pET14b:PhaC-I-Slr1975 and pET14b:NanA-PhaC-I-Slr1975.

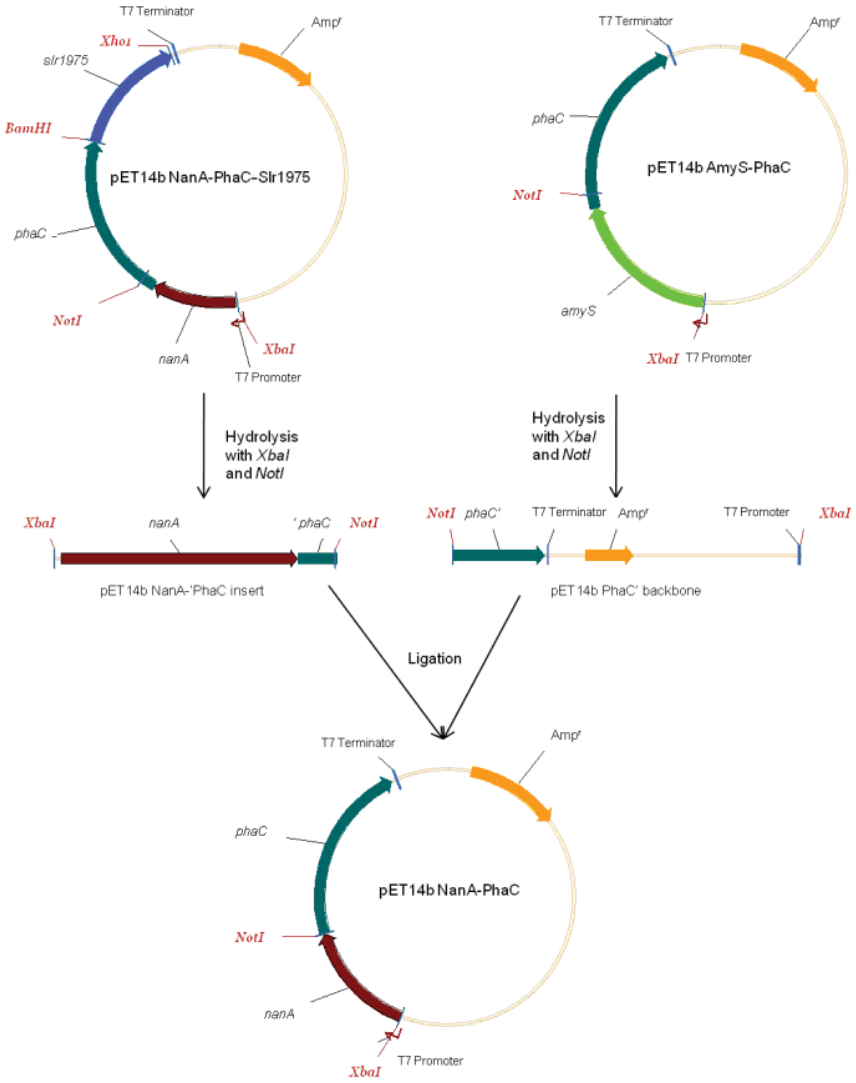

Figure S4.2: Construction of plasmid pET14b:NanA-PhaC.

Fluorescence microscopy

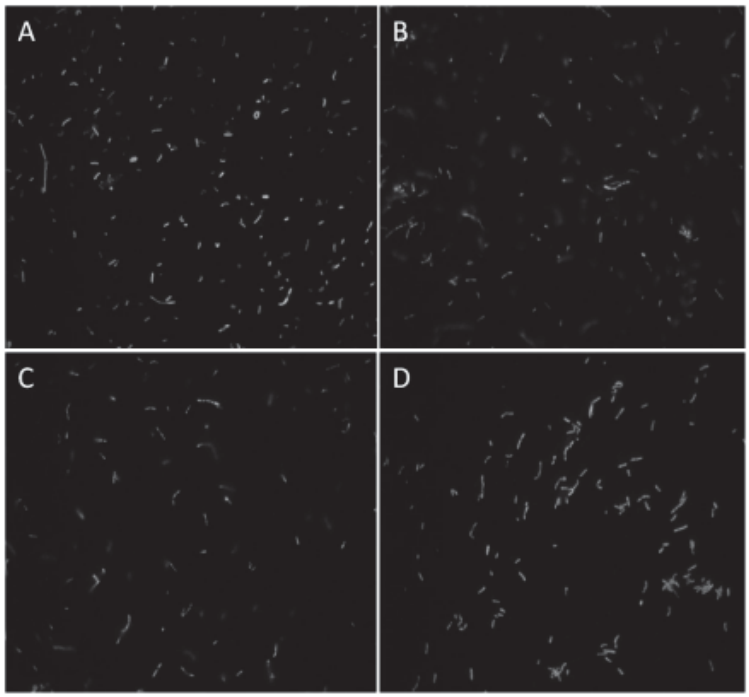

Figure S4.3: Fluorescence microscopy analysis of intact cells after staining with the lipophilic Nile Red dye. The dye is absorbed by the cells and preferentially sequestered into PHA beads. Cells were harboring various plasmids: A, pET14b:NanA-PhaC-l-Slr1975; B, pET14b:PhaC-l-Slr1975; C, pET14b:NanA-PhaC; D, pET14b:PhaC.

GC/MS PHB cell content

Table S4.2: PHB content of *E. coli* XL1 blue cells as measured by GC/MS. The *E. coli* contained either PhaC or PhaC-fusion expression plasmids and were cultivated for 48 h at 25°C after induction with IPTG.

Expression Plasmid	PHB (mg/mg cell weight)	PHB (% cell weight)
pET14b:NanA-PhaC-l-Slr1975	0.47	46.63
pET14b:NanA-PhaC	0.46	46.39
pET14b:PhaC-l-Slr1975	0.45	45.07
pET14b:PhaC	0.37	36.70

MALDI-TOF protein identification

Table S4.3: Tryptic peptides of PhaC fusion proteins as identified by MALDI-TOF/TOF MS. Total bead protein was electrophoresed onto a gel and a band corresponding to the theoretical molecular weight of the fusion protein was isolated and analysed by mass spectrometry.

Fusion Protein	Identified peptides (modifications)
NanA-PhaC-l-Slr1975	G7-K24, L147-K165, Q166-R178, Q166-R179, A287-R296, A287-R296 (oxidation), V319-R334, I361-R372, R399-R406, F413-R423, A424-K437, A424-R439, F444-R467, L468-R478, G491-R505, I493-R505, Y548-R561, H562-R576, E669-R684 (carbamidomethyl), H741-K749, R861-R871, A862-R871, Y872-R881, A887-R897, G898-R921, R922-K943, K960-R975, Q976-R986, L987-R998, A1056-R1067, E1121-R1135, E1121-R1135 oxidation, E1136-R1151, L1152-R1171, R1273-K1281
NanA-PhaC	G7-K24, L30-R59, E60-K71, L76-K96 (carbamidomethyl), A124-K146, L147-K165, Q166-R178, Q166-R179, A287-R296, A287-R296 (oxidation), V319-R334, I361-R372, D376-K388, A389-R398, A389-R399, F413-R423, A424-K437, F444-R467, F444-R467 (oxidation), L468-R478, N506-K532, Y548-R561, H562-R576, N577-R597, D604-R633 (carbamidomethyl), G634-R668, E669-R684, H741-K749, L754-R776, E777-K796, A862-R871,
PhaC-l-Slr1975	V22-R37, Q38-K63, I64-R75,A92-R101, R102-R109, F116-R126, A127-K140, A127-R142, F147-R170, L171-R181, G194-R208, I196-R208, Y251-R264, H265-R279, E372-R387 (carbamidomethyl), H444-K452, R564-R574, A565-R574, Y575-R584, A577-K587, A588-R600, A590-R600, G601-R624, R625-R646, Q679-R689, L690-R701, A759-R770, E824-R838, E824-R838 (oxidation), E839-R854, L855-R874, C946-R952 (carbamidomethyl), R976-K984

Resorcinol assays

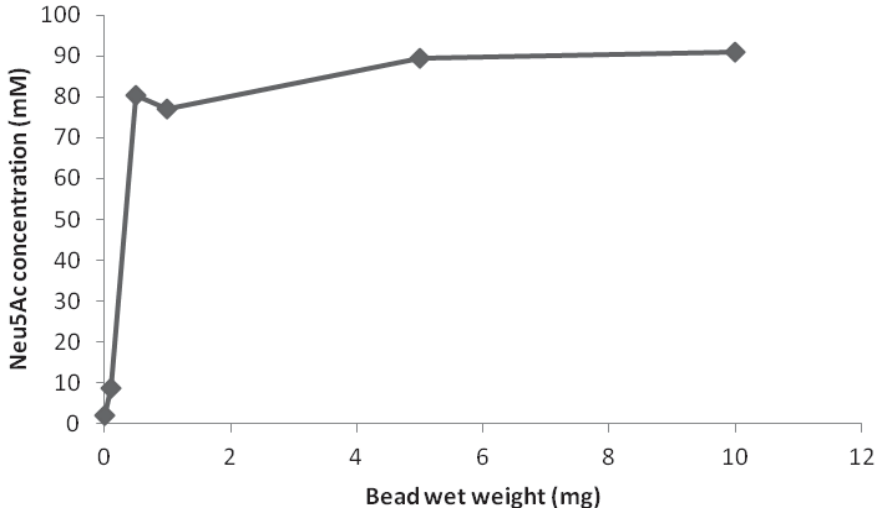

Figure S4.4: Effect of wet bead weight on the production of Neu5Ac. The reaction contained 125 mM ManNAc and 280 mM of pyruvate with increasing wet weights of NanA beads (0.1 – 10 mg). After a 43 h reaction at 37°C the resulting Neu5Ac was measured by the resorcinol assay.

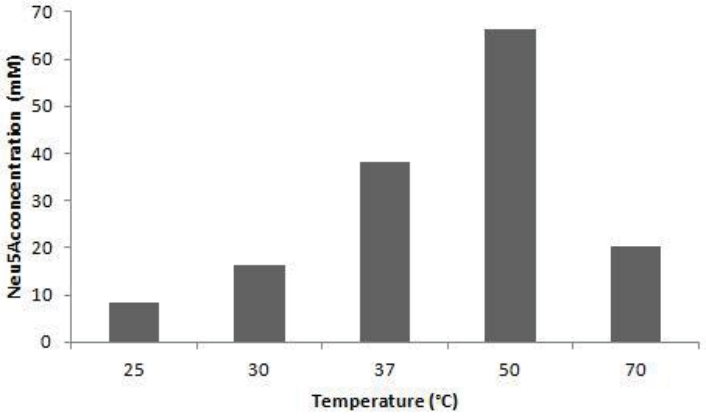

Figure S4.5: Effect of temperature on the production of Neu5Ac. The reaction contained 125mM ManNAc and 280 mM of pyruvate with 0.5 mg NanA beads. After a 24 h reaction at various temperatures the resulting Neu5Ac was measured by the resorcinol assay.

Densitometry SDS-PAGE

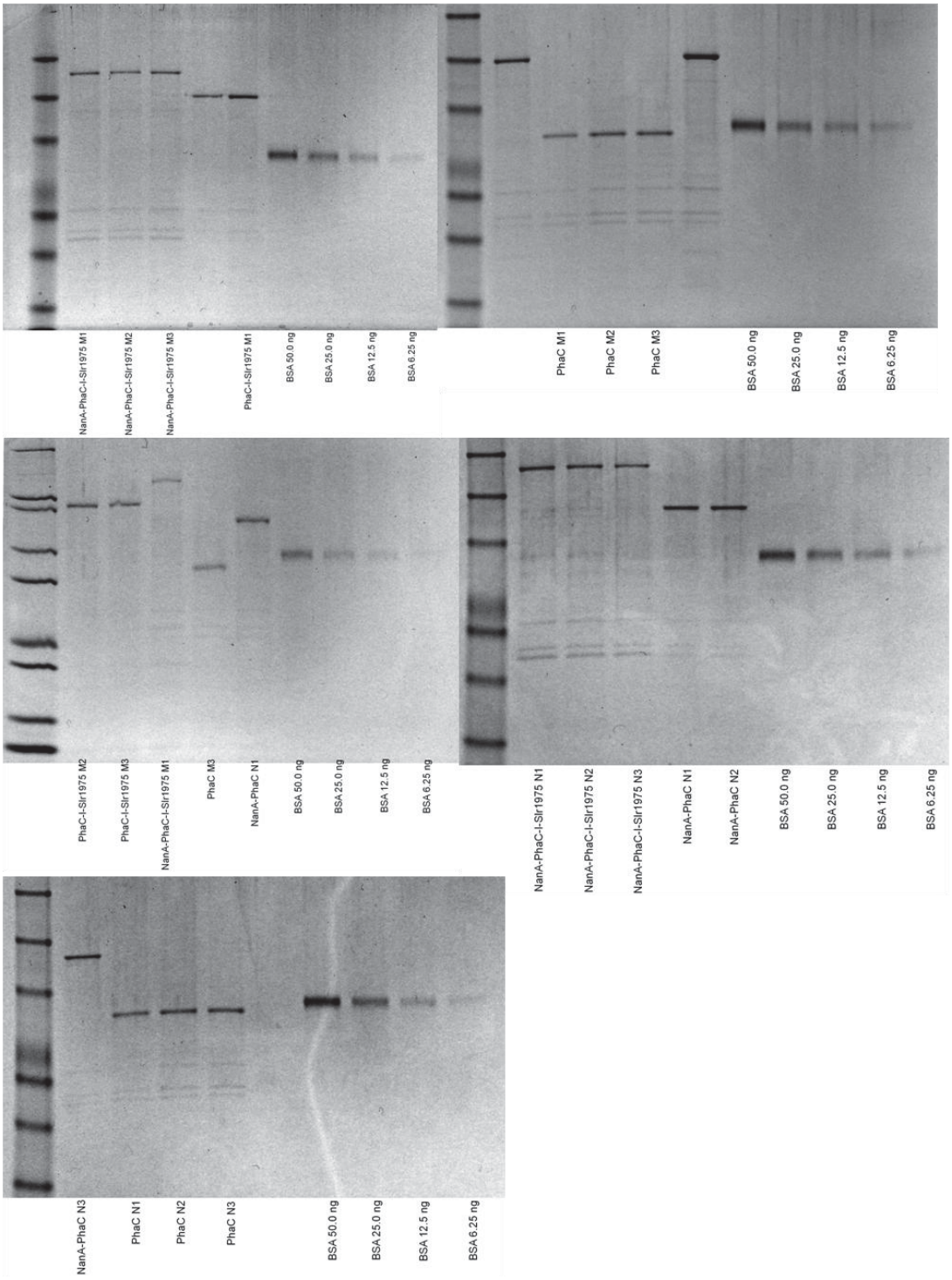

Figure S4.6: SDS-PAGE performed to assess the fusion protein content of PHA beads by densitometry. Total beads were electrophoresed onto a gel, stained with Coomassie blue, an image was taken by a gel doc (BioRad Laboratories, Hercules, CA), and analysed with the IMAGE LAB software (BioRad Laboratories, Hercules, CA) comparing the fusion protein with known quantities of BSA.

References

Amara, A. A., & Rehm, B. H. A. (2003). Replacement of the catalytic nucleophile cysteine-296 by serine in class II polyhydroxyalkanoate synthase from Pseudomonas aeruginosa-mediated synthesis of a new polyester: identification of catalytic residues. *Biochemical Journal*, *374*(Pt 2), 413–21. doi:10.1042/BJ20030431

Jahns, A. C., & Rehm, B. H. A. (2009). Tolerance of the Ralstonia eutropha class I polyhydroxyalkanoate synthase for translational fusions to its C terminus reveals a new mode of functional display. *Applied and Environmental Microbiology*, *75*(17), 5461–6. doi:10.1128/AEM.01072-09

Peters, V., & Rehm, B. H. A. (2006). In vivo enzyme immobilization by use of engineered polyhydroxyalkanoate synthase. *Applied and Environmental Microbiology*, *72*(3), 1777. doi:10.1128/AEM.72.3.1777

Rasiah, I. A., & Rehm, B. H. A. (2009). One-step production of immobilized alpha-amylase in recombinant Escherichia coli. *Applied and Environmental Microbiology*, *75*(7), 2012–6. doi:10.1128/AEM.02782-08

Chapter 5

5. Insights into the surface topology of polyhydroxyalkanoate synthase: self-assembly of functionalized inclusions

David O. Hooks[a] and Bernd H. A. Rehm[a,b,c]#

Institute of Fundamental Sciences, Massey University, Palmerston North, New Zealand[a]
MacDiarmid Institute for Advanced Materials and Nanotechnology, Wellington, New Zealand[b]

Polybatics Ltd, Palmerston North, New Zealand[c]

Address correspondence to Bernd H. A. Rehm, b.rehm@massey.ac.nz; Tel.: +64 6 350 5515 ext: 84704

Abstract

The polyhydroxyalkanoate (PHA) synthase catalyzes the synthesis of PHA, and remains attached to the hydrophobic PHA inclusions it creates. Although this feature is actively exploited to generate functionalized biobeads via protein engineering, little is known about the structure of the PHA synthase. Here, the surface topology of *Ralstonia eutropha* PHA synthase was probed to inform rational protein engineering toward the production of functionalized PHA beads. Surface-exposed residues were detected by conjugating biotin to inclusion-bound PHA synthase, and identifying the biotin-conjugated lysine and cysteine residues using peptide fingerprinting analysis. The identified sites (K77, K90, K139, C382, C459, and K518) were investigated as insertion sites for the generation of new protein fusions. Insertions of FLAG epitopes into exposed sites K77, K90, K139, and K518 were tolerated, retaining >65% of *in vivo* activity. Sites K90, K139, and K518 were also tested by insertion of the immunogobulin G (IgG) binding domain (ZZ), successfully producing PHA inclusions able to bind human IgG *in vitro*. Although simultaneous insertions of the ZZ domain into two sites was permissive, insertion at all three lysine sites inactivated the synthase. The K90/K139 double ZZ insertion had the optimum IgG binding capacity of 16 mg IgG/g wet PHA beads and could selectively purify the IgG fraction from human serum. Overall, this study identified surface-exposed flexible regions of the PHA synthase which either tolerate protein/peptide insertions, or are critical for protein function. This further elucidates the structure and function of PHA synthase and provides new opportunities for generating functionalized PHA biobeads.

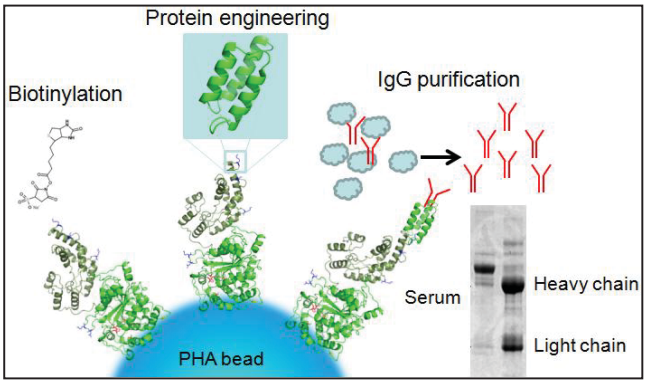

Table of contents figure: Surface exposed regions of granule-associated polyhydroxyalkanoate (PHA) synthase were probed with specific biotinylation reagents. The discovered sites were functionalized by the insertion of immunoglobulin G binding domains. The resulting PHA beads mediated the purification of IgG from human serum.

Keywords

Polyhydroxyalkanoate, Immunoglobulin G, Biotinylation, Protein immobilization

Introduction

Polyhydroxylakanoates (PHA) are a group of carbon storage polymers produced in some bacteria and archaea when subjected to nutrient-imbalanced conditions (Brandl et al 1988; Hezayen et al 2000). The final enzyme in the production pathway is PHA synthase (PhaC), which catalyzes the conversion of (*R*)-3-hydroxyacyl-CoA to the PHA polymer (Rehm and Steinbüchel 1999). PhaC remains covalently attached to the end of the nascent PHA chain, and these amphipathic PhaC-PHA chain molecules form spherical inclusions of approximately 50 - 500 nm diameter inside the cell (Grage et al 2009). PhaC from

Ralstonia eutropha (ATCC 17699) has been used as an anchor for fusion protein immobilization to the bead surface (Brockelbank et al 2006). This process allows for the *in vivo* production of functional PHA biobeads which are extracted by cell lysis and centrifugation (Rehm 2003; Draper et al 2013). Applications for these beads have included enzyme display, affinity purification, and medical uses such as vaccines and diagnostics. Until now, limited understanding of the structure of PhaC has confined protein engineering to fusions at the PhaC C-terminus and/or N-terminus (Brockelbank et al 2006; Parlane et al 2011; Blatchford et al 2012; Hooks et al 2013; Hooks et al 2014; Chen et al 2014).

As the key enzyme in PHA biosynthesis, PhaC has been extensively studied, but no three-dimensional structure has yet been obtained, perhaps in part due to its amphipathic nature. It is recognized that the protein has six conserved regions and the first 100 amino acids of the N-terminus are variable (Rehm 2003). Deletion of the first 78 amino acids of PhaC is permissive, however deletions of the first 80 amino acids reduced *in vitro* activity by 50% and deletion of the first 88 amino acids strongly impaired PHA accumulation in recombinant *R. eutropha* (Zheng et al 2006; Ye et al 2008). Despite the lack of topological information, the tolerance of PhaC to genetic manipulation through fusion to proteins of interest has previously been used in the design of functionalized PHA biobeads (Jahns and Rehm 2009).

The aim of this study was to provide insight into the topology of the inclusion-attached PHA synthase by specifically probing the surface of the synthase using conjugation of biotin labels. The structural flexibility of the identified exposed sites was further

characterized by inserting functional peptides. This approach provides data in support of a topological model of the synthase, and improves protein engineering capability for surface display of functional domains within PhaC itself.

Materials and Methods

Reagents

Biotin conjugation chemicals sulfo-NHS-biotin, iodoacetyl-LC-biotin, 1-Ethyl-3-[3-dimethylaminopropyl]carbodiimide hydrochloride (EDC), and biotin-hydrazide were purchased from ProteoChem (Loves Park, IL). Streptavidin-HRP was purchased from Invitrogen (Carlsbad, CA), anti-PhaC antibodies were produced by Genscript Corporation (Picastaway, NJ), and Anti-FLAG-HRP conjugate was purchased from Abcam (Cambridge, MA). Other chemicals were procured from Sigma-Aldrich (St. Louis, MO).

Growth conditions

Propagation of plasmids was carried out in *Escherichia coli* XL1-Blue (Stratagene, La Jolla, CA) cultivated in Luria-Bertani broth at 37 °C, 200 rpm. PHA production was performed with *E. coli* BL21(DE3) (Novagen, Madison, WI) containing the helper plasmid pMCS69 (Amara and Rehm 2003) in LB supplemented with 1% glucose at 25 °C, 200 rpm. As required, ampicillin (100 μg/mL) and chloramphenicol (50 μg/mL) were added to the media. Production of the fusion proteins was induced by the addition of IPTG to a final concentration of 1 mM. PHA beads were isolated from production cultures as described elsewhere (Hooks et al 2013); briefly, cells were lysed, and the beads were recovered from the cell lysate by ultracentrifugation in a glycerol gradient.

Biotin conjugation

Conjugation of biotin to the PHA beads was performed using Sulfo-NHS-biotin, iodoacetyl-biotin, and biotin-hydrazide according to established protocols (Hermanson 2008). For labeling lysines, a 500 µL aliquot of 1.25 mg total protein/mL PhaC beads (as determined by the method of Bradford) was dispensed into a tube, and 30 µL of 10 mM sulfo-NHS-biotin was added. The labeling reaction proceeded for two hours on a rotating mixer at 4 °C. Quenching was accomplished with Tris-HCl. Finally, the PHA beads were washed three times with phosphate buffer. For labeling cysteines, iodoacetyl-biotin was dissolved in dimethylformamide at a concentration of 2 mg/mL. PhaC beads at 4 mg total protein/mL were dispensed in a 200 µL aliquot and 45 µL of the iodoacetyl-biotin was added. The labeling reaction was incubated in the dark for 90 min on a rotating mixer at 25 °C. Finally, the PHA beads were washed three times with phosphate buffer. For labeling aspartic and glutamic acid, the PhaC beads were resuspended in 100 mM MES buffer and a 500 µL aliquot dispensed into a tube. 25 µL of biotin hydrazide dissolved in DMSO at a concentration of 13 mg/mL was added to the labeling reaction, followed by addition of 12.5 µL of EDC dissolved in water at a concentration of 100 mg/mL. The labeling proceeded for two hours on a rotating mixer. Finally, PHA beads were washed three times with 50 mM phosphate-buffer to remove residual biotinylation compounds, and resuspended in 50 mM phosphate buffer.

Biotinylated PHA samples (10 µL of 1 mg/mL wet weight) were electrophoresed through a 10% polyacrylamide gel in MOPS buffer to separate the bead-associated proteins. PhaC was identified by Western blot using an anti-PhaC antibody and a horse radish peroxidase

(HRP) labeled secondary antibody. Biotinylation of amino acids was confirmed using streptavidin-HRP conjugate. Successfully biotinylated PhaC was excised from the gel and subjected to MALDI-TOF/TOF performed by the Centre for Protein Research (Otago, New Zealand). Biotinylation sites were identified by a mass shift corresponding to the molecular weight of the conjugated chemical.

Mutagenesis of *phaC* to create FLAG insertions

The exposed sites of PhaC, as identified by biotinylation, were subjected to mutagenesis to insert FLAG epitopes. to confirm their surface exposure and assess their suitability for accepting functional insertions. The FLAG epitopes were inserted into *phaC* carried on the plasmid pET14b:PhaC (Brockelbank et al 2006) using site-directed ligation-independent mutagenesis (SLIM) as described elsewhere (Chiu et al 2004; Chiu et al 2008). SLIM primers are specified in supplementary Table S5.1 in Online Resource 1. Primers and other synthesized DNA as required were purchased from Integrated DNA technologies (Coraville, IA), while *Taq* and Platinum *Pfx* were purchased from Invitrogen (Carlsbad, CA). Successful mutagenesis was confirmed by DNA sequencing performed by the Massey Genome Centre on a capillary AB13730 genetic analyzer (Palmerston North, New Zealand).

Microscopy

Production of PHA beads was observed by fluorescent microscopy after staining with the lipophilic dye Nile Red, as described previously (Peters et al 2007).

Plasmid construction

The construction of plasmids containing *phaC* with inserted *zz* sequence (Brockelbank et al 2006) was performed using methods described elsewhere (Sambrook et al 1989). Primers were purchased from Integrated DNA Technologies (Coraville, IA) and polymerases from Invitrogen (Carlsbad, CA). Gene synthesis of the triple-*zz* inserted *phaC* was performed by Genscript Corporation (Picastaway, NJ), and inserted into pUC57 with *Nde*I and *Bam*HI restriction endonuclease sites for additional sub-cloning into a pET14b vector for protein expression (supplementary Table S5.1 in Online Resource 1). The synthesized triple-*zz* *phaC* was generated such that the site K90 *zz* was flanked by *Spe*I restriction endonuclease sites, K139 by *Afl*II, and K518 by *Mfe*I. The double and single zz-insertions were generated by subcloning restriction fragments of the pUC57 triple *zz* plasmid into pET14b:PhaC as outlined in supplementary Table S5.1 in Online Resource 1.

ELISA for detection of FLAG epitopes

The exposure and accessibility of the FLAG tags was assessed by enzyme-linked immunosorbent assay (ELISA). PHA Beads (10 mg/mL wet weight) were bound to microtiter plates by adding 100 µL of PHA bead suspension to each well and incubating overnight at 4 °C. After incubation, the wells were emptied and washed three times with PBST (PBS + 0.05% Tween 20). Anti-FLAG-HRP antibodies were diluted 1:20,000 and 100 µL added to each well. The plate was then incubated in a dark humidified container for 30 min. After incubation, the wells were emptied and washed five times with PBST. Finally, 100 µL of *o*-phenylenediamine was added to each well, and after 15 min incubation in a dark humidified container the color development was halted by addition of 100 µL H_2SO_4

(1 N). Using an ELX808 Ultra Microplate plate reader (Bio-Tek Instruments, Inc., Winooski, VT), substrate conversion was read at wavelength 490 nm. The extent of color development is based on the amount of anti-FLAG-HRP bound to the PHA beads and thus to the accessibility of the FLAG-tag within the PhaC protein.

PhaC activity after insertion of FLAG epitopes and ZZ domains

The impact of FLAG tag and ZZ domain insertions into PhaC on overall PHA production was quantified by gas chromatography-mass spectroscopy (GCMS) after conversion into 3-hydroxy-methylesters by acid-catalyzed methanolysis as described elsewhere (Brandl et al 1988). GCMS was performed by The New Zealand Institute for Plant and Food (Palmerston North, New Zealand).

IgG Binding Assays for inserted ZZ domains

The ZZ antibody binding domain of protein A from *S. aureus* was inserted into the exposed sites successfully used to display a FLAG-tag. The functionality of the inserted ZZ domain was quantified by an IgG binding assay as described previously (Brockelbank et al 2006). Briefly, PHA beads were resuspended in 450 µL of PBS buffer at a concentration of 100 mg/mL (wet bead weight), and 500 µL of 10 mg/mL human immunoglobulin (IgG) was added. The IgG was allowed to bind to the PHA beads during 30 min incubation at 25 °C on a rotating mixer. After the incubation period the beads were centrifuged at 6000 × g for 4 min. The supernatant (unbound fraction) was removed, and the sediment was washed by resuspention in 1 mL of PBS. The washing steps were repeated three times in total to remove excess unbound IgG. The remaining beads were resuspended in 1 mL of 50 mM

glycine (pH 2.7) and incubated at 25 °C for 5 min to elute bound IgG. The samples were pelleted by centrifugation at high speed (15,000 × g, 4 min) and the supernatant transferred to a new tube. This elution fraction was then neutralized by the addition of 20 µL 1 M K_2HPO_4. The amount of IgG eluted was quantified by the method of Bradford using human IgG as a standard. The purification of IgG from human serum was conducted as outlined above, except the feed material consisted of 1 mL heat-treated human serum from Invitrogen (Carlsbad, CA) -- enough to saturate the IgG binding capacity of the PHA bead.

Results

Chemical cross-linking of biotin to surface-accessible sites on PhaC

PHA beads were recombinantly produced in *E. coli* using the pET14b:PhaC and pMCS69 plasmids (described in supplementary Table S5.1 in Online Resource 1) to express the PhaA, PhaB, and PhaC enzymes from *R. eutropha*. The PHA beads were subjected to biotinylatin reactions to label surface-exposed amino acids. Three compounds with different amino acid specificities were used to probe a range of exposed amino acids. Sulfo-NHS-biotin reacts with primary amino groups found on lysine side chains and forms a stable amide bond. Iodoacetyl-biotin reacts with the reduced thiol group in cysteine residues to form an irreversible thioether bond. Finally, the crosslinker EDC is used to bond carboxyl groups to primary amines. Activation of carboxyl groups on glutamic and aspartic acid residues with EDC results in *o*-acylisourea intermediates allowing the amine-containing biotin-hydrazide to chemically bond via an amide linkage. PHA beads reacted with sulfo-NHS-biotin, iodoacetyl-LC-biotin or biotin-hydrazide (after activation with EDC)

showed successful biotinylation of bead-associated proteins (Fig. 5.1A). However, in the case of EDC and biotin-hydrazide, PhaC was lost from the beads during the reaction conditions and is absent on the Western blot using anti-PhaC antibodies (Fig. 5.1B); therefore this method of biotinylation was not further explored.

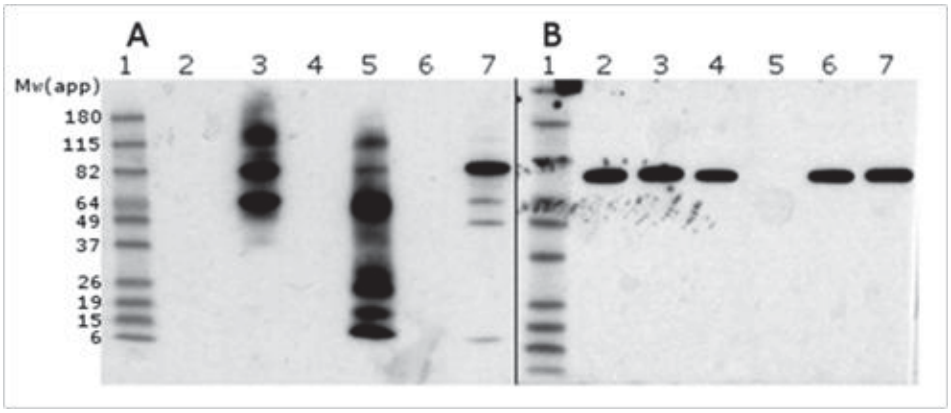

Figure 5.1 Isolated PHA beads were reacted with biotin-containing reagents to label bead-surface proteins including PhaC. A: Strepdavidin-HRP immunoblot to detect biotinylated bead-surface proteins. B: Anti-PhaC immunoblot identifying the presence of PhaC after biotinylation treatment. Lane 1: BenchMark prestained molecular weight standard, 2: Unlabelled PhaC, 3: Iodoacetyl-biotin labelled, 4: Unlabelled PhaC, 5: Biotin hydrazide labelled, 6: Unlabelled PhaC, 7: Sulfo-NHS-biotin labelled

Identification of labeled surface-accessible amino acids by MALDI-TOF mass spectrometry

Protein bands corresponding to successfully biotinylated PhaC were excised from the SDS-PAGE gel and subjected to MALDI-TOF mass spectrometry. Six amino acids along the length of PhaC were identified as having reacted with sulfo-NHS-biotin and iodoacetyl-LC-

biotin: K77, K90, K139, K518/K520, C382, and C459. Some of these sites can be visualized on the Phyre-generated threading model (Fig. 5.2) (Kelley and Sternberg 2009), which maps amino acids 205 - 534 (55%) of the PhaC C-terminal domain to the alpha/beta hydrolase domain from human epoxide hydrolase (d1zd3a2). As K518 and K520 are in close proximity, they were considered to be part of the same exposed region. K518 was chosen for further study as it was always detected as biotinylated when subjected to MALDI-TOF/MS, whereas K520 was not always detected as being biotinylated. This result showed K518 was more exposed and accessible to the biotinylation reagent than K520, and thus K518 was selected for further investigation of this protein region.

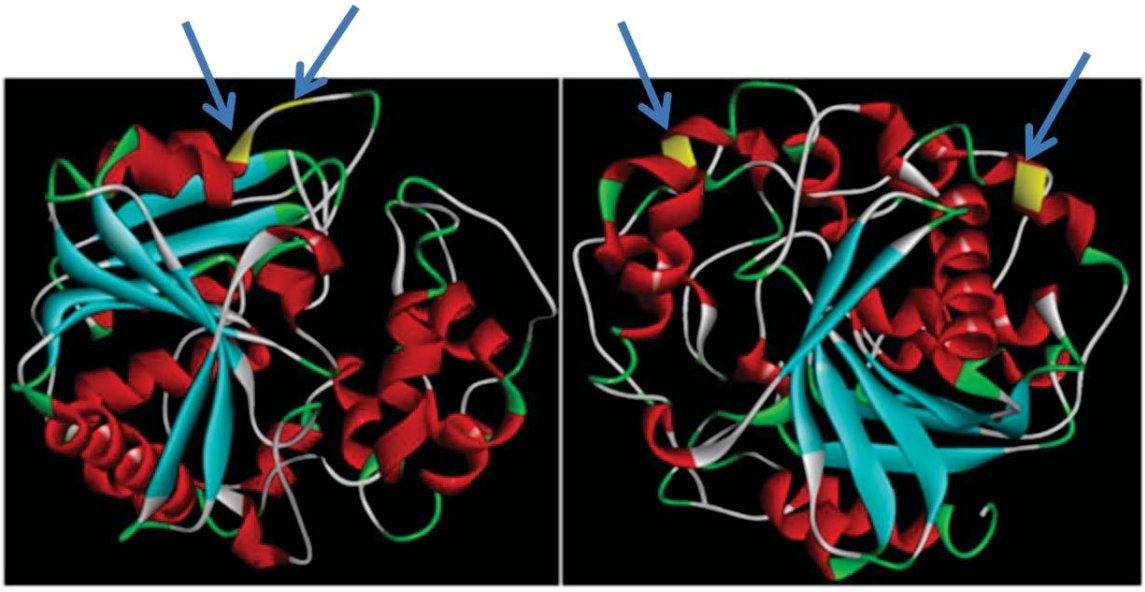

Figure 5.2 Threading model of PhaC highlighting (yellow) the location of labelled residues. Left – lysines (K518, K520). Right – cysteines (C382, C459). Lysines in the N-terminal region of PhaC are not shown as they could not be mapped in the model (K77, K90, K139). This model was generated by Phyre based on the a/b-hydrolase fold of the C-terminal domain of human expoxide hydrolase (d1zd3a2)

Assessment of structural constraints of identified surface exposed regions of bead-associated PhaC using FLAG epitope insertions

The *phaC* gene was mutagenised with site-directed ligation-independent mutagenesis (SLIM) to insert a FLAG epitope (DYKDDDDK) encoding sequence directly after each biotinylated amino acid in order to confirm surface exposure and to assess the structural flexibility of the region (Fig. 5.3). The effect of FLAG insertion on the ability of PhaC to produce polyhydroxybutyrate (PHB) was quantified by gas chromatography mass spectroscopy (GCMS) and compared to wild type PhaC (Fig. 5.4). There was no statistically significant difference between wild-type PhaC and PhaC with FLAG insertions at K139 or K518. However, insertion of FLAG at K77 or K139 did significantly reduce the amount of PHB to approximately 65% of the wild-type amount ($p < 0.05$). Insertion of FLAG at sites C382 or C459 had a dramatic effect on PHB production, with neither variant able to mediate PHB production at levels significantly greater than zero when compared to wild-type production levels. Additionally, an immunoblot of respective cell lysates showed that while the other PhaC variants with FLAG insertion were produced at high levels, C382ΩFLAG appeared at lower levels and C459ΩFLAG was not detectable (Fig. 5.5). This suggests insertion of FLAG at C459 is more deleterious and the resultant PhaC is degraded within the cell, whereas the PhaC resulting from C382ΩFLAG insertion is produced within the cell but has low or absent activity. Overall, these results demonstrate the regions around K77, K90, K139, and K518 are more flexible i.e. less structurally constrained and hence amenable to peptide insertion in order to add surface functionality.

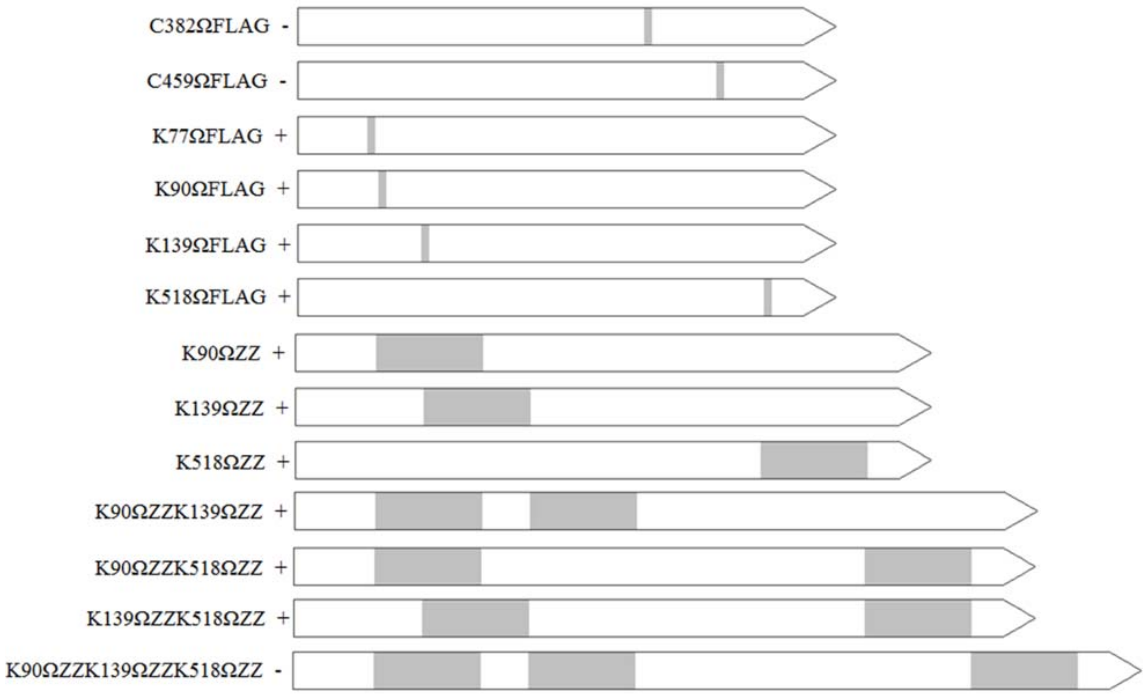

Figure 5.3 Schematics of the PhaC insertions created in this study. Shaded area indicates the location and size of insertion. The +/- indicates whether the insertion was permissive for production of PHB. Of those that were permissive, PhaC insertion variants showed additional functionality by binding anti-FLAG-HRP antibodies (FLAG insertions) or binding and eluting human IgG (ZZ insertions)

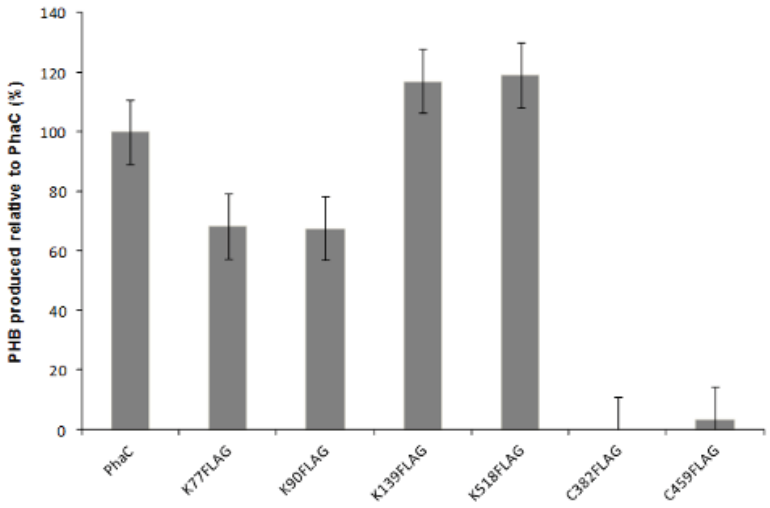

Figure 5.4 PHB production by PhaC variants with FLAG insertions. FLAG insertion at amino acids K139 or K518 had no impact on PHB production, while insertion at amino acids K77 or K139 reduced the amount of PHB to ~65% of the wild-type amount. Insertion of FLAG at sites C382 or C459 abolished PHB production. Tukey bars at experiment wide error rate of 0.05, n = 3

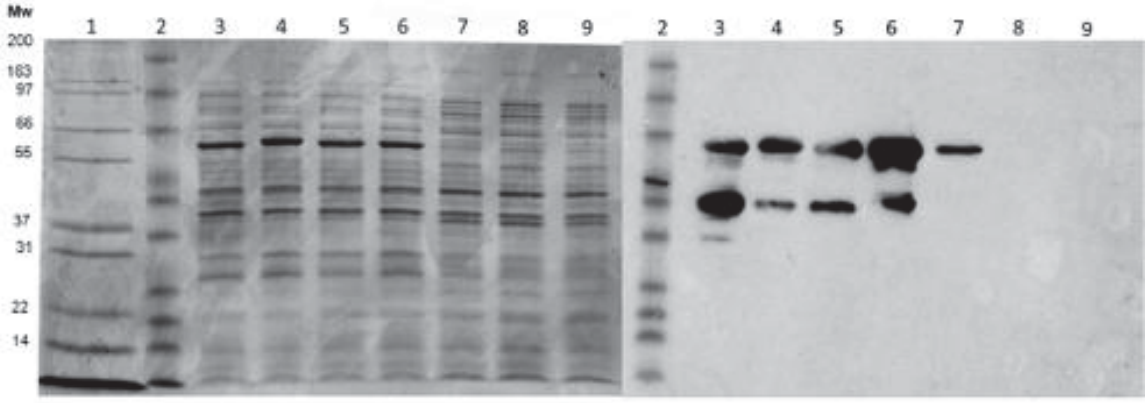

Figure 5.5 Gel electrophoresis and immunoblot analysis of whole cell lysates from PhaC FLAG variants. Left, SDS-PAGE. Right, Anti-PhaC immunoblot. Lane 1: Mark 12 protein ladder, 2: BenchMark prestained ladder, 3: K77ΩFLAG, 4: K90ΩFLAG, 5: K139ΩFLAG, 6: K518ΩFLAG, 7: C382ΩFLAG, 8: C459ΩFLAG, 9: K90ΩZZK139ΩZZK518ΩZZ. On the SDS-PAGE gel, PhaC overproduction is visible (arrows) at ~64 kDa in lanes 3 - 6 but not in lanes 7 - 9. For the anti-PhaC Western blot, PhaC is visible (arrows) in lanes 3 - 7 indicating some amount of PhaC is produced in the C382ΩFLAG variant, even though it is not visible by SDS-PAGE

FLAG insertions into accessible lysine sites are surface exposed in the bead-associated PHA synthase

PHA beads coated with synthase variants containing FLAG epitopes were subjected to enzyme-linked immunosorbent assay (ELISA) using anti-FLAG-HRP conjugated antibodies (Fig. 5.6). PHA beads were normalized by weight and adsorbed overnight to the wells of 96-well plates. Excess beads were removed with repeated wash steps. Anti-FLAG-HRP

antibodies were allowed to bind to the exposed FLAG epitopes and then reacted with *o*-phenylenediamine in a colorimetric assay. The negative control, PHA beads coated with wildtype PhaC, had no detectable absorbance at 490 nm whereas the FLAG-containing constructs had absorbance measured from 0.61 - 2.91. Of these K90ΩFLAG, K139ΩFLAG, and K518ΩFLAG had approximately the same absorbance reading across the 6.25 - 50 µg bead mass range of 0.61 - 1.44. K77ΩFLAG had an approximately 70% higher reading, from 1.39 - 2.91, at all bead mass levels compared to the other sites. These results demonstrated that the FLAG insertions at amino acids K90, K139, and K518 were exposed to approximately the same level. Site K77 appeared to be more accessible to the anti-FLAG-HRP antibody, likely due to its location in the highly flexible N-terminal region of PhaC. All four of the FLAG insertions showed both PhaC enzyme activity as well as functionalization of the PHA bead surface with a detectable epitope.

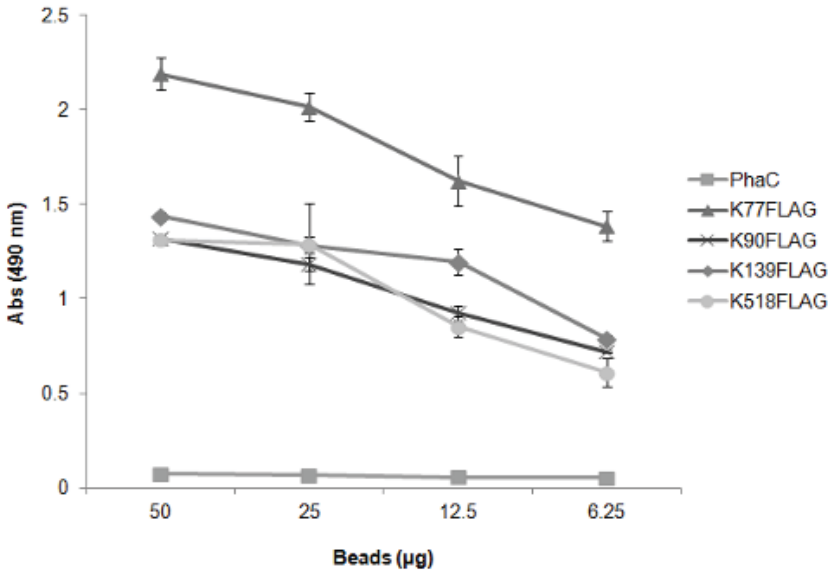

Figure 5.6 ELISA using anti-FLAG-HRP antibodies to determine the exposure of the FLAG insertion for potential functional display. PHA beads containing FLAG tags at the indicated site were bound to microtiter plates and incubated with anti-FLAG-HRP antibodies. The HRP substrate *o*-phenylenediamine was added and color allowed to develop for 15 min. Absorbance was read at 490 nm. A higher absorbance correlates with a higher level of and accessibility for the antibody. Error bars ± SEM, n = 3

Targeting surface exposed lysine sites toward functionalization of PHA beads

The IgG binding domain ZZ based on protein A from *Staphylococcus aureus* was selected as a model for functionality, as its strong folding potential and hair-pin like structure would potentially allow the internally-modified PhaC to fold correctly (Nilsson et al 1987; Löwenadler et al 1987). Surface exposed sites K90, K139, and K518 were targeted for insertion of the ZZ domain. K77 was not considered for further functionalization, as it is

accepted that at least the first 78 amino acids of PhaC can be deleted without significant negative consequence on the ability of PhaC to produce PHB (Zheng et al 2006; Ye et al 2008). In addition to the single ZZ domain insertions at K90, K139, and K518, the three double and single triple ZZ insertion variants were also produced (Fig. 5.3). PHB production analysis by GCMS revealed that single insertions were tolerated well, with no discernible impact on PHB production; PHB content of cells ranged from 39 - 42% PHB per mg dry cell weight compared to 32% PHB per mg dry cell weight of the wild type (Fig. 5.7). In contrast, PhaC containing double ZZ domain insertions produced lower amounts of PHB, 3 - 22% PHB per mg dry cell weight, and the triple ZZ insertion strain produced no detectable PHB (Fig. 5.7). Immunoblot analysis of respective cell lysates revealed that the triple inserted PhaC protein was not produced in detectable amounts (Fig. 5.5). These results show that a single insertion of 116 amino acids at one of three identified surface exposed lysine sites can be well tolerated by the PhaC enzyme, but further insertions of the same size at the other sites interferes with synthase activity. When three ZZ domains were inserted, the PhaC variant protein could not be detected and no PHB was produced, indicating a deleterious effect on protein production and/or stability within the cell.

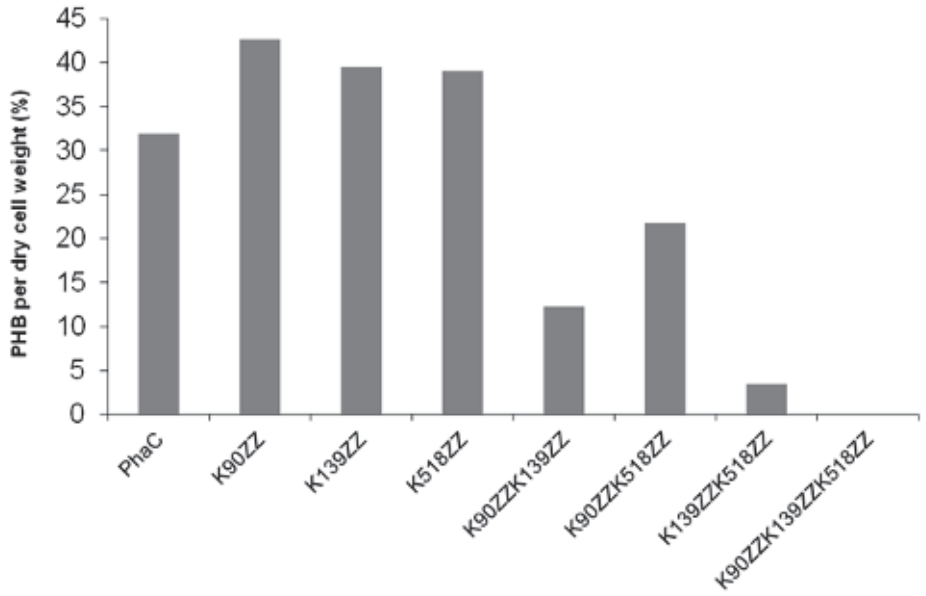

Figure 5.7 PHB production mediated by PhaC variants with ZZ domain insertion. The 116 amino acid ZZ domain was inserted after the indicated amino acid and PHB production assessed. Single insertions of ZZ were well tolerated with no apparent impact on PHB production. PhaC containing double ZZ domain insertions decreased the amount of PHB produced, and the triple ZZ insertion strain produced no detectable PHB. n = 1, only one repeat performed due to cost constraints

Assessment of engineered PhaC surface functionality

The functionality of the ZZ inserted into the surface of attached PhaC was examined by incubating the respective ZZ-displaying beads with human immunoglobulin G (IgG) and measuring the amount of IgG which could be bound and subsequently eluted from the beads with a low pH treatment. All PHA beads coated by PhaC variants with ZZ domain insertions were able to bind and elute human IgG (Fig. 5.8), but the amount of IgG eluted varied depending on the number and positioning of the ZZ domains within the PhaC

enzyme. Insertion of the ZZ domain at amino acid K90 resulted in the highest amount of eluted IgG, while insertion at amino acid K518 resulted in the lowest elution amount. Having a ZZ domain at site K518 appeared to have a negative impact on the quantity of IgG bound by the PHA beads possibly due to a less stable or lower amount of PhaC present on the bead surface. Single insertions of the ZZ domain bound between 9.1 - 13.6 µg IgG/mg PHA beads. Double insertions were not strictly additive, with K90ΩZZK139ΩZZ binding more at 16.0 µg IgG/mg bead while K90ΩZZK518ΩZZ and K139ΩZZK518ΩZZ bound less at 7.9 and 7.1 µg IgG/mg bead, respectively.

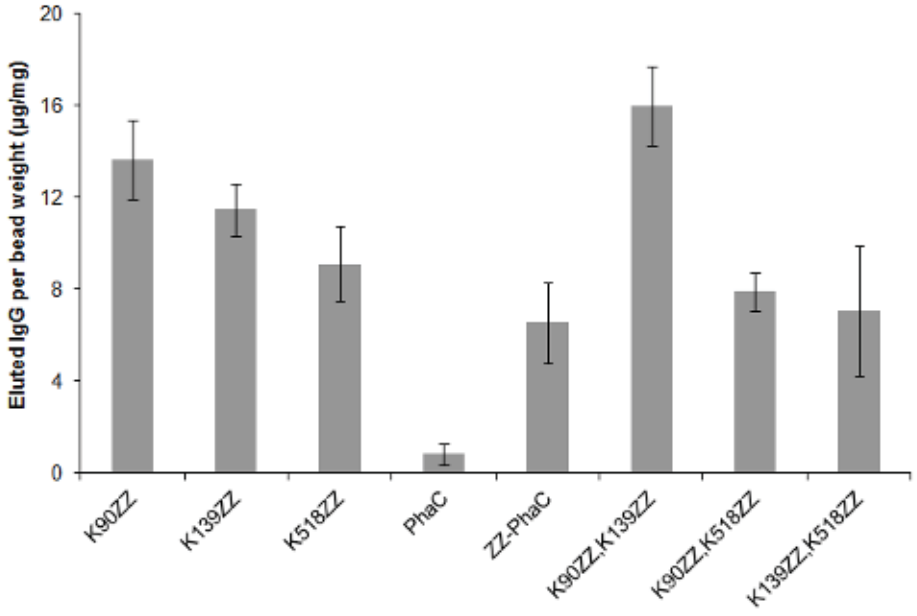

Figure 5.8 Human IgG binding capacity of PHA beads formed by PhaC with ZZ insertions. Beads (30 mg) containing the indicated ZZ domain insertions were incubated with 5 mg of IgG for 30 min at 25 ^{o}C. Bound IgG was eluted with glycine-HCl (pH 2.7) and measured by the method of Bradford. Error bars ± SEM, n = 3

PhaC beads displaying immobilized ZZ domains fused directly to the N-terminus of PhaC have previously been shown to purify IgG from human serum to a similar quality as commercial protein A-sepharose beads (Brockelbank et al 2006). In this study, these previously published ZZ-PhaC beads, used as a positive control, bound a similar amount of IgG to the lowest performing ZZ insertion beads of 6.6 μg IgG/mg bead (Fig 8). Therefore, we assessed the ZZ-insertion displaying beads with the highest binding capacity (K90ΩZZK139ΩZZ) for their ability to purify the IgG fraction from human serum (Fig. 5.9). SDS-PAGE analysis of eluted proteins revealed protein bands at ~50 kDa and ~25 kDa, representing the heavy and light chains of human IgG respectively. The protein elution profile of wild-type PHA beads suggests non-specific binding of IgG to the PhaC-only beads is not a significant issue. The proteins eluted at pH 2.7 from the K90ΩZZK139ΩZZ beads showed a high degree of purity demonstrating the inserted ZZ domains mediate IgG purification.

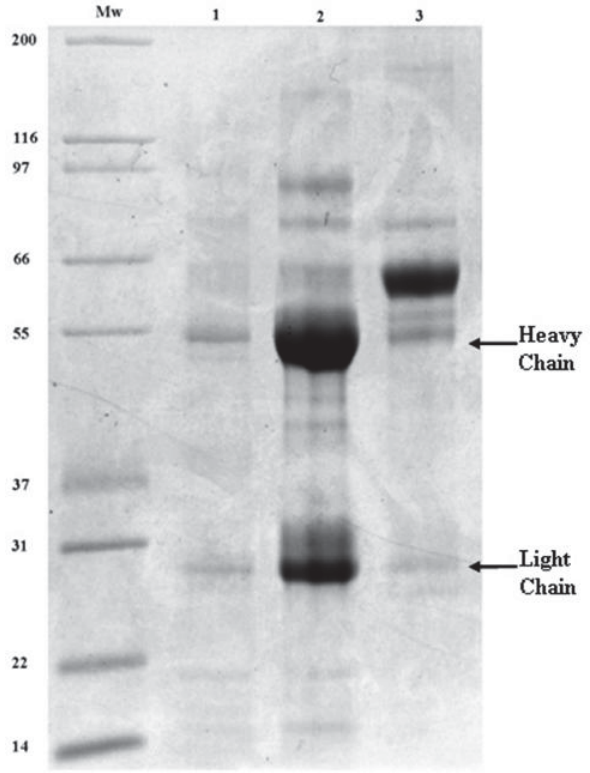

Figure 5.9 SDS-PAGE of human serum proteins bound *in vitro* to wild-type or PhaCK90ΩZZK139ΩZZ beads and released after low pH elution, showing the purification ability of ZZ-inserted PHA beads. Lane Mw: Mark 12 protein ladder; 1: proteins eluted from wild-type PHA beads; 2, proteins eluted from PhaCK90ΩZZK139ΩZZ beads; 3: human serum (1:200). Indicated are the heavy and light chains of human IgG.

Discussion

This study explored the surface topology of granule-associated PHA synthase by probing the folded protein with biotinylation reagents (Hermanson 2008) followed by identification of the biotinylated amino acid residues using MALDI-TOF/MS. Two different

biotinylation reactions with sulfo-NHS-biotin and iodoacetyl-biotin resulted in identification of five lysine residues of interest: K77, K90, K139, K518, and K520, and two cysteine residues: C382 and C459. A Phyre model of PhaC based on a human epoxide hydrolase (d1zd3a2) covering 56% of the PhaC sequence (Fig 5.2) is consistent with surface exposure of the identified residues present in the model (K518, K520, C382, C459). Attempts at using *ab initio* structure prediction tools to visualize the remaining variable N-terminal structure were not convincing (data not shown).

Multiple alignments of PHA synthases have previously shown there are six conserved regions of the enzyme (Rehm, B.H.A., Steinbüchel 2001). Sites K77 and K90 are located before the first conserved region, K139 is located between conserved regions one and two, C382 and C459 are located within the fourth conserved region, and K518 is located between conserved regions five and six (Rehm 2003). It is therefore reasonable that the non-conserved regions (K77, K90, K139, K518) could be modified with functional insertions without disrupting protein function, as opposed to the conserved regions (C382 and C459). In this work, only the lysine sites could be confirmed as surface exposed and amenable to insertion by detectable FLAG sequences (Fig. 5.6). Previously, the tuberculosis-related antigens ESAT6, CFP10, and Rrv3615c were shown to be highly accessible to their respective antibodies in ELISA assays when directly fused to the N-terminus of PhaC (Chen et al 2014). Additionally, the ZZ domain fused directly to the N-terminus of PhaC is accessible for antibody binding in ELISA assays (Brockelbank et al 2006). Ultimately, three sites: K90, K139, and K518, were targeted by ZZ domain insertions which mediated binding of IgG (Nilsson et al 1987; Löwenadler et al 1987) by

the respective isolated PHA beads (Fig. 5.8). The K90/K139 double ZZ insertion had the highest IgG binding capacity and could selectively purify the IgG fraction from human serum (Fig. 5.9), indicating the suitability of these sites for functionalized insertions. Single insertions of either FLAG or ZZ had little impact on the ability of PhaC to synthesize PHA in vivo, however multiple insertion did have a negative impact on PHA production (Figs. 5.5, 5.8). Commercially available protein A resins include crosslinked agarose, porous glass, and other polymeric matrices ranging in size 50 - 300 µm in diameter. The dynamic binding capacity of these materials has been measured under operating conditions in a variety of column set-ups to be between 5 - 30 mg of IgG per mL of settled resin (Hahn et al 2003). Previous ZZ-displaying PHA beads have been shown to bind up to 100 mg IgG per g drained beads, and the use of internal ZZ display in conjunction with N- and C-terminal display could potentially increase overall IgG binding capacity.

Using these new surface-display sites will allow the immobilization of additional functionalities such as binding domains (e.g., biotin acceptor peptide) or multiple epitopes while leaving the more flexible N- and C-terminal binding sites free for larger fusion partners. This approach of using a single engineered PhaC as the sole protein anchor on PHA beads will maintain the simplicity of the PHA bead over-expression system and purification processes while allowing more complex applications, such as novel multivalent particulate vaccines, to be explored.

Acknowledgments

This work was supported by the Institute of Fundamental Sciences and Massey University,

Palmerston North, New Zealand. DOH received a PhD scholarship from Massey University.

Conflict of Interest: The authors declare that they have no conflict of interest.

References

Amara AA, Rehm BHA (2003) Replacement of the catalytic nucleophile cysteine-296 by serine in class II polyhydroxyalkanoate synthase from *Pseudomonas aeruginosa*-mediated synthesis of a new polyester: identification of catalytic residues. Biochem J 374:413–21. doi: 10.1042/BJ20030431

Blatchford PA, Scott C, French N, Rehm BHA (2012) Immobilization of organophosphohydrolase OpdA from *Agrobacterium radiobacter* by overproduction at the surface of polyester inclusions inside engineered *Escherichia coli*. Biotechnol Bioeng 109:1101–8. doi: 10.1002/bit.24402

Brandl H, Gross RA, Lenz RW, Fuller RC (1988) *Pseudomonas oleovorans* as a Source of Poly(beta-Hydroxyalkanoates) for Potential Applications as Biodegradable Polyesters. Appl Environ Microbiol 54:1977–82.

Brockelbank JA, Peters V, Rehm BHA (2006) Recombinant *Escherichia coli* strain produces a ZZ domain displaying biopolyester granules suitable for immunoglobulin G purification. Appl Environ Microbiol 72:7394–7. doi: 10.1128/AEM.01014-06

Chen S, Parlane NA, Lee J, Wedlock DN, Buddle BM, Rehm BHA (2014) New skin test for detection of bovine tuberculosis on the basis of antigen-displaying polyester inclusions produced by recombinant *Escherichia coli*. Appl Environ Microbiol 80:2526–35. doi: 10.1128/AEM.04168-13

Chiu J, March PE, Lee R, Tillett D (2004) Site-directed, Ligase-Independent Mutagenesis (SLIM): a single-tube methodology approaching 100% efficiency in 4 h. Nucleic Acids Res 32:e174. doi: 10.1093/nar/gnh172

Chiu J, Tillett D, Dawes IW, March PE (2008) Site-directed, Ligase-Independent Mutagenesis (SLIM) for highly efficient mutagenesis of plasmids greater than 8kb. J Microbiol Methods 73:195–8. doi: 10.1016/j.mimet.2008.02.013

Draper J, Du J, Hooks DO, Lee JW, Parlane NA, Rehm BHA (2013) Polyhyroxyalkanoate inclusions: polymer synthesis, self-assembly, and display technology. In: Rehm BHA (ed) Bionanotechnol. Biol. Self-assembly Its Appl. Caister Academic Press, Norfolk, pp 1–36

Grage K, Jahns AC, Parlane N, Palanisamy R, Rasiah IA, Atwood JA, Rehm BHA (2009) Bacterial polyhydroxyalkanoate granules: biogenesis, structure, and potential use as nano-/micro-beads in biotechnological and biomedical applications. Biomacromolecules 10:660–9. doi: 10.1021/bm801394s

Hahn R, Schlegel R, Jungbauer A (2003) Comparison of protein A affinity sorbents. J Chromatogr B Anal Technol Biomed Life Sci 790:35–51. doi: 10.1016/S1570-0232(03)00092-8

Hermanson GT (2008) Bioconjugate Techniques. Bioconjugate Tech 506–545. doi: 10.1016/B978-0-12-370501-3.00011-4

Hezayen FF, Rehm BHA, Eberhardt R, Steinbüchel A (2000) Polymer production by two newly isolated extremely halophilic archaea: application of a novel corrosion-resistant bioreactor. Appl Microbiol Biotechnol 54:319–325.

Hooks DO, Blatchford PA, Rehm BHA (2013) Bioengineering of bacterial polymer inclusions catalyzing the synthesis of N-acetylneuraminic acid. Appl Environ Microbiol 79:3116–21. doi: 10.1128/AEM.03947-12

Hooks DO, Venning-Slater M, Du J, Rehm BHA (2014) Polyhydroyxalkanoate synthase fusions as a strategy for oriented enzyme immobilisation. Molecules 19:8629–43. doi: 10.3390/molecules19068629

Jahns AC, Rehm BHA (2009) Tolerance of the *Ralstonia eutropha* class I polyhydroxyalkanoate synthase for translational fusions to its C terminus reveals a new mode of functional display. Appl Environ Microbiol 75:5461–6. doi: 10.1128/AEM.01072-09

Kelley LA, Sternberg MJE (2009) Protein structure prediction on the Web: a case study using the Phyre server. Nat Protoc 4:363–71. doi: 10.1038/nprot.2009.2

Löwenadler B, Jansson B, Paleus S, Houngren E, Nilsson B, Moks T, Palm G, Josephson S, Philipson L, Uhlén M (1987) A gene fusion system for generating antibodies against short peptides. Gene 58:87–97. doi: 10.1016/0378-1119(87)90032-1

Nilsson B, Moks T, Jansson B, Abrahmsén L, Elmblad A, Holmgren E, Henrichson C, Jones TA, Uhlén M (1987) A synthetic IgG-binding domain based on staphylococcal protein A. "Protein Eng Des Sel 1:107–113. doi: 10.1093/protein/1.2.107

Parlane NA, Grage K, Lee JW, Buddle BM, Denis M, Rehm BHA (2011) Production of a particulate hepatitis C vaccine candidate by an engineered *Lactococcus lactis* strain. Appl Environ Microbiol 77:8516–22. doi: 10.1128/AEM.06420-11

Peters V, Becher D, Rehm BHA (2007) The inherent property of polyhydroxyalkanoate synthase to form spherical PHA granules at the cell poles: the core region is required for polar localization. J Biotechnol 132:238–45. doi: 10.1016/j.jbiotec.2007.03.001

Rehm BHA (2003) Polyester synthases: natural catalysts for plastics. Biochem J 376:15–33. doi: 10.1042/BJ20031254

Rehm BHA, Steinbüchel A (1999) Biochemical and genetic analysis of PHA synthases and other proteins required for PHA synthesis. Int J Biol Macromol 25:3–19.

Rehm, B.H.A., Steinbüchel A (2001) Biopolymers. Wiley-VCH, Heidelberg

Sambrook J, Fritsch E, Maniatis T (1989) Molecular cloning: A laboratory manual. Cold Spring Harbor Laboratory Press, Plainview, NY

Ushimaru K, Sangiambut S, Thomson N, Sivaniah E, Tsuge T (2013) New insights into activation and substrate recognition of polyhydroxyalkanoate synthase from *Ralstonia eutropha*. Appl Microbiol Biotechnol 97:1175–1182. doi: 10.1007/s00253-012-4089-x

Ye Z, Song G, Chen G, Chen J (2008) Location of functional region at N-terminus of polyhydroxyalkanoate (PHA) synthase by N-terminal mutation and its effects on PHA synthesis. Biochem Eng J 41:67–73. doi: 10.1016/j.bej.2008.03.006

Zheng Z, Li M, Xue X-J, Tian H-L, Li Z, Chen G-Q (2006) Mutation on N-terminus of polyhydroxybutyrate synthase of *Ralstonia eutropha* enhanced PHB accumulation. Appl Microbiol Biotechnol 72:896–905. doi: 10.1007/s00253-006-0371-0

Supplementary material for: Insights into the surface topology of polyhydroxyalkanoate synthase: self-assembly of functionalized inclusions

Journal:

Applied Microbiology and Biotechnology

Authors:

David O. Hooks[a] and Bernd H. A. Rehm[a,b,c]#

Affiliations:

Institute of Fundamental Sciences, Massey University, Palmerston North, New Zealand[a]
MacDiarmid Institute for Advanced Materials and Nanotechnology, Wellington, New Zealand[b]

Polybatics Ltd, Palmerston North, New Zealand[c]

Address correspondence to Bernd H. A. Rehm, b.rehm@massey.ac.nz; Tel.: +64 6 350 5515 ext: 84704

Table S5.1: Primers used in this study. Site-directed ligation -independant mutagenesis (SLIM) primers include forward and reverse short (Fs and Rs) as well as forward and reverse tailed (Ft and Rt) with the FLAG sequence.

Name	Characteristics	Source
***E. coli* Strains**		
XL1-Blue	*recA1*, *endA1*, *gyrA96*, *thi-1*, *hsdR17*($r-_k$, $m+_k$), *supE44*, *relA1*, -, *lac*[*F'*, *proAB*, *lacI*^{q}, *lacZΔM15*, *Tn10*(*Tc*^{r})]	Stratagene
BL21(DE3)	*F-*, *ompT*, *hsdS*$_B$ (r_B- m_B-), *gal*, *dcm* (DE3)	Novagen
SLIM primers		
PhaCK77Fs	cttcatgtagcgctgctggatat	
PhaCK77Ft	CTTGTCGTCGTCGTCCTTGTAGTCcttcatgtagcgctgctggatat	
PhaCK77Rs	gacttctcagcgctgtggca	
PhaCK77Rt	GACTACAAGGACGACGACGACAAGgacttctcagcgctgtggca	
PhaCK90Fs	cttgccctcggccatggcct	
PhaCK90Ft	CTTGTCGTCGTCGTCCTTGTAGTCcttgccctcggccatggcct	
PhaCK90Rs	gccgaggccaccggtccgct	
PhaCK90Rt	GACTACAAGGACGACGACGACAAGgccgaggccaccggtccgct	
PhaCK139Fs	cttggcatcggcctcgacgg	
PhaCK139Ft	CTTGTCGTCGTCGTCCTTGTAGTCcttggcatcggcctcgacgg	
PhaCK139Rs	acccgccagcgcatccgctt	
PhaCK139Rt	GACTACAAGGACGACGACGACAAGacccgccagcgcatccgctt	
PhaCK518Fs	cttggccggcgggttgatca	
PhaCK518Ft	CTTGTCGTCGTCGTCCTTGTAGTCcttggccggcgggttgatca	
PhaCK518Rs	aacaagcgcagccactggactaa	
PhaCK518Rt	GACTACAAGGACGACGACGACAAGaacaagcgcagccactggactaa	
Plasmids		
pMCS69	pBBR1MCS derivative containing genes *phaA* and *phaB* of *R. eutropha* colinear to lac promoter, Cp^r	(Amara and Rehm 2003)
pET14b	Ap^r, T7 promoter	Novagen
pET14b:PhaC	Coding for PhaC wild-type	(Brockelbank et al 2006)
ZZ insertion plasmids		
pUC57:PhaC-K90ΩZZK139ΩZZK518ΩZZ	*phaC* with three insertions of *zz* sequence flanked by restriction endonuclease sites: *Spe*I, *Afl*II, and *Mfe*I respectively	Genscript Corporation
pET14b:PhaC-K90ΩZZ	pET14b:PhaC-K90ΩZZK139ΩZZ with the zz sequence between flanking *Afl*II sites removed	This study
pET14b:PhaC-K139ΩZZ	pET14b:PhaC-K90ΩZZK139ΩZZ with the zz sequence between flanking *Spe*I sites removed	This study
pET14b:PhaC-K518ΩZZ	Containing the *Sac*II to *Bam*HI sequence of pUC57:PhaC-K90ΩZZK139ΩZZK518ΩZZ inserted into pET14b-PhaC	This study
pET14b:PhaC-K90ΩZZK139ΩZZ	Containing the *Nde*I to *Sac*II sequence of pUC57:PhaC-K90ΩZZK139ΩZZK518ΩZZ inserted into pET14b-PhaC	This study
pET14b:PhaC-K90ΩZZK518ΩZZ	Containing the *Sac*II to *Bam*HI sequence of pUC57:PhaC-K90ΩZZK139ΩZZK518ΩZZ inserted into pET14b-PhaC-K90ΩZZ	This study
pET14b:PhaC-K139ΩZZK518ΩZZ	Containing the *Sac*II to *Bam*HI sequence of pUC57:PhaC-K90ΩZZK139ΩZZK518ΩZZ inserted into pET14b-PhaC-K139ΩZZ	This study
pET14b:PhaC-K90ΩZZK139ΩZZK518ΩZZ	Containing the *Nde*I to *Bam*HI sequence of pUC57:PhaC-K90ΩZZK139ΩZZK518ΩZZ inserted into pET14b-PhaC	This study

References

Amara AA, Rehm BHA (2003) Replacement of the catalytic nucleophile cysteine-296 by serine in class II polyhydroxyalkanoate synthase from *Pseudomonas aeruginosa*-mediated synthesis of a new polyester: identification of catalytic residues. Biochem J 374:413–21. doi: 10.1042/BJ20030431

Brockelbank JA, Peters V, Rehm BHA (2006) Recombinant *Escherichia coli* strain produces a ZZ domain displaying biopolyester granules suitable for immunoglobulin G purification. Appl Environ Microbiol 72:7394–7. doi: 10.1128/AEM.01014-06

Chapter 7

7. Discussion

Key Findings

This thesis has focused on three aspects of the PHA beads as a platform technology for protein immobilisation (Fig. 7.1). First, the scope of the system was expanded by demonstrating the possibility of a dual enzyme fusion. Both NanA and Slr1975 were displayed on a single PHA bead and the biosynthesis of Neu5Ac from GlcNAc and pyruvate was achieved. Second, the surface exposed regions of the granule-associated PhaC were explored with specific biotinylation. Three new sites were confirmed as surface exposed and amenable to function insertion as demonstrated with the ZZ domain and IgG binding experiments. Finally, the bioremediation potential of the technology was expanded by immobilisation of the enhanced DvCA to the PHA bead surface. These enzyme beads were tolerant to harsh conditions similar to those found in their potential application of carbon dioxide conversion and capture within coal-fired power plant exhaust streams. These three aspects all expand the scope of the PHA biobeads into new areas allowing more complex arrangements of fusion partners than was previously possible. Each of the aspects of this thesis is further discussed below.

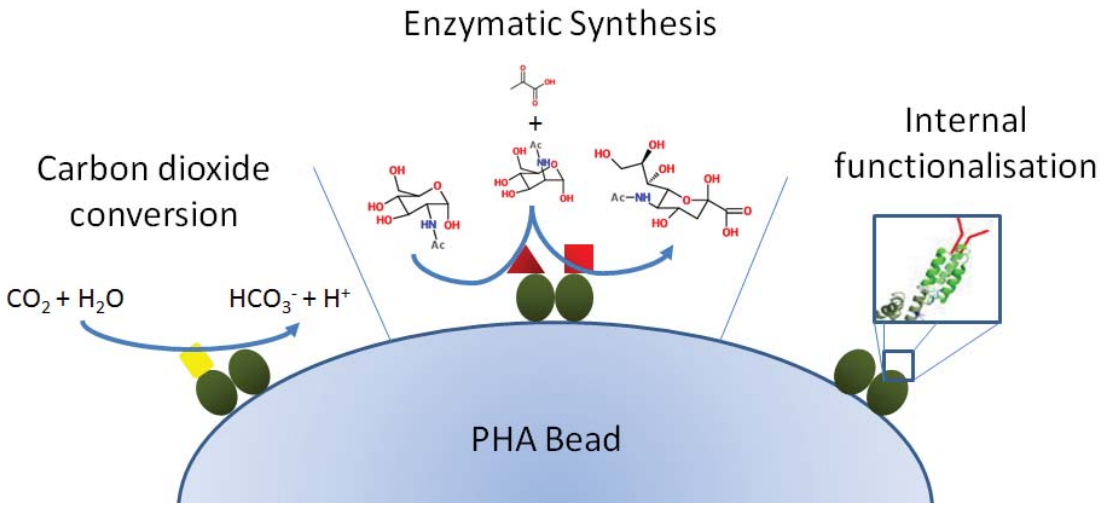

Figure 7.1: The three studies described in this thesis for the enhancement of the PHA bead protein display platform. Immobilisation of carbonic anhydrase for the conversion and capture of carbon dioxide (Chapter 6). Synthesis of N-acetyl neuraminic acid by immobilisation of Slr1975 and NanA (Chapter 4). Internal functionalisation of PhaC internal sites K90, K139, and K518 by insertion of ZZ domain for the binding of IgG (Chapter 5).

One aspect of this thesis was to investigate the tolerance of PhaC and the PHA biobead system for dual fusion of two different enzymes. This possibility was investigated using an aldolase and an epimerase to recapitulate a fine chemical synthesis pathway. In Chapter 4, the NanA and Slr1975 enzymes were both active in the dual fusion construct. However, this dual approach limited flexibility during optimisation by fixing the ratio of each enzyme present in a reaction mixture at 1:1. The use of two single enzyme displaying biobeads for

NanA and Slr1975 was necessary to achieve maximum production of Neu5Ac (22% yield) by shifting the ratio to three times as many Slr1975 PHA beads compared to the NanA beads. This secondary approach set reaction conditions to favour the production of the ManNAc intermediate from GlcNAc pushing the overall reaction towards synthesis of Neu5Ac. The result achieved by the two-bead system can be compared to the traditional approach of chemi-enzymatic synthesis reported to yield up to 33% (Blayer, Woodley, Dawson, & Lilly, 1999). Higher conversion by the PHA-bead display system may be achievable using a continuous process with consistent extraction of Neu5Ac as it is produced consistently pushing the reaction equilibrium towards the desired product. Although this research demonstrated dual fusion can result in two active enzymes on a single PHA bead, a higher productivity per unit input was achieved using single enzyme fusions. This was due to the flexibility allowed by the single bead system in altering the ratio of Slr1975 to NanA present in the synthesis reaction.

A secondary aspect to Chapter 4 was the observation that the choice of fusion point of the enzyme to the PhaC was critical for activity of the final construct. The Slr1975 was fused to the C-terminus via a specially designed linker that had previously been considered necessary for functional attachment (Jahns & Rehm, 2009). However, when the NanA was fused directly to the C-terminus without this linker both the PhaC and the NanA remained active producing NanA-immobilised PHA beads. In contrast, when the Slr1975 was fused to the N-terminus not only was it completely inactive, it also inactivated the previously

functional NanA attached to the C-terminus of the dual fusion bead. It has previously been suggested that the termini of PhaC interact in some way promoting steric hindrance when large fusion partners are added to the construct. The results described in Chapter 4 provide supporting evidence to this claim as the addition of Slr1975 to the construct prevented the functioning of both fusion partners.

The PhaC protein has been extensively studied and utilised in many different biotechnological applications including not only fine-chemical synthesis but also bioremediation, bioseparation, and vaccine development (Brockelbank, Peters, & Rehm, 2006; N. A. Parlane et al., 2011; Robins, Hooks, Rehm, & Ackerley, 2013). Despite the success of this research, very little is known about the structure of PhaC as a three-dimensional structure remains elusive. Further information about the topology of PhaC on the PHA beads would prove useful to further develop this platform technology beyond the current single fusions to the N- and/or C- terminus. While it is known that the PhaC remains attached to the PHA bead *in vivo*, the orientation of the enzyme on the bead is not known. Detecting regions of the granule-associated PhaC may open new design space for functionalised biobeads as well as provide topological insights into the enzyme itself. Several methods were used to gain these insights including crosslinking and partial digestion, both of which were ultimately unsuccessful. Partial digestion involved treatment of the PhaC beads with trypsin and examination of the protein profile by SDS-PAGE. Due to the number of other granule-associated proteins present in the gel, it was

impossible to isolate PhaC fragments in a rigorous way. If the process of partial digestion was to be repeated, beginning with PHA beads of a higher purity would be necessary in order to progress. The downside of a higher purity PHA bead is the harshness of the cleaning process which may alter the PhaC structure and change the overall outcome of the digestion process. As partial digestion would give similar information to the biotinylation experiments of exposed loop structures, this method was not continued beyond initial experiments. The second approach that was unsuccessful was crosslinking of the granule-attached PhaC which would then be viewed on and isolated from an SDS-PAGE gel. Similar to the partial digestion, the problem with this method was the multitude of other granule-associated proteins that made it impossible to identify multimers of the PhaC as opposed to multimers consisting of mixed proteins. To proceed with this method would also require a high purity of PhaC on the PHA beads. In the case of crosslinking, the potential information about the length of the space between different residues would be quite valuable due to the lack of a crystal structure. If successful, a crosslinking experiment could even lead to a low-resolution structure of PhaC and further functionalisation of the platform technology.

However, the research described in Chapter 5 was successful in locating several exposed regions of granule-associated PhaC. Amino acids K77, K90, K139, K518, C382, and C459 were all found labelled after the biotinylation reactions for specific surface-exposed amino acids and MALDI-TOF MS were performed. Further confirmation of the exposed nature of

these discovered regions and their tolerance for short (8 amino acid) insertions was explored using insertions of FLAG epitopes. Although neither cysteine site was able to tolerate insertion with FLAG epitope, all of the lysine site FLAG insertions were tolerated showing the potential flexibility of these sites. FLAG was then detected ELISA and an anti-FLAG-HRP antibody. This was strong confirmatory evidence that the lysine sites on PhaC were surface exposed an amenable to functional insertion. Labelled sites K90, K139, and K518 were further functionalised with IgG-binding ZZ domain insertions. Exposed site K77 was not further explored as it is widely acknowledged that at least the first 80 amino acids of PhaC can be deleted without impact on the function of PhaC. Each of these three ZZ insertions into PhaC were tolerated by the enzyme and the functionalised PHA beads were able to bind and elute significant amounts of human IgG, up to 16 mg IgG/g wet PHA beads for the highest performing construct. Double insertions were also functional with K90ZZK139ZZ demonstrated to purify IgG from human serum with an apparent purity similar to IgG purification seen in PHA beads with terminal fusions of ZZ to PhaC (Brockelbank et al., 2006). Further work could be done to quantitatively assess the purification power of the ZZ insertion beads and compare their performance to that of commercial available IgG binding beads. These three sites along the length of PhaC were clearly shown in Chapter 5 to tolerate large (<100 amino acids) insertions demonstrating their surface exposure and potential application for further functionalisation of the PHA biobead technology.

Finally, carbonic anhydrase immobilised to PHA biobeads was active and results in Chapter 6 clearly demonstrate it was thermotolerant and able to remain functional after pre-incubation over a range of pH conditions. The carbonic anhydrase of choice was from *Desulfovibrio vulgaris* str. "Miyazaki F" and had previously been further enhanced with 35 point mutations selecting for thermotolerance and high activity in tertiary amine solvents. This includes retaining 54% activity after pre-incubation for 1 h at 90 °C and 75% activity after pre-incubation for 30 min at pH 12. Industrial conditions within a carbon dioxide remediation unit at a coal-fired power plant include elevated (>40 °C) temperatures and exposure to carbon dioxide carrying solvents high on the pH scale (pH 10 - 12). Thus the stability tests indicate the suitability of this immobilisation system for deployment in an industrial setting. The activity of the immobilised DvCA was 114 U/mg enzyme. This value is low compared to commercially available carbonic anhydrases although it is unknown whether the decrease in DvCA enzyme activity is due to the mutagenesis, the immobilisation, or a mixture of both processes. In addition to the DvCA fusion a simultaneous fusion of the R5 silica binding peptide to the C-terminus of PhaC was made. Functionalised PhaC beads had previously been shown to bind silica and this was an attempt to expand on that work by growing metal-organic frameworks (MOF) on the silica coating (Jahns, Haverkamp, & Rehm, 2008). MOF have a large surface-to-volume ratio and had a conceived role in carbon dioxide storage. Although MOF synthesis on the bead surface was attempted, no MOF was ever detected or visualised and time constraints meant the work had to be discontinued.

Outlook

Fusion of enzymes relevant to fine chemical synthesis revealed a new application of the biobeads which had not previously been explored. The focus of the research described in Chapter 4 was on a producing a high value optically pure fine chemical as this may be a field where high production costs for bioplastics are not viewed as a drawback. Dual fusion of these enzymes was successful and could be potentially used in other synthesis pathways such as production of the optically pure antibiotic precursor p-hydroxyphenylglycine using the enzymes D-hydantoinase and D-carboamylase, or even to synthetically recreate multi-enzyme complexes (Aranaz, Ramos, De La Escalera, & Heras, 2003). Alternatively the model two enzyme system glucose oxidase and horse radish peroxidase could be used to determine if the need to alter enzyme ratios in order to achieve maximum production is always necessary or simply a feature of the particular NanA/Slr1975 enzymatic pathway chosen in this study (Pescador, Katakis, Toca-Herrera, & Donath, 2008).

As the beads produced in the studies described in Chapters 4, 5, and 6 were produced in transgenic *E. coli* and isolated with a simple mechanical disruption they likely contain significant levels of lipopolysaccharide (LPS). LPS is a known toxin and cannot be present in medical products such as vaccines. Further use of the PHA bead platform in the biomedical field will require production of PHA beads free from significant levels of LPS. Although this issue is not a concern in applications such as bioremediation, alternate

production hosts such as Gram-negative bacteria and low LPS *E. coli* as well as a more rigorous purification process are currently being developed to overcome this issue and further the vaccine and biomedical work.

The formation of the Neu5Ac synthesis pathway on a single PHA bead demonstrates the possibilities of using two fusion sites simultaneously. Uncovering more sites for PhaC modification will undoubtedly lead to even more advanced applications of the PHA biobeads. Although the FLAG tag and ZZ domains were tolerated after insertion into PhaC at K90, K139, and K518, these three internal sites are unlikely to be as flexible as the N- and C-termini which can tolerate large functional fusions, sometimes of multiple proteins (Chen et al., 2014). The small size and possibly hairpin-like fold of ZZ may have contributed to the success of the approach taken here. Regardless, locating several new sites for PhaC modification will result in new applications for the PHA biobeads. Much interest has formed on the potential to use these biobeads as a basis for new vaccines and routine diagnostic screens (Chen et al., 2014; Natalie A Parlane, Rehm, Wedlock, & Buddle, 2014). Potentially, small epitopes or peptide adjuvants (<100 amino acids) could be inserted into PhaC leaving the termini free for larger antigen partners. Alternatively, these sites could be further functionalised with other small binding domains or genetically engineered peptides for inorganics (GEPI) of interest such as the biotin acceptor peptide or a his-tag. Further work in this area will be able to determine the limits in terms of size and fold for functional peptide insertions into the granule-associated PhaC. All biotinylated amino

acids were visualised on a full protein model of PhaC generated by the I-TASSER server with a mixture of threading and *ab initio* folding. While the I-TASSER server for protein structure prediction has performed well in the critical assessment of protein structure prediction challenge, the output for PhaC subjectively appears artificial and likely differs from the actual PhaC structure. It is interesting to note that the full model of PhaC places the N- and C-terminus in close proximity potentially explaining the repeated observations of steric hindrance in dual fusion partners. However, the location of the termini are the least certain aspect of the model so very little weight can be given to this finding. The PhaC model also places all the biotinylated sites on the surface, agreeing with experimental data and lending some weight to its potential accuracy. Ultimately, producing a three-dimensional structure of PhaC would greatly aid research progress in this field and is still a high priority target. If crystallising PhaC remains problematic there is the potential for further investigation using techniques such as partial digestion and crosslinking. As was demonstrated in Chapter 5, even limited knowledge about certain structural aspects of PhaC can be exploited in the rational design of functionalised biobeads and provide insights into the topological nature of this important enzyme.

As atmospheric carbon dioxide has increased more interest has developed around technological solutions to stabilise or reduce CO_2 levels (Huesemann, 2006). Thermostable DvCA immobilised to PHA beads may help to reduce the CO_2 emissions from coal-fired power plants, one of the largest sources of CO_2 worldwide. The demonstration of

immobilised DvCA tolerance to extremes of temperature and pH suggest its suitability for this application. A likely CO_2 remediation unit would consist of two columns with immobilised carbonic anhydrase with a CO_2 solvent continuously cycling between them. In the first column CO_2 would be extracted from the feed gas as it bubbles through the column converting it into bicarbonate ions. The enriched solvent would then flow through to the second column which reverses the conversion and releases pure CO_2 for capture and storage. Ultimately, the immobilised DvCA would need to be adapted to a column set-up with continuous flow capabilities before deployment to an industrial location. Further work will need to be done to test the stability of immobilised DvCA over longer time periods but the results reported in Chapter 6 appear encouraging. The DvCA-displaying PHA beads could potentially even incorporate CO_2 capture material within the second column itself. This approach would add value to the PHA biobead material and help mitigate the drawback of expensive bioplastic production. Finally, the knowledge gained in the different aspects of this thesis, including enzyme display, multiple fusion partners, and internal modification of PhaC, could lead to the rational design of more advanced projects further enhancing the potential of this exciting platform for protein immobilisation.

References

Aranaz, I., Ramos, V., De La Escalera, S., & Heras, A. (2003). Co-immobilization of d -hydantoinase and d -carboamylase on Chitin: Application to the Synthesis of p-hydroxyphenylglycine. *Biocatalysis and Biotransformation*, *21*(6), 349–356. doi:10.1080/10242420310001597829

Blayer, S., Woodley, J. M., Dawson, M. J., & Lilly, M. D. (1999). Alkaline biocatalysis for the direct synthesis of N-acetyl-D-neuraminic acid (Neu5Ac) from N-acetyl-D-glucosamine (GlcNAc). *Biotechnology and Bioengineering*, *66*(2), 131–6. Retrieved from http://www.ncbi.nlm.nih.gov/pubmed/10567071

Brockelbank, J. A., Peters, V., & Rehm, B. H. A. (2006). Recombinant Escherichia coli strain produces a ZZ domain displaying biopolyester granules suitable for immunoglobulin G purification. *Applied and Environmental Microbiology*, *72*(11), 7394–7. doi:10.1128/AEM.01014-06

Chen, S., Parlane, N. A., Lee, J., Wedlock, D. N., Buddle, B. M., & Rehm, B. H. A. (2014). New skin test for detection of bovine tuberculosis on the basis of antigen-displaying polyester inclusions produced by recombinant Escherichia coli. *Applied and Environmental Microbiology*, *80*(8), 2526–35. doi:10.1128/AEM.04168-13

Huesemann, M. H. (2006). *Can Advances in Science and Technology Prevent Global Warming? Mitigation and Adaptation Strategies for Global Change* (Vol. 11). doi:10.1007/s11027-006-2166-0

Jahns, A. C., Haverkamp, R. G., & Rehm, B. H. A. (2008). Multifunctional inorganic-binding beads self-assembled inside engineered bacteria. *Bioconjugate Chemistry*, *19*(10), 2072–80. doi:10.1021/bc8001979

Jahns, A. C., & Rehm, B. H. A. (2009). Tolerance of the Ralstonia eutropha class I polyhydroxyalkanoate synthase for translational fusions to its C terminus reveals a new mode of functional display. *Applied and Environmental Microbiology*, *75*(17), 5461–6. doi:10.1128/AEM.01072-09

Parlane, N. A., Grage, K., Lee, J. W., Buddle, B. M., Denis, M., & Rehm, B. H. A. (2011). Production of a particulate Hepatitis C vaccine candidate by engineered Lactococcus lactis. *Applied and Environmental Microbiology*, *77*(24), 8516–8522. doi:10.1128/AEM.06420-11

Parlane, N. A., Rehm, B. H. A., Wedlock, D. N., & Buddle, B. M. (2014). Novel particulate vaccines utilizing polyester nanoparticles (bio-beads) for protection against

Mycobacterium bovis infection - a review. *Veterinary Immunology and Immunopathology*, *158*(1-2), 8–13. doi:10.1016/j.vetimm.2013.04.002

Pescador, P., Katakis, I., Toca-Herrera, J. L., & Donath, E. (2008). Efficiency of a bienzyme sequential reaction system immobilized on polyelectrolyte multilayer-coated colloids. *Langmuir : The ACS Journal of Surfaces and Colloids*, *24*(24), 14108–14. doi:10.1021/la8027435

Robins, K. J., Hooks, D. O., Rehm, B. H. A., & Ackerley, D. F. (2013). Escherichia coli NemA is an efficient chromate reductase that can be biologically immobilized to provide a cell free system for remediation of hexavalent chromium. *PloS One*, *8*(3), e59200. doi:10.1371/journal.pone.0059200

MASSEY UNIVERSITY
GRADUATE RESEARCH SCHOOL

STATEMENT OF CONTRIBUTION TO DOCTORAL THESIS CONTAINING PUBLICATIONS

(To appear at the end of each thesis chapter/section/appendix submitted as an article/paper or collected as an appendix at the end of the thesis)

We, the candidate and the candidate's Principal Supervisor, certify that all co-authors have consented to their work being included in the thesis and they have accepted the candidate's contribution as indicated below in the *Statement of Originality*.

Name of Candidate: David Hooks

Name/Title of Principal Supervisor: Prof. Bernd Rehm

Name of Published Research Output and full reference:

Polyhydroxyalkanoate inclusions: Polymer synthesis, self-assembly and display technology.

Draper, J.; Du, J.; Hooks, D. O.; Lee, J. W.; Parlane, N. A.; Rehm, B. H. A. Polyhydroxyalkanoate inclusions: Polymer synthesis, self-assembly and display technology. In Bionanotechnology: Biological Self-assembly and Its Applications; Rehm, B. H. A., Ed.; Caister Academic Press: Norfolk, 2013; pp. 1–36.

In which Chapter is the Published Work: Chapter 2

Please indicate either:

- The percentage of the Published Work that was contributed by the candidate 20%

  and / or
- Describe the contribution that the candidate has made to the Published Work:

David Hooks
Digitally signed by David Hooks
DN: cn=David Hooks, o=Massey University, ou, email=dohooks@gmail.com, c=NZ
Date: 2014.10.02 14:31:14 +13'00'

Candidate's Signature

2/10/14
Date

Bernd Rehm
Digitally signed by Bernd Rehm
DN: cn=Bernd Rehm, o=MU, ou=IMBS, email=b.rehm@massey.ac.nz, c=NZ
Date: 2014.12.08 08:38:06 +13'00'

Principal Supervisor's signature

8/12/14
Date

MASSEY UNIVERSITY
GRADUATE RESEARCH SCHOOL

STATEMENT OF CONTRIBUTION TO DOCTORAL THESIS CONTAINING PUBLICATIONS

(To appear at the end of each thesis chapter/section/appendix submitted as an article/paper or collected as an appendix at the end of the thesis)

We, the candidate and the candidate's Principal Supervisor, certify that all co-authors have consented to their work being included in the thesis and they have accepted the candidate's contribution as indicated below in the *Statement of Originality*.

Name of Candidate: David Hooks

Name/Title of Principal Supervisor: Prof. Bernd Rehm

Name of Published Research Output and full reference:

Hooks, D. O.; Venning-Slater, M.; Du, J.; Rehm, B. H. A. Polyhydroyxalkanoate Synthase Fusions as a Strategy for Oriented Enzyme Immobilisation. Molecules 2014, 19, 8629–8643.

In which Chapter is the Published Work: Chapter 3

Please indicate either:

- The percentage of the Published Work that was contributed by the candidate 50%

  and / or
- Describe the contribution that the candidate has made to the Published Work:

David Hooks
Digitally signed by David Hooks
DN: cn=David Hooks, o=Massey University, ou, email=dohooks@gmail.com, c=NZ
Date: 2014.10.02 14:31:14 +13'00'

Candidate's Signature

2/10/14
Date

Bernd Rehm
Digitally signed by Bernd Rehm
DN: cn=Bernd Rehm, o=MU, ou=IMBS, email=b.rehm@massey.ac.nz, c=NZ
Date: 2014.12.08 08:38:43 +13'00'

Principal Supervisor's signature

8/12/14
Date

MASSEY UNIVERSITY
GRADUATE RESEARCH SCHOOL

STATEMENT OF CONTRIBUTION TO DOCTORAL THESIS CONTAINING PUBLICATIONS

(To appear at the end of each thesis chapter/section/appendix submitted as an article/paper or collected as an appendix at the end of the thesis)

We, the candidate and the candidate's Principal Supervisor, certify that all co-authors have consented to their work being included in the thesis and they have accepted the candidate's contribution as indicated below in the *Statement of Originality*.

Name of Candidate: David Hooks

Name/Title of Principal Supervisor: Prof. Bernd Rehm

Name of Published Research Output and full reference:

Hooks, D. O.; Blatchford, P. A.; Rehm, B. H. A. Bioengineering of bacterial polymer inclusions catalyzing the synthesis of N-acetyl neuraminic acid. Appl. Environ. Microbiol. 2013, 79, 3116–3121.

In which Chapter is the Published Work: Chapter 4

Please indicate either:

- The percentage of the Published Work that was contributed by the candidate 80%

  and / or
- Describe the contribution that the candidate has made to the Published Work:

David Hooks
Digitally signed by David Hooks
DN: cn=David Hooks, o=Massey University, ou, email=dohooks@gmail.com, c=NZ
Date: 2014.10.02 14:31:14 +13'00'

Candidate's Signature

2/10/14
Date

Bernd Rehm
Digitally signed by Bernd Rehm
DN: cn=Bernd Rehm, o=MU, ou=IMBS, email=b.rehm@massey.ac.nz, c=NZ
Date: 2014.12.08 08:35:54 +13'00'

Principal Supervisor's signature

8/12/14
Date

MASSEY UNIVERSITY
GRADUATE RESEARCH SCHOOL

STATEMENT OF CONTRIBUTION TO DOCTORAL THESIS CONTAINING PUBLICATIONS

(To appear at the end of each thesis chapter/section/appendix submitted as an article/paper or collected as an appendix at the end of the thesis)

We, the candidate and the candidate's Principal Supervisor, certify that all co-authors have consented to their work being included in the thesis and they have accepted the candidate's contribution as indicated below in the *Statement of Originality*.

Name of Candidate: David Hooks

Name/Title of Principal Supervisor: Prof. Bernd Rehm

Name of Published Research Output and full reference:

Hooks, D. O.; Rehm, B. H. A. Insights into the surface topology of polyhydroxyalkanoate synthase toward self-assembly of functionalized supramolecular inclusions. Applied microbiology and biotechnology 2015, 1-9

In which Chapter is the Published Work: Chapter 5

Please indicate either:

- The percentage of the Published Work that was contributed by the candidate 80%

  and / or
- Describe the contribution that the candidate has made to the Published Work:

David Hooks
Digitally signed by David Hooks
DN: cn=David Hooks, o=Massey University, ou=IFS, email=dohooks@gmail.com, c=NZ
Date: 2014.11.30 10:41:52 +13'00'

Candidate's Signature

30/11/14

Date

Bernd Rehm
Digitally signed by Bernd Rehm
DN: cn=Bernd Rehm, o=MU, ou=IMBS, email=b.rehm@massey.ac.nz, c=NZ
Date: 2014.12.08 08:36:48 +13'00'

Principal Supervisor's signature

8/12/14

Date

MASSEY UNIVERSITY
GRADUATE RESEARCH SCHOOL

STATEMENT OF CONTRIBUTION TO DOCTORAL THESIS CONTAINING PUBLICATIONS

(To appear at the end of each thesis chapter/section/appendix submitted as an article/paper or collected as an appendix at the end of the thesis)

We, the candidate and the candidate's Principal Supervisor, certify that all co-authors have consented to their work being included in the thesis and they have accepted the candidate's contribution as indicated below in the *Statement of Originality*.

Name of Candidate: David Hooks

Name/Title of Principal Supervisor: Prof. Bernd Rehm

Name of Published Research Output and full reference:

Hooks, D. O.; Rehm, B. H. A. Surface display of highly-stable carbonic anhydrase on polyester beads for carbon dioxide capture. Biotechnology letters 2015, 1-6

In which Chapter is the Published Work: Chapter 6

Please indicate either:

- The percentage of the Published Work that was contributed by the candidate 80%

  and / or
- Describe the contribution that the candidate has made to the Published Work:

David Hooks
Digitally signed by David Hooks
DN: cn=David Hooks, o=Massey University, ou=IFS, email=dohooks@gmail.com, c=NZ
Date: 2014.11.30 10:41:12 +13'00'

Candidate's Signature

30/11/14

Date

Bernd Rehm
Digitally signed by Bernd Rehm
DN: cn=Bernd Rehm, o=MU, ou=IMBS, email=b.rehm@massey.ac.nz, c=NZ
Date: 2014.12.08 08:40:34 +13'00'

Principal Supervisor's signature

8/12/14

Date

MASSEY UNIVERSITY
TE KUNENGA KI PŪREHUROA
UNIVERSITY OF NEW ZEALAND

COPYRIGHT FORM AND DECLARATION CONFIRMING CONTENT OF DIGITAL VERSION OF THESIS

Student ID number: 1 0 2 1 3 6 5 7

Student's name: David Hooks

Thesis title:

Polyhydroxyalkanoate granules: surface protein topology and rational design of functionalised biobeads

Have you published articles/material from your thesis? (•) Yes ( ) No

If 'Yes', have you received copyright permission from the third party to include this published material in your thesis which will be placed in the Library's electronic repository? (•) Yes ( ) No

Student's signature:

David Hooks

Digitally signed by David Hooks
DN: cn=David Hooks, o=Massey University, ou=IFS, email=dohooks@gmail.com, c=NZ
Date: 2014.11.30 10:51:46 +13'00'

Date: Day 3 0 Month 1 1 Year 2 0 1 4

If you opted to self-print your thesis, please complete the following declaration:

I confirm that the content of the digital version of this thesis is the final amended version following the examination process, and is identical to the bound paper copy.

Student's signature:

David Hooks

Digitally signed by David Hooks
DN: cn=David Hooks, o=Massey University, ou=IFS, email=dohooks@gmail.com, c=NZ
Date: 2014.11.30 10:51:33 +13'00'

Date: Day 3 0 Month 1 1 Year 2 0 1 4